



Thèse

2012

Open Access

This version of the publication is provided by the author(s) and made available in accordance with the copyright holder(s).

On Testing Modified Gravity : with Solar System Experiments and Gravitational Radiation

Sanctuary, Hillary

How to cite

SANCTUARY, Hillary. On Testing Modified Gravity : with Solar System Experiments and Gravitational Radiation. Doctoral Thesis, 2012. doi: 10.13097/archive-ouverte/unige:28935

This publication URL: <https://archive-ouverte.unige.ch/unige:28935>

Publication DOI: [10.13097/archive-ouverte/unige:28935](https://doi.org/10.13097/archive-ouverte/unige:28935)

UNIVERSITÉ DE GENÈVE
Département de physique théorique

FACULTÉ DES SCIENCES
Professeur Michele Maggiore

On Testing Modified Gravity

with Solar System Experiments and Gravitational Radiation

THÈSE

présentée à la Faculté des Sciences de l'Université de Genève
pour obtenir le grade de Docteur ès Sciences, mention Physique

par

Hillary Sanctuary

de

Montréal, Canada

Thèse N° 4524
Genève, juillet 2012
Reprographie EPFL



**UNIVERSITÉ
DE GENÈVE**

FACULTÉ DES SCIENCES

**Doctorat ès sciences
Mention physique**

Thèse de *Madame Hillary Adrienne SANCTUARY*

intitulée :

**"On Testing Modified Gravity
With Solar System Tests and Gravitational Radiation"**

La Faculté des sciences, sur le préavis de Messieurs M. MAGGIORE, professeur ordinaire et directeur de thèse (Département de physique théorique), A. RIOTTO, professeur ordinaire (Département de physique théorique), M. KUNZ, docteur (Département de physique théorique), A. KEHAGIAS, professeur (Physics Division, School of Applied Sciences, National Technical University of Athens) et S. SIBIRYAKOV, docteur (Institute for Nuclear Research, Russian Academy of Sciences, Moscow, Russia), autorise l'impression de la présente thèse, sans exprimer d'opinion sur les propositions qui y sont énoncées.

Genève, le 31 juillet 2012

Thèse - 4524 -



Le Doyen, Jean-Marc TRISCONE

N.B. - La thèse doit porter la déclaration précédente et remplir les conditions énumérées dans les "Informations relatives aux thèses de doctorat à l'Université de Genève".

Publications

D. Blas and H. Sanctuary, “Gravitational Radiation in Horava Gravity,” *Phys.Rev.* **D84** (2011) 064004, [arXiv:1105.5149 \[gr-qc\]](#).

U. Cannella, S. Foffa, M. Maggiore, H. Sanctuary, and R. Sturani, “Extracting the three- and four-graviton vertices from binary pulsars and coalescing binaries,” *Phys. Rev.* **D80** (2009) 124035, [arXiv:0907.2186 \[gr-qc\]](#).

H. Sanctuary and R. Sturani, “Effective field theory analysis of the self-interacting chameleon,” *Gen.Rel.Grav.* **42** (2010) 1953–1967, [arXiv:0809.3156 \[gr-qc\]](#).



ON TESTING MODIFIED GRAVITY

WITH SOLAR SYSTEM EXPERIMENTS
AND GRAVITATIONAL RADIATION

Hillary Sanctuary

Thesis N° 4524
Docteur ès Sciences, Physics

University of Geneva
Faculty of Science
Department of Theoretical Physics

Contents

Résumé	ix
Remerciements	xiii
Summary	xv
Acknowledgements	xix
Conventions	xxiii
1 General Relativity	1
1.1 The field equations	1
1.2 The action	2
1.3 Gravitational waves in weak-field gravity	3
1.3.1 Linearized gravity	3
1.3.2 Vacuum spacetimes	4
1.3.3 Spacetimes with an isolated matter source	5
1.3.4 Generation of gravitational waves	5
1.4 A PN technique - NRGR	10
2 Modified Gravity	19
2.1 Foundations	20
2.2 Solar-System tests	22
2.2.1 Tests involving null trajectories	22
2.2.2 Tests involving time-like trajectories	23
2.3 Parametrized post-Newtonian formalism	24
2.3.1 The method	24
2.4 Gravitational radiation tests	27
2.4.1 Indirect detection	27
2.4.2 Direct detection	30
2.5 Theoretical considerations	31
3 Gravitational Radiation in Hořava gravity	35
3.1 Action for khronometric theory at low energies	37
3.2 Equations of motion in the far-zone	40
3.2.1 Wave equations	41
3.3 Post-Newtonian expressions	42
3.4 The source: conservation properties	45

3.5	Wave forms in the far-zone	46
3.6	Notion of energy for an asymptotically flat spacetime	47
3.7	Energy-loss formulae for post-Newtonian systems	51
3.8	Energy loss by a Newtonian binary system	53
3.9	The Einstein-aether and the monopole	56
3.10	Discussion	57
4	Effective field theory analysis of general relativity	59
4.1	Measuring the three-graviton vertex	61
4.1.1	The modified bound system	62
4.1.2	The modified power radiated	63
4.1.3	The modified phase	66
4.2	The four-graviton vertex	71
4.3	The method	72
4.4	Discussion	75
5	Effective Field Theory Analysis of the Chameleon	77
5.1	The chameleon in brief	78
5.1.1	The chameleon equation of motion	79
5.1.2	The chameleon mass and non-linear couplings	79
5.1.3	The chameleon profile	80
5.1.4	A threat from chameleon self-couplings	82
5.2	Analysis of chameleon self-interactions	84
5.2.1	An effective field theory approach	84
5.2.2	Tests of the chameleon	89
5.3	Discussion	90
	Acronyms	91
	Bibliography	91

Résumé

La théorie de la gravitation d'Einstein, la relativité générale, a sculptée notre compréhension des interactions gravitationnelles. Confirmée expérimentalement par la précession de la périhélie de Mercure ou la perte d'énergie due au rayonnement gravitationnel dans un système binaire d'étoiles à neutrons [1], elle est l'une des théories les plus réussies et influentes de notre temps.

Cependant, aux extrêmes de l'échelle d'énergie, il apparaît que la relativité générale n'est plus valable en tant que théorie gravitationnelle. Dans l'ultraviolet (ou à énergie élevée), les méthodes employées afin de quantifier la relativité générale, à la base une théorie classique des champs, sont incapables de donner une théorie quantique, cohérente, de la gravitation [2]. Par conséquent, la relativité générale est perçue comme une théorie effective des champs, avec une version quantique gravitationnelle encore à découvrir [3].

Dans l'infrarouge (où à basse énergie), des phénomènes étranges deviennent apparents, comme l'accélération du taux d'expansion de l'univers [4]. La prise en compte de la présence de nouvelles sources invisibles permet de réconcilier ces observations avec la théorie [5]. La nécessité d'introduire des composantes (de matière et d'énergie) que l'on ne peut détecter que de façon gravitationnelle pourrait être l'indication d'une mauvaise compréhension de la dynamique gravitationnelle aux échelles allant au-delà du kiloparsec [6]. Il est donc intéressant de réfléchir à des théories alternatives de la gravitation.

Ces dernières décennies, la recherche sur la gravitation a beaucoup progressé, donnant lieu à un nouveau domaine de recherche qui s'appelle la 'gravitation modifiée'. Ici, nous en adoptons la définition¹ donnée en [7]. La théorie de base est la relativité générale d'Einstein. La gravitation modifiée fait référence, quant à elle, à un ensemble de théories gravitationnelles qui modulent d'une manière ou une autre la théorie d'Einstein dans l'infrarouge et/ou dans l'ultraviolet. Afin de conserver la plus grande cohérence dans la définition de ces théories, des formalismes sont proposés dans le but de les mettre à l'épreuve des observations expérimentales. L'importance des théories métriques de la gravitation émerge des tests des principes d'équivalences. Les tests à l'échelle du système solaire donnent lieu à des limites strictes sur les phénomènes gravita-

¹Dans la littérature, le sens de l'expression 'gravitation modifiée' n'est pas unanime. Remarque que certains auteurs font la distinction entre 'gravitation modifiée' et une 'théorie UV complète'. Dans ce cas, l'expression 'gravitation modifiée' parle d'une modification dans l'infrarouge de la relativité générale, tandis qu'une théorie UV complète parle d'une extension à hautes énergies de la relativité générale.

tionnels. Le formalisme ‘post-newtonien paramétré’ (PPN) a été développé afin de mettre à l’épreuve des théories candidates gravitationnelles [8, 9, 10, 11]. Essentiellement, le formalisme compare les premiers termes post-newtoniens avec les contraintes expérimentales. Un nouvel ensemble d’outils est actuellement en train d’apparaître. Il s’agit de l’approche "post-friedmannien paramétrée" [12, 13, 14, 15], qui analyse des théories à l’échelle cosmologique (voir [7] pour une vue d’ensemble).

Dans cette thèse, nous mettons à l’épreuve trois théories gravitationnelles en les appliquant à certains corps célestes. Nous utilisons des outils de base et d’autres adaptés aux principes post-newtoniens. En particulier, nous étudions la relativité générale, le chaméléon et la gravitation d’Hořava. Le système solaire, les pulsars binaires et les détections futures aux observatoires gravitationnels font office de laboratoire.

La gravitation d’Hořava et le rayonnement gravitationnel

La gravitation Hořava-Lifschitz est une théorie candidate de la gravitation renormalisable et possédant une réalisation ultraviolette, complétant la relativité générale, mais tout en violant l’invariance de Lorentz [16]. En effet, la recherche dans le domaine de la gravitation quantique suggère que la symmétrie de Lorentz n’est peut-être pas une symmétrie valable pour toute énergie [17]. La proposition d’origine d’Hořava a en effet, à l’origine, des problèmes de cohérence. Ceux-ci ont ensuite été résolus, donnant lieu à une théorie scalaire-tenseur dans l’infrarouge et violant l’invariance de Lorentz. Elle s’appelle la théorie khronométrique [18, 19, 20]. La foliation temporelle préférée est définie par le champ scalaire, d’où son nom de ‘khronon’ ou de ‘champ-T’. Cette théorie est une alternative prometteuse à la relativité générale.

Nous testons la gravitation d’Hořava en étudiant l’émission du rayonnement gravitationnel dans la limite des champs faibles pour des sources post-newtoniennes, en utilisant des techniques qui profitent pleinement du formalisme PPN de Will [10]. En particulier, nous donnons une généralisation de la formule quadrupolaire d’Einstein, et nous montrons qu’un terme monopolaire persiste, même dans la limite pour laquelle les paramètres PPN sont identiques à ceux de la relativité générale. Notre résultat complète ce que l’on a trouvé pour les théories tenseurs multi-scalaires [21] et les théories Einstein-Æther [22]. En comparant nos résultats avec les observations du système binaire Hulse-Taylor, nous obtenons les meilleures contraintes jamais enregistrées sur les paramètres libres de la théorie khronométrique, quand les paramètres PPN sont identiques à ceux de la relativité générale.

La relativité générale et les méthodes théorie de champs effective

Dans ce travail, nous étudions la déviation des vertexes d’interaction trilineaires et quartiques gravitationnelles de leurs valeurs telles qu’elles sont définies dans la relativité générale. Or, nous nous trouvons face à des limites expérimentales lorsque nous observons ces déviations possibles à partir d’expériences sur le système solaire, les pulsars binaires et les interféromètres gravitationnels. Si la

relativité générale est effectivement la théorie la plus adéquate pour ce qui est de la gravitation à basse énergie, ces mesures imposent des limites strictes aux théories qui complètent la relativité générale à hautes-énergies.

Comme le modèle standard de la physique des particules, la relativité générale est considérée comme une théorie effective. Elle fournit un modèle valable de la gravitation à basse énergie mais devient peu fiable à hautes énergies, proche du cutoff de la théorie. En théorie effective, l'effet des processus quantiques sur des énergies arbitrairement élevées contribue à ce que l'on observe à basse énergie. Ces processus renormalisent les constantes de couplage de la théorie. Alors que les physiciens cherchent des moyens pour compléter la relativité générale à des énergies élevées avec une théorie quantique de la gravitation, il n'est pas nécessaire de connaître la théorie quantique complète afin de faire des prédictions censées, tant que le système à étudier est bien en-dessous du cutoff.

Nous testons la relativité générale à l'aide d'une technique de théorie effective qui s'appelle NRGR (non-relativistic general relativity) [23, 24] afin de déterminer les corrections post-newtoniennes pour des corps en interaction gravitationnelle. En se basant sur cette technique post-newtonienne, nous proposons une façon phénoménologique pour mesurer les déviations de la relativité générale provenant d'une théorie complète dans l'ultraviolet, qui est encore inconnue.

Le chaméléon et les méthodes théorie de champs effective

Le chaméléon est une théorie scalaire-tenseur possédant un mécanisme qui supprime son comportement longue portée, tout en gardant un couplage de l'ordre de l'unité avec la matière. Ceci est réalisé en ajoutant un potentiel monotone à l'action tel qu'un potentiel effectif agisse sur le chaméléon. Une expansion de Taylor du potentiel effectif révèle que le chaméléon est en interaction avec lui-même. En l'absence d'auto-interaction, le champ scalaire chaméléonique est médiateur d'interactions à longue portée tout en évadant les contraintes imposées par la violation du principe d'équivalence faible. Cependant, ces auto-interactions scalaires sont potentiellement dangereuses car elles changent le comportement du champ à longue portée. Or, l'effet des auto-interactions quartiques n'a été jusqu'alors étudié que dans la littérature.

En adaptant NRGR au chaméléon, nous étudions les effets du chaméléon en auto-interaction à tous les ordres. En particulier, l'auto-interaction trilineaire conduit à une correction proportionnelle au logarithme de la distance. Nous montrons systématiquement que ces contributions provenant des auto-interactions d'ordre trois et plus ne mettent pas en danger la théorie du chaméléon pour ce qui est des objets du type du système solaire.

Remerciements

Plusieurs événements importants, dans le domaine de la physique théorique, jalonnent l'histoire de l'Université de Genève. En 1909, cette institution décernait à Albert Einstein son tout premier doctorat honorifique. De 1930 à 1975, Ernst Stueckelberg était professeur en physique théorique aux deux universités de Genève et de Lausanne. Or, ces deux brillants physiciens du XXe siècle sont intimement liés à ma recherche de thèse au sujet de la gravitation.

Aujourd'hui, le département de physique théorique de l'Université de Genève offre un cadre de travail stimulant et la possibilité de rencontrer des physiciens ayant des intérêts convergents, tout en bénéficiant de la proximité d'organisations de recherche prestigieuses tels que le CERN et l'EPFL. Pour toutes ces raisons, c'était un honneur de pouvoir poursuivre ma recherche et faire mon doctorat à l'Université de Genève. Je suis reconnaissante à Michele Maggiore pour cette opportunité.

C'est grâce à la collaboration de Diego Blas, collègue et ami, que mes projets de recherche se sont tournés vers les théories de la gravitation au-delà de la relativité. Notre amitié a commencé avec la pratique de la plongée dans le lac Léman, des duos de musique, des tours en peaux-de-phoque dans les Alpes suisses, et, en route, une sorte de rêve sur la gravitation quantique. Il m'a également encouragée à participer à des ateliers uniques sur ce thème. À Peyresq, un village médiéval, perché dans les Alpes de Haute-Provence, j'ai appris à adapter mon langage à deux espèces distinctes de physiciens théoriciens: ceux de la gravitation et ceux de la physique des particules. J'ai aussi découvert un mélange enivrant (et non incompatible) de gravitation, de physique quantique, de musique médiévale et de génépi. Merci, Diego, pour ton influence décisive sur ma recherche, et pour ton amitié.

Je souhaiterais remercier mes collègues pour les discussions, les visites et les échanges de courriels stimulants et souvent passionnants, ainsi que pour leur hospitalité et leur soutien précieux, ou tout simplement encore pour les bons moments partagés avec eux: Bruce Bassett, Luc Blanchet, Céline Boehm, Mariam Bouhmadi Lopez, Umberto Cannella, Chiara Caprini, Steve Carlip, Timothy Clifton, Claudia de Rham, Peter Dunsby, Ruth Durrer, Gilles Esposito-Farese, Valerio Faraoni, Elisa Fenu, Stefano Foffa, Brendan Foster, Sergey Frolov, Kevin Govender, Edgard Gunzig, Lukas Hollenstein, Bei-Lok Hu, Ted Jacobson, Alex Kehagias, Nima Khosravi, Martin Kunz, David Langlois, Julien Lesgourgues, Marcos Mariño, Alexis Martin, James Newling, Nathaniel Obadia, Carolina Ödman-Govender, Charles Pfister, Martin Pohl, Rafael Porto, Max Rinaldi, An-

tonio Riotto, Albert Roura, Marcus Ruser, Domenico Sapon, Tanya Schmah, Sergey Sibiryakov, Thomas Sotiriou, Charles Stuart, Riccardo Sturani, Andrew Tolley, Bill Unruh, Peter Wittwer. Un grand merci à Céline Boehm, Ruth Durrer, Martin Kunz et Julien Legourgues, pour leur investissement envers leurs étudiants, leur enseignement et pour l'organisation des Cosmo Coffees, ateliers, cours du 3e cycle, et conférences à Genève, au CERN et un peu partout en Europe. Merci au jury de thèse et en particulier à Sergey pour le retour précieux. Un merci chaleureux à mes étudiants en électrodynamique, physique mathématique et mécanique quantique. Aucun institut de recherche ne fonctionnerait comme il le faut sans son personnel administratif, que je souhaiterais également remercier pour son soutien continu, en particulier Nathalie Chaduiron, Danièle Chevalier, Francine Gennai-Nicole, Marie-Anne Gervais, Cécile Jaggi-Chevalley, Andreas Malaspinas. Merci au Fonds National Suisse et à l'Association pour la Recherche Fondamentale OLAM.

La recherche en physique théorique exige de l'imagination, de la rigueur, et un travail soutenu. Aujourd'hui, elle consiste aussi entre autres en collaborations, partages, débats, respect, réseautage. Elle demande de la persévérance et une inspiration toujours renouvelée malgré les obstacles.

Charles Roth de l'Université de McGill - un enseignant dévoué et une source d'inspiration - aimait à distribuer une liste de citations à ses étudiants dans le but de les soutenir lors de son cours en analyse avancée. Dans un premier temps, cette liste m'a bien amusée. Elle m'a ensuite accompagnée depuis le Canada jusqu'en Suisse, où elle m'a aidée à travers toutes mes études, durant ma recherche et plus généralement, dans la vie de tous les jours. Merci Professeur Roth.

La physique nous permet de naviguer les mystères de la Nature, mais les entreprises artistiques, eux aussi, nous offrent la possibilité de sonder notre existence. Je souhaiterais saluer deux musiciens contemporains qui appartiennent au monde transdisciplinaire de l'art et de la science. L'un est le guitariste anglais, Brian May, du célèbre groupe de rock Queen. Il a reçu sa thèse de doctorat en astrophysique du Collège Imperial à l'âge de 60 ans. Il est pour moi un musicien-physicien exemplaire et prouve que les passions artistiques et scientifiques sont compatibles. L'autre est la musicienne Islandaise Björk. Non seulement est-elle constamment à la recherche de manières créatives d'intégrer la science et la technologie dans sa musique, mais elle a généreusement incorporé une installation scientifique dans sa tournée «Biophilia». Par ses efforts pédagogiques, elle parvient à éveiller de manière admirable la curiosité et l'imagination des enfants et des adultes.

Enfin, je souhaite dire merci, à vous, famille et amis, ici en Europe et éparpillés dans le monde. Aux familles Martin, Weber, Weibel et Woo. À ma famille. À ma mère. À mes amis proches et de longue date, Bastien, Cynthia, Joëlaki, Mariska, Paula, Simon, pour votre soutien infini, pour votre amitié et pour les aventures partagées.

Hillary Sanctuary
Lausanne, 2012

Summary

Einstein’s theory of gravitation, general relativity, has sculpted our understanding of gravitational interactions. It is one of the most successful and influential theories of our times, with experimental confirmation ranging from the precession of Mercury’s perihelion to the power loss due to gravitational radiation in a binary system of neutron stars[1].

At extremes of the energy scale, however, there is evidence that general relativity breaks down as a theory of gravitation. In the [ultraviolet \(UV\)](#) (or high-energy), procedures to quantify general relativity, an inherently classical theory, fail to provide a consistent quantum theory of gravity [2]. In light of this, general relativity is considered to be an effective field theory of gravity [3], with a quantum description yet to be discovered.

In the [infrared \(IR\)](#) (or low-energy), strange phenomena become apparent such as the acceleration of the expansion rate of the universe [4]. New sources of unseen matter and energy are a way to deal with these observations [5]. The need to introduce matter-energy components that we detect only gravitationally may indicate a poor understanding of gravitational dynamics at scales larger than the kiloparsec. These observations may be an indication that general relativity is not adequate to describe gravitation at extremes of the energy scale [6]. It is therefore worth considering alternative theories of gravity.

Over the past few decades, research in gravity has progressed substantially, giving way to a whole new field called ‘Modified Gravity’. Here we adopt the definition² of Modified Gravity given in [7]. The theory of reference is Einstein’s theory of general relativity, and modified gravity refers to a host of candidate theories of gravitation that alter in some way or other Einstein’s original theory in the [IR](#) and/or the [UV](#). Given the abundance of ways to go about building theories of gravitation, formalisms are developed to test these theories against experiment. The importance of metric theories of gravity emerge from tests of the equivalence principles. Solar system tests provide stringent bounds on gravitational phenomena. The [parametrized post-Newtonian \(PPN\)](#) formalism was developed to test candidate theories of gravity [8, 9, 10, 11]. Essentially, the formalism compares the theory’s leading post-Newtonian terms with experimental constraints. A new set of tools is currently being developed, called the

²In the literature, the significance of the expression ‘Modified Gravity’ is not unanimous. Note that some authors make the distinction between ‘Modified Gravity’ and a ‘UV complete theory’. The term ‘Modified Gravity’ then refers to an [IR](#) modification of general relativity, whereas a [UV](#) completion refers to a high-energy extension of general relativity.

Parametrized Post-Friedmannian approach [12, 13, 14, 15], analyzing theories at cosmological scales (see [7] for a review).

In this thesis, we test three theories of gravitation with celestial bodies, using standard and adapted [post-Newtonian \(PN\)](#) tools. In particular, the theories we study are general relativity, the chameleon and Hořava gravity. The laboratory is provided by the Solar System, Binary Pulsars and future detections at [gravitational wave observatories \(GWO\)](#).

Hořava gravity and gravitational radiation

Hořava-Lifschitz gravity is a candidate for a renormalizable, UV completion of general relativity that violates Lorentz invariance [16]. Indeed, research in quantum gravity suggests that Lorentz symmetry may not be a valid symmetry at all energies [17]. While Hořava’s initial proposal has consistency issues, the latter were resolved leading to a scalar-tensor theory in the [IR](#) that breaks Lorentz invariance, called khronometric theory [18, 19, 20]. The preferred time-foliation is defined by the scalar-field, hence its name the ‘khronon’ or the ‘T-field’. Khronometric theory is a promising alternative to general relativity.

We test Hořava gravity by studying emission of gravitational radiation in the weak-field limit for [PN](#) sources using techniques that take full advantage of the [PPN](#) formalism described by Will [10]. In particular, we provide a generalization of Einstein’s quadrupole formula and show that a monopole persists even in the limit in which the [PPN](#) parameters are identical to those of general relativity. The result extends results previously discovered for Multi-Scalar Tensor [21] and Einstein-Æther Theories [22]. Constraining our results with observations of the Hulse-Taylor binary pulsar provides the strongest constraints yet on the free parameters of khronometric theory, when the [PPN](#) parameters are identical to those of general relativity.

General relativity and effective field theory methods

We study the deviation of the three- and four-graviton vertices from their standard general relativity values, and place experimental bounds on these possible deviations from Solar-System experiments, binary pulsars and gravitational-wave interferometers. If general relativity is indeed the correct low-energy theory describing gravity, these measurements then provide strict bounds on theories that complete general relativity at high-energies.

Like the Standard Model of Particle Physics, general relativity is considered to be an effective field theory, providing a valid description of gravity at low energies but becoming unreliable at high energies, near the theory’s cutoff. In effective field theory, the effect of quantum processes at arbitrarily high energies contribute to what is observed at low energies. These high energy processes renormalize the coupling constants of the theory. While many physicists today are searching for ways to complete general relativity at high energies with some quantum theory of gravity, it is not necessary to know the full quantum theory in order to make meaningful predictions, as long as the system of study is well below the cutoff.

We test general relativity with the help of a technique called [non-relativistic General Relativity \(NRGR\)](#) [23, 24], used to determine [PN](#) corrections for the problem of gravitating bodies. Based on this [PN](#) technique, we propose a phenomenological way to measure deviations from general relativity coming from an unknown [UV](#) completion.

The chameleon and effective field theory methods

The chameleon is a scalar-tensor theory endowed with a special mechanism that suppresses its long range behaviour while maintaining order unity coupling to matter. This is done by adding a monotonic potential to the action so that the chameleon is subject to an effective potential. Taylor expanding the potential around the scalar's background value reveals that the chameleon is self-interacting. In the absence of self-interactions, the chameleon scalar field can mediate long range interactions and simultaneously evade constraints from violation of the weak equivalence principle. These scalar self-interactions are potentially dangerous, however, since they change the long-range behaviour of the field. Only the effect of quartic self-interactions had been studied in the literature.

Adapting [NRGR](#) to the chameleon, we study the effects of the self-interacting chameleon at arbitrary order. In particular, the trilinear self-interaction leads to a correction which is logarithmic in distance. We systematically show that these self-interacting contributions at orders three and higher do not jeopardize the chameleon theory for Solar System type objects.

Chapters 1 and 2 aim to provide a context for the three theories of gravity that we study throughout the thesis and how we test them. In Chapter 1, we present general relativity and its main features. Given the importance of gravitational radiation throughout this manuscript, we discuss in detail the generation of gravitational waves. We then present, in Chapter 2, the basics of Modified Gravity, namely the tests and theoretical considerations that have framed our understanding of gravity. We discuss the Equivalence Principles, Solar System tests, the [PPN](#) formalism and radiation tests. We also provide a glimpse of the field of research called Modified Gravity. In Chapter 3, we study radiation damping from an astrophysical binary system in Hořava Gravity. In the remaining two chapters, the effective field theory technique [NRGR](#) is adapted to test general relativity and the chameleon. In Chapter 4, this technique allows us to measure deviations from the three- and four- graviton vertices in general relativity. Finally, in Chapter 5, this effective field theory method is used to study self-interactions present in the chameleon. These three chapters are based on the articles written in collaboration with Diego Blas [25], Umberto Cannella, Stefano Foffa, Michele Maggiore and Riccardo Sturani [26],[27].

Acknowledgements

The University of Geneva has seen its share of historic moments for theoretical physics. Two prominent physicists of the 20th century come to mind and are intimately related to my thesis research in gravitation, Albert Einstein and Ernst Stueckelberg. In 1909, the University of Geneva awarded Albert Einstein his first honorary doctorate. From 1930 - 1975, Ernst Stueckelberg was a Professor of Theoretical Physics at both the University of Geneva and of Lausanne.

Today, the Department of Theoretical Physics constitutes a stimulating environment in which to work and meet physicists with similar research interests. In addition, it is close to other prestigious research organisations like CERN and EPFL. For these reasons, it was an honour to be able to pursue my research and earn my doctorate at the University of Geneva - I am thankful to Michele Maggiore for this opportunity.

My research interests took a conceptual turn towards theories of gravitation beyond Einstein's theory of general relativity thanks to collaborations with Diego Blas, colleague and friend. Our friendship began with scuba diving in lake Geneva, music duos, ski-touring in the Swiss Alps, and some dream about quantum gravity along the way. Besides research collaborations, he encouraged me to participate in unique workshops dedicated to quantum gravity. Located in a remote Medieval village named Peyresq, perched in the Alps of Haute-Provence, I learned to tailor my language to two very distinct species of theoretical physicists: gravitational physicists and particle physicists. I also discovered an ethereal (and not incompatible) mix of gravitation, quantum physics, medieval music and génépi - no pun intended. Thank you, Diego, for your decisive influence on my research, and for your friendship.

I would like to express my sincere thanks and appreciation to colleagues for valuable, stimulating and often captivating discussions, email exchanges, visits, hospitality, for your support or simply for good times. Bruce Bassett, Luc Blanchet, Céline Boehm, Mariam Bouhmadi Lopez, Umberto Cannella, Chiara Caprini, Steve Carlip, Timothy Clifton, Claudia de Rham, Peter Dunsby, Ruth Durrer, Gilles Esposito-Farese, Valerio Faraoni, Elisa Fenu, Stefano Foffa, Brendan Foster, Sergey Frolov, Kevin Govender, Edgard Gunzig, Lukas Holenstein, Bei-Lok Hu, Ted Jacobson, Alex Kehagias, Nima Khosravi, Martin Kunz, David Langlois, Julien Lesgourgues, Marcos Mariño, Alexis Martin, James Newling, Nathaniel Obadia, Carolina Ödman-Govender, Charles Pfister, Martin Pohl, Rafael Porto, Max Rinaldi, Antonio Riotto, Albert Roura, Marcus Ruser, Domenico Sapone, Tanya Schmah, Sergey Sibiryakov, Thomas Sotiriou,

Charles Stuart, Riccardo Sturani, Andrew Tolley, Bill Unruh, Peter Wittwer. A special thanks to Céline Boehm, Ruth Durrer, Martin Kunz and Julien Lesgourgues, for their dedication to students, to teaching and for organizing stimulating Cosmo Coffees, workshops, advanced courses and conferences in Geneva, at CERN and all over Europe for that matter. Thanks to my thesis jury, and to Sergey Sibiryakov, for providing valuable feedback. A warm thanks to my students in electrodynamics, mathematical physics and quantum mechanics. No research institute would function properly without the administrative staff, to whom I would like to extend my thanks for their endless support, in particular Nathalie Chaduiron, Danièle Chevalier, Francine Gennai-Nicole, Marie-Anne Gervais, Cécile Jaggi-Chevalley, Andreas Malaspinas. Thank you to the Swiss National Fund SNF and the Association for Fundamental Research OLAM.

Research in theoretical physics is about imagination, rigour and hard work. Today, it is also about collaboration, sharing, debate, respect, networking, to mention a few. It is about perseverance and renewing inspiration despite obstacles.

Charles Roth of McGill University - an inspiring and dedicated lecturer - liked to distribute a list of motivational sayings to his students to encourage us through his course in Advanced Calculus. This list has accompanied me from Canada to Switzerland, and has helped me throughout my studies, my research, and more importantly, in everyday life. Thank you Professor Roth.

Physics allows us to navigate the mysteries of Nature, but artistic endeavours also provide profound insight into our existence. In the transdisciplinary realm where the arts and sciences mingle, I would like to salute two prominent musicians of today. One is British guitarist Brian May of the famous rock band Queen. He received his Ph.D. in Astrophysics at the age of 60 from Imperial College. He is exemplary of a musical physicist ("physical musician" doesn't quite mean the same thing) and proof that artistic and scientific passions are compatible. The other is Icelandic musician Björk. Not only does she constantly search for creative ways to integrate science and technology into her music, but she has also generously incorporated a science installation into her "Biophilia" tour, complete with guided visits for children. Her outreach efforts - mixing art and science - are a tremendous way to awaken curiosity and imagination in children and adults alike.

Finally, I would like to thank my family and friends - here in Europe and scattered around the World - for your support and caring. To the Martin, Weber, Weibel and Woo families. To my family. To my Mom. To close friends for your endless support and shared adventures, Bastien, Cynthia, Joëlaki, Mariska, Paula, Simon.

Hillary Sanctuary
Lausanne, 2012

FAMOUS QUOTES

1. **THE HARDER YOU WORK THE LUCKIER YOU GET.**
2. **NOTHING IS GOOD OR BAD, BUT THINKING MAKES IT SO. W. SHAKESPEARE**
3. **CHALLENGES CAN BE STEPPING STONES OR STUMBLING BLOCKS. IT'S JUST A MATTER OF HOW YOU VIEW THEM.**
4. **IF YOU DON'T STAND FOR SOMETHING YOU'LL FALL FOR EVERYTHING.**
5. **YOU HAVE TO LEARN FROM OTHER PEOPLES'S MISTAKES-- YOU DON'T HAVE TIME TO DO THEM ALL YOURSELF.**
6. **DON'T BE AFRAID TO TAKE BIG STEPS. YOU CAN'T CROSS A CHASM IN TWO SMALL JUMPS.**
7. **ONE MAN WITH COURAGE IS A MAJORITY. A. JACKSON**
8. **EXCELLENCE IS NEVER AN ACCIDENT.**
9. **IT'S A FUNNY THING ABOUT LIFE; IF YOU REFUSE ANYTHING BUT THE BEST, YOU VERY OFTEN GET IT. SOMERSET MAUGHAN**
10. **WELL DONE IS BETTER THAN WELL SAID. B. FRANKLIN**
11. **IT'S NOT HOW FAR YOU FALL, BUT HOW HIGH YOU BOUNCE.**
12. **DON'T JUDGE THOSE WHO TRY AND FAIL. JUDGE ONLY THOSE WHO FAIL TO TRY.**
13. **HAPPINESS IS NOT AN ABSENCE OF PROBLEMS; BUT THE ABILITY TO DEAL WITH THEM.**
14. **SUCCESS IS GETTING WHAT YOU WANT. HAPPINESS IS LIKING WHAT YOU GET.**
15. **MOST PEOPLE ARE ABOUT AS HAPPY AS THEY MAKE UP THEIR MINDS TO BE. A. LINCOLN**
16. **WHEN YOU TELL THE TRUTH, YOU NEVER HAVE TO WORRY ABOUT YOUR LOUSY MEMORY.**
17. **HONESTY IS THE FIRST CHAPTER IN THE BOOK OF WISDOM. T. JEFFERSON**
18. **MANS MIND ONCE STRETCHED BY A NEW IDEA, NEVER REGAINS ITS ORIGINAL DIMENSION.**
19. **IMAGINATION IS MORE IMPORTANT THAN KNOWLEDGE. A. EINSTEIN**
20. **THE SMALLEST ACT OF KINDNESS IS WORTH MORE THAN THE GRANDEST INTENTION.**
21. **REAL GENEROSITY IS DOING SOMETHING NICE FOR SOMEONE WHO'LL NEVER FIND IT OUT.**
22. **IF YOU'RE LOOKING FOR A BIG OPPORTUNITY, SEEK OUT A BIG PROBLEM.**
23. **SUCCESS SEEMS TO BE LARGELY A MATTER OF HANGING IN AFTER OTHERS HAVE LET GO.**
24. **WE DO NOT SEE THINGS AS THEY ARE. WE SEE THINGS AS WE ARE.**
25. **NO ONE CAN MAKE YOU FEEL INFERIOR WITHOUT YOUR CONSENT.**
26. **THE CLOSEST WE COME TO PERFECTION IS WHEN WE WRITE OUR RESUMES.**
27. **FAILURE IS SUCCESS IF WE LEARN FROM IT.**
28. **THE ROAD TO SUCCESS IS NOT DOING ONE THING 100% BETTER, BUT DOING 100 THINGS 1% BETTER.**
29. **SUCCESS COMES BEFORE WORK ONLY IN THE DICTIONARY.**
30. **WE MAKE A LIVING BY WHAT WE GET, BUT WE MAKE A LIFE BY WHAT WE GIVE.**
31. **THERE IS NEVER A WRONG TIME TO DO THE RIGHT THING.**
32. **PEOPLE WHO ARE RESTING ON THEIR LAURELS ARE WEARING THEM ON THE WRONG END.**
33. **THE GREATEST IGNORANCE IS TO REJECT SOMETHING YOU KNOW NOTHING ABOUT.**
34. **A DIAMOND IS A CHUNK OF COAL THAT MADE GOOD UNDER PRESSURE.**
35. **TO TEACH IS TO LEARN AGAIN.**
36. **EVEN IF YOU'RE ON THE RIGHT TRACK, YOU'LL GET RUN OVER IF YOU JUST SIT THERE.**
37. **YOU NEVER GET A SECOND CHANCE TO MAKE A GOOD FIRST IMPRESSION.**
38. **PEOPLE DON'T CARE HOW MUCH YOU KNOW, UNTIL THEY KNOW HOW MUCH YOU CARE.**
39. **PEOPLE NEED LOVE ESPECIALLY WHEN THEY DON'T DESERVE IT.**
40. **THE PERSON WHO MAKES NO MISTAKES DOES NOT USUALLY MAKE ANYTHING.**

Conventions

Let us first set the conventions that are used throughout this manuscript. We use the mostly minus signature, so that when the metric is diagonalized it has the signature $(+---)$. An exception is made in chapter 5 where we adopt the opposite signature for the chameleon. Spacetime indices use the Greek alphabet, whereas space indices use the Latin alphabet. For an arbitrary expression X , the overbar \bar{X} denotes the part of X linear in perturbations. The superscript X^{NL} is the non-linear part of X , i.e. $X^{NL} \equiv X - \bar{X}$. The dot \dot{X} denotes the derivative of X with respect to time. Repeated Latin indices are to be summed, e.g. $X_{ii} = \delta^{ij} X_{ij}$. We define symmetrization of indices by $T_{\mu\nu} = \frac{1}{2}(T_{\mu\nu} + T_{\nu\mu})$. The speed of light and Planck's constant are set to unity $c = \hbar = 1$. We also define the Laplacian by D'Alembertian operator $\square \equiv \partial_\mu \partial^{\mu\nu} \equiv \partial_0^2 - \Delta$ where we have used the Laplacian $\Delta \equiv \partial_i \partial_i$.

With these conventions, the line-element for Minkowski space can be written as

$$ds^2 = \eta_{\mu\nu} dx^\mu dx^\nu = dt^2 - dx^2 - dy^2 - dz^2 \quad (1)$$

Otherwise, we use the conventions of Wald [28]. The Riemann and Einstein curvature tensors are given by

$$\begin{aligned} R^\mu{}_{\nu\alpha\beta} &= \partial_\alpha \Gamma^\mu{}_{\nu\beta} - \partial_\beta \Gamma^\mu{}_{\nu\alpha} + \Gamma^\mu{}_{\sigma\alpha} \Gamma^\sigma{}_{\nu\beta} - \Gamma^\mu{}_{\sigma\beta} \Gamma^\sigma{}_{\nu\alpha}, \\ G_{\mu\nu} &= R_{\mu\nu} - \frac{1}{2} g_{\mu\nu} R, \end{aligned} \quad (2)$$

where the Ricci tensor $R_{\mu\nu}$ is given by contracting the 1st and 3rd indices of the Riemann tensor $R_{\mu\nu} = R^\alpha{}_{\mu\alpha\nu}$, and the Ricci Scalar R is given by contracting the Ricci tensor $R^\alpha{}_\alpha$. The matter energy momentum tensor is defined by the matter action S_m as

$$T_{\mu\nu} = \frac{2}{\sqrt{-g}} \frac{\delta S_m}{\delta g^{\mu\nu}} \quad (3)$$

Some important terminology:

- **weak equivalence principle (WEP)** : All uncharged, freely-falling test particles follow the same trajectories, once an initial position and velocity have been prescribed.
- **Einstein equivalence principle (EEP)** : The **WEP** is valid, and furthermore, in all freely-falling frames one recovers (locally, and up to tidal gravitational forces) the same laws of special relativistic physics, independent of position or velocity.
- **strong equivalence principle (SEP)** : The **WEP** is valid for massive gravitating objects as well as test particles, and in all freely-falling frames one recovers (locally, and up to tidal gravitational forces) the same special relativistic physics, independent of position or velocity.

Chapter 1

General Relativity

Einstein's theory of general relativity has drastically changed our understanding of gravity. In searching for alternative theories of gravity, the point of reference is inevitably general relativity. In this preliminary chapter, we present Einstein's theory of general relativity and some of its key features. Given the importance of gravitational radiation in testing theories of gravity, we derive in detail the generation of gravitational waves. This chapter is based on discussions in [29, 30, 31, 28, 10, 7].

1.1 The field equations

Let us consider Einstein's theory of general relativity. General relativity can be summarized as follows [28]: Spacetime is a 4-dimensional manifold M on which a Lorentz metric $g_{\mu\nu}$ is defined. The curvature of $g_{\mu\nu}$ is related to the matter distribution in spacetime by Einstein's equation

$$G_{\mu\nu} \equiv R_{\mu\nu} - \frac{1}{2}Rg_{\mu\nu} = 8\pi G_N T_{\mu\nu}, \quad (1.1)$$

where $T_{\mu\nu}$ is the energy-momentum tensor of matter fields in spacetime, $G_{\mu\nu}$ is the Einstein tensor and G_N is Newton's constant. General relativity also assumes that the connection $\Gamma_{\mu\nu}^\rho$ satisfies the following two conditions:

- torsion-free : $\Gamma_{[\mu\nu]}^\rho = 0$;
- metric compatible : $\nabla_\rho g_{\mu\nu} = 0$.

These conditions ensure that the connection is unique and is given by

$$\Gamma_{\mu\nu}^\rho = \frac{1}{2}g^{\rho\sigma}(\partial_\mu g_{\nu\sigma} + \partial_\nu g_{\sigma\mu} - \partial_\sigma g_{\mu\nu}). \quad (1.2)$$

This unique connection is known by several names : the 'Christoffel' connection, the 'Levi-Civita' connection or sometimes the 'Riemannian' connection. A manifold endowed with a metric and a connection that is torsion-free and metric compatible is called a Riemannian manifold (or pseudo-Riemannian when

the metric has Lorentzian signature). An important property of Riemannian manifolds is that the Bianchi identities are always satisfied:

$$\nabla_\mu \left(R^{\mu\nu} - \frac{1}{2} g^{\mu\nu} R \right) = 0. \quad (1.3)$$

Equations (1.1) together with (1.3) imply that the energy-momentum tensor is always conserved,

$$\nabla^\mu T_{\mu\nu} = 0. \quad (1.4)$$

1.2 The action

From a field theory point of view, the field equations of general relativity (1.1) can be derived from an action,

$$S = S_{EH} + S_m, \quad (1.5)$$

where

$$S_{EH} = -\frac{1}{16\pi G_N} \int d^4x \sqrt{-g} R \equiv -\frac{M_{Pl}^2}{2} \int d^4x \sqrt{-g} R \quad (1.6)$$

is known as the Hilbert action or the Einstein-Hilbert action, Newton's constant G_N is related to the Planck mass M_{Pl} by $M_{Pl}^2 = 1/8\pi G_N$, and,

$$S_m = \int d^4x L_m(g_{\mu\nu}, \psi), \quad (1.7)$$

is the matter action. L_m is the Lagrangian density of the matter fields ψ . Variation of the action (1.5) with respect to the metric $\delta S/\delta g_{\mu\nu} = 0$ leads to the Einstein field equations (1.1), which we re-express as,

$$\mathcal{Q}^{GR}_{\mu\nu} \equiv G_{\mu\nu} - M_{Pl}^{-2} T_{\mu\nu}^m = 0 \quad (1.8)$$

where

$$T_{\mu\nu}^m \equiv \frac{2}{\sqrt{-g}} \frac{\delta S_m}{\delta g^{\mu\nu}}. \quad (1.9)$$

Riemannian geometry then tells us that at every point on the manifold there exists a tangent plane, which in cases with Lorentzian signature is taken to be Minkowski space. This allows us to recover special relativity at every point, up to the effects of second derivatives in the metric (i.e. tidal forces), so both the WEP and EEP are satisfied.

Birkhoff's Theorem: All spherically symmetric solutions of Einstein's equations in vacuum must be static and asymptotically flat.

While exact spherical symmetric and vacuums are not found in Nature, Birkhoff's theorem still provides deep insight into the gravitational field that surrounds an isolated mass. Given the asymptotic nature of gravitational fields, Birkhoff's theorem tells us that it makes sense to treat the weak-field treatment of general relativity as a perturbation around Minkowski space.

No-hair theorem: The generic final state of gravitational collapse is a Kerr-Newmann black hole, fully specified by its mass, angular momentum and charge.

1.3 Gravitational waves in weak-field gravity

Einstein's field equations are highly non-linear and exact solutions are rare. Bursts of gravitational radiation arise from collapsing phenomena, where gravity is strong and linear approximations cannot be applied. The full non-linear Einstein field equations must be solved to describe such strong field scenarios and our knowledge of these systems are limited.

To gain insight into the propagation of gravitational disturbances, it is therefore instructive to work in the approximation in which gravity is *weak*. In particular, the linearized theory is useful for displaying the wave nature of gravitational phenomena. Outside of the source, where the energy-momentum is naught, the transverse traceless gauge is introduced and the existence of two polarizations of gravitational waves is shown. Next, we discuss the generation of gravitational waves from sources where self-gravity may be important.

1.3.1 Linearized gravity

In weak-field gravity, we assume that

$$g_{\mu\nu} = \eta_{\mu\nu} + h_{\mu\nu}, \quad (1.10)$$

where $|h_{\mu\nu}| \ll 1$. In other words, deviations $h_{\mu\nu}$ of the metric $g_{\mu\nu}$ around Minkowski $\eta_{\mu\nu}$ are taken to be small. We mean by *linearized gravity* substitution of (1.10) into Einstein's field equations (1.8) and only retaining terms linear in metric perturbations $h_{\mu\nu}$.

In terms of the metric perturbation $h_{\mu\nu}$, the linear Einstein tensor is given by,

$$\bar{G}_{\mu\nu} = -\frac{1}{2}\square h_{\mu\nu} - \frac{1}{2}h_{,\mu\nu} + h_{\rho(\mu,\nu)}{}^\rho + \frac{1}{2}\eta_{\mu\nu} \left(\square h - h_{\alpha\beta,}{}^{\alpha\beta} \right). \quad (1.11)$$

Let us introduce the trace-reversed perturbation $\theta_{\mu\nu} \equiv h_{\mu\nu} - \frac{1}{2}h\eta_{\mu\nu}$. Its name is appropriate since $\theta = \eta^{\mu\nu}\theta_{\mu\nu} = -h$ where $h \equiv \eta^{\mu\nu}h_{\mu\nu}$ is the trace of the metric perturbation. Using this notation, the linear Einstein tensor becomes

$$\bar{G}_{\mu\nu} = -\frac{1}{2}\square\theta_{\mu\nu} + \theta_{\rho(\mu,\nu)}{}^\rho + \frac{1}{2}\eta_{\mu\nu}\theta_{\alpha\beta,}{}^{\alpha\beta} \quad (1.12)$$

The linear Einstein tensor $\bar{G}_{\mu\nu}$ can be simplified by taking advantage of the gauge freedom. A gauge transformation generated by the vector field ξ^a is

$$h_{\mu\nu} \rightarrow h_{\mu\nu} + \mathcal{L}_\xi h_{\mu\nu} \quad (1.13)$$

where the Lie derivative of the metric along ξ_a is $\mathcal{L}_\xi g_{ab} = 2\nabla_{(\alpha}\xi_{b)}$. In our context where the background metric is Minkowski and covariant derivatives become partial derivatives, we have

$$h_{\mu\nu} \rightarrow h_{\mu\nu} + 2\partial_{(\mu}\xi_{\nu)} \quad (1.14)$$

which represents the change of the metric perturbation under an infinitesimal diffeomorphism along the vector field ξ^μ . By solving

$$\square \xi_\mu = -\partial^\nu \theta_{\mu\nu}$$

for ξ^μ , we can make a gauge transformation such that

$$\partial^\nu \theta_{\mu\nu} = 0. \quad (1.15)$$

This choice of gauge, called the ‘harmonic’ gauge, is particularly useful in general relativity since it substantially simplifies the linear Einstein tensor, which becomes

$$\bar{G}_{\mu\nu} = -\frac{1}{2}\square\theta_{\mu\nu}. \quad (1.16)$$

Then the Einstein field equations can be rewritten as,

$$\square\theta_{\mu\nu} = -2M_{Pl}^{-2}T_{\mu\nu}. \quad (1.17)$$

and in vacuum,

$$\square\theta_{\mu\nu} = 0. \quad (1.18)$$

In other words, the linearized Einstein equation can be rewritten in terms of a wave equation with perturbations that travel at the speed of light $c = 1$.

1.3.2 Vacuum spacetimes

Let us first consider the propagation of gravitational disturbances in globally vacuum spacetimes, i.e. we assume that the linearized Einstein equations are valid everywhere in spacetime, and that the solutions are asymptotically flat. The source is therefore set to zero $T_{\mu\nu} = 0$ and we are interested in the linearized Einstein’s equations in vacuum (1.18). Notice that this situation is unrealistic in that we have not specified the source of the gravitational disturbances: a non-zero energy-momentum tensor is treated in the next subsection.

Eqs (1.15) and (1.18) describe a massless spin-2 field propagating in flat spacetime as initially proposed by Pauli and Fierz. In the linear approximation, general relativity therefore describes a theory of a massless spin-2 field. As stated by Wald [28], “The full theory of general relativity thus may be viewed as a massless spin-2 field which undergoes a non-linear self-interaction. It should be noted, however, that the notion of the mass and spin of a field require the presence of a flat background metric $\eta_{\mu\nu}$ which one has in the linear approximation but not in the full theory, so the statement that, in general relativity, gravity is treated as a massless spin-2 field is not one that can be given precise meaning outside the context of the linear approximation.”

The solution to the wave equation (1.18) is given by plane waves. It is possible to take advantage of a residual gauge freedom present in the harmonic gauge. We can choose ξ_a such that,

$$\begin{aligned} h &= 0, \\ h_{0i} &= 0. \end{aligned} \quad (1.19)$$

The gauge choice (1.15) together with (1.19) is called the **transverse-traceless (TT)** or the ‘radiation’ gauge. In this gauge, the trace-reversed metric and the metric perturbations are identical $\theta_{\mu\nu} = h_{\mu\nu}$. The metric perturbation is represented by a symmetric 4×4 tensor, so there are 10 independent variables. The **TT** gauge represents 8 conditions and reduces the number of independent variables from 10 down to 2 in the metric perturbation. By imposing the **TT** gauge, we therefore see that the metric perturbation contains only 2 propagating degrees of freedom.

1.3.3 Spacetimes with an isolated matter source

Let us now consider generation of gravitational waves from isolated matter sources, where the energy-momentum tensor is non-zero. We assume that the linearized Einstein equations are valid everywhere in spacetime, and that the solutions are asymptotically flat. Using Green’s function for the d’Alembertian operator \square , it is possible to solve the wave equation Eq. (1.17) in the harmonic gauge (1.15) in the slow motion limit. We assume that the source velocity is much smaller than the speed of light.

At first glance, the wave equation (1.17) is misleading since it suggests that all of the components of the metric satisfy the wave equation and are therefore propagating degrees of freedom. Actually, the metric perturbation contains:

- (i) gauge degrees of freedom;
- (ii) physical, propagating degrees of freedom, and;
- (iii) physical, non radiative components tied to the matter sources.

In four dimensional spacetime, there are 4 gauge degrees of freedom, 2 physical, propagating degrees of freedom which are contained in the *transverse-traceless projection* of the metric perturbations and satisfy the wave equation. There are 4 components which are physical but do not propagate and which satisfy Poisson equations [30].

1.3.4 Generation of gravitational waves

Let us now consider generation of gravitational waves from isolated matter sources, where the energy-momentum tensor is non-zero, but where self-energies may become important. We continue to assume that the solutions are asymptotically flat, but we no longer assume that the linearized Einstein’s equations are valid. Instead, we allow the metric perturbations to depend on the non-linear contributions coming from the Einstein tensor. Although slightly more complicated, we deliberately avoid casting the linearized equations into the trace-reversed metric and the harmonic gauge. Instead, we choose a gauge that provides insight into the propagating degrees of freedom.

To derive the equations governing the perturbations $h_{\mu\nu}$, we split Einstein’s equations (1.8) into linear and non-linear parts as follows

$$\bar{G}_{\mu\nu} = M_{Pl}^{-2} \tau_{\mu\nu}, \quad (1.20)$$

The expression for $\tau_{\mu\nu}$ reads

$$\tau_{\mu\nu} = T_{\mu\nu}^m - M_{Pl}^2 G_{\mu\nu}^{NL}. \quad (1.21)$$

This separation into linear and non-linear parts allows us to solve for $h_{\mu\nu}$ perturbatively in M_{Pl}^{-2} . The term $\tau_{\mu\nu}$ can be interpreted to be source terms for the linear equations at different orders in M_{Pl}^{-2} . They include contributions from both matter and non-linear gravitational fields of lower order.

We are interested in matter sources that are weakly self-gravitating, slowly moving and weakly stressed. These are known as **PN** sources [32]. For these systems, one has

$$v \sim |h_{00}^{1/2}| \sim \left| \frac{T_{0i}^m}{T_{00}^m} \right| \sim \left| \frac{T_{ij}^m}{T_{00}^m} \right|^{1/2} \ll 1, \quad (1.22)$$

where v is the typical three-velocity of the source. Thus, we can introduce v as a new parameter of expansion and consider the predictions of the theory at different orders in v , also known as **PN** orders. We content ourselves with the first **PN** corrections, which amounts to considering Eqs. (1.20) where the source terms also include **PN** corrections. In particular, the metric should be substituted by its first **PN** expression whenever it appears in the non-linear source terms.

This analysis is only suited for the first **PN** corrections. Beyond that, the analysis becomes more complicated due to the presence of tails and retardation effects. The correct treatment of the problem in general involves the separation into a near-zone and a wave-zone. In the near-zone, one can find the metric to any **PN** order including non-linearities and minimizing retardation effects. This corresponds to an expansion in the small parameter to desired order in v . In the wave zone, one can solve the equations of motion perturbatively in the fields and match the solution to the one found in the near-zone in a region where both approximations are valid [32, 31, 33, 34]. For the first **PN** corrections considered, this analysis reduces to the one outlined in the previous paragraph. For higher order corrections the matching is much less trivial [32, 31, 33, 35].

A straightforward calculation shows that $\partial^\mu \bar{G}_{\mu\nu} = 0$. By the linearized Einstein equations (1.20), we therefore have the following conservation relation for the source tensor $\tau_{\mu\nu}$

$$\partial^\mu \tau_{\mu\nu} = 0. \quad (1.23)$$

Irreducible parameterization

To extract the physical degrees of freedom contained in the metric perturbation $h_{\mu\nu}$, we start by decomposing $h_{\mu\nu}$ into irreducible representations of $SO(3)$ [36, 30],

$$\begin{aligned} h_{00} &= 2\phi, & h_{0i} &= -\frac{\partial_i}{\sqrt{\Delta}} B + V_i, \\ h_{ij} &= t_{ij} + 2\partial_{(i} F_{j)} + 2\frac{\partial_i \partial_j}{\Delta} E + 2\left(\delta_{ij} - \frac{\partial_i \partial_j}{\Delta}\right) \psi, \end{aligned} \quad (1.24)$$

with constraints $t_{ii} = \partial_i t_{ij} = \partial_i V_i = \partial_j F_j = 0$. A priori, there are 16 free functions in the parametrization for the metric perturbation fields (1.24): a symmetric tensor t_{ij} (6 functions), transverse vectors V_i, F_i , (3 + 3 functions) and scalars ϕ, B, F, ψ (4 functions). There are 6 constraints so the number of independent variables in the metric parameterization is 10, consistent with a 4×4 symmetric tensor.

Let us study the linearized equations of motion (1.8) in terms of this irreducible decomposition.

Tensors

To single out the tensorial part of the equations of motion, we introduce the transverse-traceless projector $P_{ij,kr}$ and the transverse projector P_{ij}

$$P_{ij,kr} \equiv P_{ik}P_{jr} - \frac{1}{2}P_{ij}P_{kr}, \quad P_{ij} \equiv \delta_{ij} - \frac{\partial_i \partial_j}{\Delta}. \quad (1.25)$$

Applying the projector $P_{ij,kr}$ to \mathcal{Q}^{GR}_{kr} yields

$$P_{ij,kr} \mathcal{Q}^{GR}_{kr} \equiv -\frac{1}{2}P_{ij,kr}(\partial_0^2 - \Delta)h_{kr} - 2M_b^{-2}\tau_{kr} = 0.$$

leading to the wave equation for the tensor modes

$$\square t_{ij} \equiv (\partial_0^2 - \Delta)t_{ij} = -2M_b^{-2}P_{ij,ks}\tau_{ks}, \quad (1.26)$$

Vectors

Consider now the vectorial part of the linearized field equations. One finds

$$\begin{aligned} P_{ij} \mathcal{Q}_{0j}^{GR} &= \frac{1}{2}\Delta (V_i - \dot{F}_i) - M_b^{-2}P_{ij}\tau_{j0} = 0, \\ P_{ik}\partial_j \mathcal{Q}_{kj}^{GR} &= \frac{1}{2}\Delta (\dot{V}_i - \ddot{F}_i) - M_b^{-2}P_{ik}\partial_j\tau_{kj} = 0. \end{aligned} \quad (1.27)$$

Notice that the time derivative of the first equation is related to the second equation.

Scalars

For the scalar sector of the equations, the non-redundant equations of motion derived from Eq. (1.20) are,

$$\begin{aligned} \mathcal{Q}_{00}^{GR} &= 2\Delta\psi - M_0^{-2}\tau_{00} = 0, \\ \mathcal{Q}_{ii}^{GR} &= 2\left(2\ddot{\psi} - \Delta\psi + \ddot{E} + \sqrt{\Delta}\dot{B} + \Delta\phi\right) - M_0^{-2}\tau_{ii} = 0, \end{aligned} \quad (1.28)$$

Choosing the gauge

Of the 10 independent variables contained in the metric perturbation $h_{\mu\nu}$, it is not yet obvious which ones are the physical degrees of freedom. We saw in 1.3.1 that the usual choice of gauge in *vacuum* general relativity is the Lorentz gauge, $\partial^\mu \theta_{\mu\nu} = 0$ where $\theta_{\mu\nu} = h_{\mu\nu} - \frac{1}{2}h\eta_{\mu\nu}$ is the trace-reversed metric. The residual gauge is then exploited further allows us to impose $\theta_{0i} = 0$ and $\theta = 0$. When matter sources are present, the residual gauge cannot be exploited to set $\theta_{0i} = 0$ and $\theta = 0$. It is possible to choose the Lorentz gauge [10], but for the sake of illustration, we use the following unusual gauge choice [22, 37],

$$h_{kk} = 0, \quad h_{0i,i} = 0, \quad h_{i[j,k]i} = 0. \quad (1.29)$$

In terms of the irreducible decomposition (1.24), the gauge choice is equivalent to the following conditions on the components,

$$F_k = 0, \quad B = 0, \quad E + 2\psi = 0. \quad (1.30)$$

This choice represents 4 conditions and fixes the gauge degrees of freedom. This choice is accessible by choosing the vector field ξ_μ in the gauge transformation (1.14) to satisfy

$$\xi_0 = \frac{1}{\sqrt{\Delta}}B + \frac{2}{\Delta}\dot{E} + \frac{4}{\Delta}\dot{\psi}, \quad \xi_i = -\frac{\partial_i}{\sqrt{\Delta}}(2E + 4\psi) - F_i. \quad (1.31)$$

With this gauge choice, the physical degrees of freedom are contained in the following expressions,

$$\begin{aligned} \square t_{ij} &= -2M_{Pl}^{-2}P_{ij,ks}\tau_{ks}, \\ \Delta V_i &= -2M_{Pl}^{-2}P_{ij}\tau_{j0}, \\ \Delta\psi &= \frac{1}{2}M_{Pl}^{-2}\tau_{00}, \\ \Delta(\phi - \psi) &= \frac{1}{2}M_{Pl}^{-2}\tau_{ii}. \end{aligned} \quad (1.32)$$

The first of these equations is a wave equation for the transverse-traceless tensor t_{ij} traveling at the speed of light $c = 1$ and contains 2 propagating degrees of freedom. The remaining equations are Poisson equations for V_i , ψ and ϕ and represent 4 non-propagating physical degrees of freedom.

Far-zone expressions and post-Newtonian approximation

The equations of motion (1.32) contain two types of equations to be solved, Poisson and wave equations. The Poisson equation is of the form

$$\Delta\xi(t, x) = -4\pi\rho(t, x),$$

whose solution for vanishing boundary conditions at infinity is given by

$$\xi(t, x) = \int d^3\tilde{x} \frac{\rho(t, \tilde{x})}{|x - \tilde{x}|}.$$

We assume that the isolated source of GWs can be confined within a sphere of radius R . At distances far away from the source, $r \equiv |x| \gg R$, we can perform the expansion ($\hat{\mathbf{r}}^i = x^i/r$)

$$|x - \tilde{x}| = r - \hat{\mathbf{r}}^i \tilde{x}^i + r O(R/r)^2. \quad (1.33)$$

We refer to this zone as the ‘‘far-zone’’. The leading contribution of the solution to the Poisson equation at large distances is then

$$\xi_f(t, x) = \frac{1}{r} \int d^3 \tilde{x} \rho(t, \tilde{x}). \quad (1.34)$$

The sourced wave equations are of the form

$$(c_\sigma^{-2} \partial_0^2 - \Delta) \sigma(t, x) = 4\pi \mu(t, x), \quad (1.35)$$

with speed of propagation c_σ . The solution to this equation with radiation boundary conditions is given by (see, e.g. [31])

$$\sigma(t, x) = \int d^3 \tilde{x} \frac{\mu(t - |x - \tilde{x}|/c_\sigma, \tilde{x})}{|x - \tilde{x}|}. \quad (1.36)$$

where $t_r \equiv t - |x - \tilde{x}|/c_\sigma$ is the *retarded time*. We see then that the disturbance of the field σ at (t, x) is influenced by the energy and momentum sources at the point $(t_r, x - \tilde{x})$ on a past light cone. Besides adopting the far-zone approximation and using (1.33), we also assume that r is such that $r \gg \omega R^2/c_\sigma$, where ω is the largest characteristic frequency of the source. This allows us to write the leading contribution as

$$\begin{aligned} \sigma_f(t, x) &= \frac{1}{r} \int d^3 \tilde{x} \mu(t - r/c_\sigma + \hat{\mathbf{r}}^i \tilde{x}^i/c_\sigma, \tilde{x}) \\ &= \frac{1}{r} \sum_{n=0}^{\infty} \frac{1}{n!} \partial_0^n \int d^3 \tilde{x} \mu(t - r/c_\sigma, \tilde{x}) (\hat{\mathbf{r}}^i \tilde{x}^i/c_\sigma)^n, \end{aligned} \quad (1.37)$$

where the last identity holds formally. This expression can be simplified further for the PN sources of interest [10, 32, 38]. Thus, for a typical velocity $v \sim \omega R$ of the source, the sum in Eq. (1.37) represents a well-defined expansion in the small parameter,

$$v \ll 1,$$

i.e. it is a PN expansion, cf. Eq. (1.22). In other words, every time derivative in the near zone represents an extra $O(v)$.

The source: conservation properties

Eqs. (1.37) and (1.34) indicate that we need to evaluate various integrals of $\tau_{\mu\nu}$. By virtue of (1.23), we have the following useful integral conservation relations for the source $\tau_{\mu\nu}$,

$$\int d^3 x \tau_{ij} = \frac{1}{2} \int d^3 x \ddot{\tau}_{00} x^i x^j, \quad (1.38a)$$

$$\int d^3 x \dot{\tau}_{0i} x^j = - \int d^3 x \tau_{ij}, \quad (1.38b)$$

$$\int d^3 x \dot{\tau}_{00} x^i = - \int d^3 x \tau_{i0}, \quad (1.38c)$$

where we have neglected boundary terms since we are dealing with isolated sources.

Wave forms in the far-zone

We are now ready to compute the explicit form of the wave solutions in the far-zone. For the tensor and vector modes, the solutions of Eqs. (1.32) are

$$t_{ij}(t, x) = -\frac{1}{4\pi M_{Pl}^2 r} \hat{\mathbf{P}}_{ij,ks} \ddot{Q}_{ks}(t - r/c_t), \quad (1.39a)$$

$$V_i(t, x) = -\frac{c_t^2}{2\pi M_{Pl}^2} \left(\frac{1}{r} \int d^3 \tilde{x} P_{ij} \tau_{j0}(t, \tilde{x}) \right), \quad (1.39b)$$

where

$$Q(t)_{ij} \equiv I(t)_{ij} - \frac{1}{3} \delta_{ij} I_{kk}(t), \quad I_{ij}(t) \equiv \int d\tilde{x} \tau_{00}(t, \tilde{x}) \tilde{x}^i \tilde{x}^j, \quad (1.40)$$

The quantity Q_{ij} represents the quadrupole of τ_{00} . Note that in the far-zone, the transverse projector P_{ij} of Eq. (1.25) can be substituted by the transverse part of the algebraic projector,

$$\hat{\mathbf{P}}_{ij} \equiv \delta_{ij} - \hat{\mathbf{r}}^i \hat{\mathbf{r}}^j.$$

This substitution is valid up to $O(R/r)$ terms. The object $\hat{\mathbf{P}}_{ij,ks}$ is defined as

$$\hat{\mathbf{P}}_{ij,kr} \equiv \hat{\mathbf{P}}_{ik} \hat{\mathbf{P}}_{jr} - \frac{1}{2} \hat{\mathbf{P}}_{ij} \hat{\mathbf{P}}_{kr}.$$

Ultimately we are interested in calculating the radiation loss due to the radiation of gravitational wave. Static contributions to the wave solutions are ignored. Moreover, the scalar and vector parts that satisfy Poisson equations can be neglected. To see this, consider the vector part. The previous expression yields

$$\dot{h}_{0i} = \dot{V}_i = -\frac{c_t^2}{2\pi M_{Pl}^2} \left(\frac{1}{r} \int d^3 \tilde{x} P_{ij} \dot{\tau}_{j0}(t, \tilde{x}) \right) \quad (1.41)$$

where we have neglected static contributions. From the conservation law (1.23), this term can be expressed as the integration over the boundary of the transverse component of the source, which cancels away from the source, so we can neglect the vector perturbations altogether. The same argument applies to ϕ and ψ .

1.4 A PN technique - NRGR

In this section, we give an introduction to calculating PN corrections using NRGR, a technique based on the effective field theory (EFT) formulation of the slow-motion, weak-field sources. This applies to the slow inspiral phase of compact binary stars i.e. with neutron star (NS) or black hole (BH) constituents. It provides a systematic approach to calculating PN corrections to the bound and radiative systems.

Developed by Goldberger and Rothstein, the method was first presented in [23] and has been developed to include spin, higher orders, arbitrary spacetime dimensions and extreme mass ratios [39, 40, 41, 42] to mention a few. Similar EFT techniques had already been developed to calculate PN corrections in the context of scalar-tensor theories [21, 43]. NRGR’s novelty lies in that it provides a straightforward framework with which to calculate PN corrections at a given order, called power-counting, identifying the conservative and the radiative sectors of the system to any order. It conveniently abolishes the need for zones which is prevalent in the usual analytical techniques [44, 10, 32].

Many scales are involved given the nature of a coalescing binary system, from the minute size of the source’s internal structure to the long wavelength of gravitational waves emitted. In order to obtain post-Newtonian corrections, which are corrections to Newton’s potential in powers of 3-velocity v , Golberger and Rothstein provide a consistent way to keep track of these powers. To do so, we must clearly separate these different scales which may have different contributions in powers of v . Let’s go through the steps outlined by Goldberger and Rothstein which allow for this separation of scales.

Consider a (binary) system of gravitating bodies of total mass m and separated by a distance r . During the inspiral of the binary system, the motion of the bodies can be considered to be non-relativistic and slow-moving so that the relative 3-velocity $v \ll 1$. In a system that is described to a good approximation by Newtonian interaction, notice that these parameters r , m and v are interdependent. By the virial theorem,

$$v^2 \sim \frac{G_N m}{r} \quad (1.42)$$

Also notice that the typical angular momentum of the system is given by

$$L = mvr. \quad (1.43)$$

Neglecting spin and finite-size effects, the starting point of the EFT method is a theory of point particles coupled to Einstein gravity:

$$\begin{aligned} S &= S_{EH} + S_{pp} \\ S_{EH} &= -2M_{Pl}^2 \int d^4x \sqrt{-g} R(x) \\ S_{pp} &= - \sum_a m_a \int d\tau_a \end{aligned} \quad (1.44)$$

where $a = 1, 2$ labels the bodies for a binary system and $d\tau_a = \sqrt{g_{\mu\nu}(x_a) dx_a^\mu dx_a^\nu}$ is the a th body’s proper time.

The metric is expanded around flat space as follows

$$g_{\mu\nu} = \eta_{\mu\nu} + \kappa_g h_{\mu\nu}, \quad (1.45)$$

where $\kappa_g = 1/M_{Pl}$ is the gravitational coupling. With this expansion around Minkowski, the first thing to notice is that the proper time can be expanded as follows:

$$d\tau = dt \left[1 - \frac{1}{2}v^2 + \frac{1}{2} \frac{h_{00}}{M_{Pl}} + \frac{h_{0i}}{M_{Pl}} v^i + \dots \right]. \quad (1.46)$$

So far, the graviton that we have considered $h_{\mu\nu}$ is fully relativistic since it does not yet distinguish between gravitons that bind the system together (through the gravitational potential) from the gravitons that are emitted as gravitational radiation. The next step is to then separate this fully relativistic graviton $h_{\mu\nu}$ into two parts

$$h_{\mu\nu}(x) = \bar{h}_{\mu\nu}(x) + H_{\mu\nu}(x) \quad (1.47)$$

where $\bar{h}_{\mu\nu}$ and $H_{\mu\nu}$ represent ‘radiation’ and the ‘potential’ gravitons respectively. To ensure homogeneous scaling in v , the graviton can be split into two regions of momenta as follows.

- *Potential Gravitons.* The forces between the two bodies separated by a distance r are mediated by the potential gravitons whose momentum k^μ scales as ($k^0 \sim v/r, |\mathbf{k}| \sim 1/r$). In the language of [EFT](#), these potential gravitons are off-shell and can only appear as internal lines. But the potential graviton still contains two very different scales: hard momenta $\mathbf{k} \sim 1/r$ and long wavelengths $x_\mu \sim r/v$. To further untangle the scales, it is useful to work with a Fourier transformation of the potential gravitons instead:

$$H_{\mu\nu}(x) = \int \frac{d^3\mathbf{k}}{(2\pi)^3} e^{i\mathbf{k}\cdot\mathbf{x}} H_{\mathbf{k}\mu\nu}(x_0) \quad (1.48)$$

so that all derivatives on fields scale according to $\partial_\mu \sim v/r$.

- *Radiation Gravitons.* Gravitational waves, on the other hand, consist of ‘radiation’ gravitons whose momentum scales as ($k^0 \sim v/r, |\mathbf{k}| \sim v/r$). In the language of [EFT](#), these gravitons are on-shell. Again to ensure homogenous scaling in v , the radiation gravitons are multipole expanded around \mathbf{X} :

$$\bar{h}_{\mu\nu}(x^0, \mathbf{x}) = \bar{h}_{\mu\nu}(x^0, \mathbf{X}) + \delta x_i \partial_i \bar{h}_{\mu\nu}(x^0, \mathbf{X}) + \frac{1}{2} \delta x_i \delta x_j \partial_i \partial_j \bar{h}_{\mu\nu}(x^0, \mathbf{X}) + \dots \quad (1.49)$$

where $\delta \mathbf{x} = \mathbf{x} - \mathbf{X}$ and \mathbf{X} is chosen to be the center of mass $\mathbf{X} = \frac{1}{m} \sum_a m_a \mathbf{x}_a = 0$, $m = \sum_a m_a$.

The following table is useful for counting powers of v related to different quantities:

\mathbf{k}	$H_{\mu\nu}^{\mathbf{k}}$	$\bar{h}_{\mu\nu}$	m/M_{Pl}
$1/r$	$r^2 v^{1/2}$	v/r	$\sqrt{L}v$

Using the separation of scales as outlined by equations (1.45), (1.46) and (1.47), the action (1.44) can be expressed in terms of velocity v , and potential and radiation gravitons $\bar{h}_{\mu\nu}$ and $H_{\mathbf{k}\mu\nu}(x^0 \equiv t)$, each with distinct scaling in terms of velocity. The resulting terms in this expanded action can be represented with a diagram, the building blocks of Feynman diagrams. In this way, it is possible to build Feynman diagrams with clear power counting rules in terms of v . For a classical system, whose angular momentum $L \gg \hbar$, only tree diagrams contribute.

In the following paragraphs, we summarize the basic [NRGR](#) results with their respective diagrams. A mass moving along its worldline is represented by a solid line. Dashed lines represent the exchange of potential gravitons $H_{\mathbf{k}\mu\nu}$. Curly lines represent radiation gravitons $\bar{h}_{\mu\nu}$. For details, see [23, 24].

$$\begin{aligned}
S_{EH} &= (\text{wiggly line})^{-1} + \text{wiggly line} + \text{wiggly line} + \dots \\
S_{pp} &= \text{wiggly line} + \text{wiggly line} + \text{wiggly line} + \dots
\end{aligned}$$

Figure 1.1: The action schematically expanded in powers of $h_{\mu\nu}$ (represented here by a wiggly line).

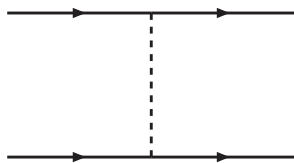


Figure 1.2: The diagram that contributes to the Newtonian potential and scales as Lv^0 .

The bound system. Using standard techniques in quantum field theory, the effective Lagrangian built by collecting appropriate terms in powers of v reproduces the classical Lagrangian that is usually derived from general relativity to find the [PN](#) expansion. To see this for the bound system, first notice that the Newtonian potential is given by the diagram in [fig. 1.2](#).

$$\begin{aligned}
\text{Fig. (1.2)} &= \frac{im_1m_2}{8M_{Pl}^2} \int dt_1 dt_2 \delta(t_1 - t_2) \int_{\mathbf{k}} \frac{1}{\mathbf{k}^2} e^{-i\mathbf{k}\cdot(\mathbf{x}_1 - \mathbf{x}_2)} \\
&= i \int dt \frac{G_N m_1 m_2}{|x_1(t) - x_2(t)|}
\end{aligned} \tag{1.50}$$

where $\int_{\mathbf{k}} \equiv \int \frac{d^3k}{(2\pi)^3}$. The δ -function comes from the potential graviton propagator and has the effect of making the graviton exchange simultaneous. Notice that the Newtonian potential scales as the orbital angular momentum $L = mvr$. We then expect Post-Newtonian corrections to the Newtonian potential to carry extra powers of velocity.

Collecting terms that scale as Lv^2 , we obtain the 1 [PN](#) correction to the New-

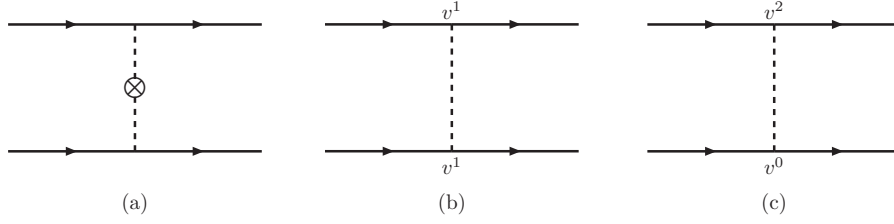


Figure 1.3: Diagrams that contribute to the EIH Lagrangian and scale as Lv^2 . The \otimes denotes the insertion of the potential graviton kinetic term.

tonian potential as shown in figures 1.3 and 1.4.

$$\begin{aligned}
 \text{Fig. (1.3)a} &= \frac{i}{2} \int dt \frac{G_N m_1 m_2}{|x_1(t) - x_2(t)|} \\
 \text{Fig. (1.3)b} &= -4i \int dt \frac{G_N m_1 m_2}{|x_1(t) - x_2(t)|} (\mathbf{v}_1 \cdot \mathbf{v}_2) \\
 \text{Fig. (1.3)c} &= \frac{3i}{2} \int dt \frac{G_N m_1 m_2}{|x_1(t) - x_2(t)|} \mathbf{v}_1^2 \\
 \text{Fig. (1.4)a} &= -i \int dt \frac{G_N^2 m_1 m_2^2}{|x_1(t) - x_2(t)|^2} \\
 \text{Fig. (1.4)b} &= \frac{i}{2} \int dt \frac{G_N^2 m_1 m_2^2}{|x_1(t) - x_2(t)|^2}
 \end{aligned} \tag{1.51}$$

Summing the contributions from these diagrams, including their mirror images under the exchange of the labels of the massive bodies $1 \leftrightarrow 2$ and the relativistic corrections to the kinetic energy of the point particles, we obtain the effective Lagrangian at PN:

$$\begin{aligned}
 L_{EIH} &= \frac{1}{8} m_1 \mathbf{v}_1^4 + \frac{1}{8} m_2 \mathbf{v}_2^4 \\
 &+ \frac{G_N m_1 m_2}{2|\mathbf{x}_1 - \mathbf{x}_2|} \left(3(\mathbf{v}_1^2 + \mathbf{v}_2^2) - 7\mathbf{v}_1 \cdot \mathbf{v}_2 - \frac{(\mathbf{x}_{12} \cdot \mathbf{v}_1)(\mathbf{x}_{12} \cdot \mathbf{v}_2)}{|\mathbf{x}_1 - \mathbf{x}_2|^2} - \frac{G_N(m_1 + m_2)}{|\mathbf{x}_1 - \mathbf{x}_2|} \right)
 \end{aligned} \tag{1.52}$$

This Lagrangian describes the correction to Newtonian motion between two bodies, coming from general relativity, and was first derived in 1937 by [Einstein, Infeld and Hoffmann \(EIH\)](#).

In general, the n^{th} PN correction to the Newtonian potential is found by collecting Feynman diagrams that scale as Lv^{2n} .

The radiative system. In the center-of-mass frame $\bar{h}_{\mu\nu} \equiv \bar{h}_{\mu\nu}(x^0, \mathbf{X})$ and by requiring gauge invariance under infinitesimal coordinate transformations,



Figure 1.4: Diagrams that contribute to the EIH Lagrangian and scale as Lv^2 .

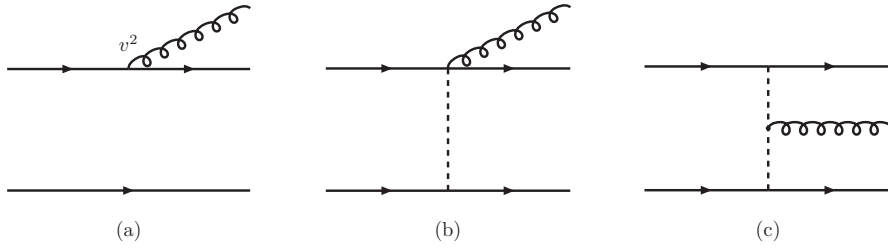


Figure 1.5: Diagrams that contribute to the radiation action and scale as $L^{1/2}v^{5/2}$. The optical theorem leads to the quadrupole formula. Note that the three-graviton vertex already contributes at this order.

the leading order processes can be determined from the following Lagrangian:

$$\begin{aligned}
L = & \frac{1}{2} \sum_a m_a \mathbf{v}_a^2 + \frac{G_N m_1 m_2}{|\mathbf{x}_1 - \mathbf{x}_2|} - \frac{m}{2M_{Pl}} \bar{h}_{00} \\
& - \frac{\bar{h}_{00}}{2M_{Pl}} \left[\frac{1}{2} \sum_a m_a \mathbf{v}_a^2 - \frac{G_N m_1 m_2}{|\mathbf{x}_1 - \mathbf{x}_2|} \right] \\
& - \frac{1}{2M_{Pl}} \epsilon_{ijk} \mathbf{L}_k \partial_j \bar{h}_{0i} + \frac{1}{2M_{Pl}} \sum_a m_a \mathbf{x}_{ai} \mathbf{x}_{aj} R_{0i0j},
\end{aligned} \tag{1.53}$$

where $\mathbf{L} = \sum_a m_a \mathbf{x}_a \times \mathbf{v}_a$ is the angular momentum. Of the terms in this Lagrangian, only the coupling of the (linearized) Riemann tensor to the moment $I_{ij} = \sum_a m_a \mathbf{x}_{ai} \mathbf{x}_{aj}$ gives rise to gravitational radiation. Other terms in this Lagrangian cannot radiate because they couple to conserved quantities.

More explicitly, the diagrams that contribute to gravitational radiation at leading order scale as $L^{1/2}v^{5/2}$, and are shown in fig.(1.5). They have the following contributions,



Figure 1.6: Self-energy diagram that leads to the quadrupole formula.

$$\begin{aligned}
\text{Fig. (1.5)a} &= -\sum_a \frac{m_a}{2M_{Pl}} \left(\frac{1}{2} \bar{h}_{00} \mathbf{v}_a^2 + \frac{1}{2} \mathbf{x}_{ai} \mathbf{x}_{aj} \partial_i \partial_j \bar{h}_{00} + 2 \mathbf{x}_{ai} \mathbf{v}_{aj} \partial_i \bar{h}_{0j} + \bar{h}_{ij} \mathbf{v}_{ai} \mathbf{v}_{aj} \right) \\
\text{Fig. (1.5)b} &= -\frac{i}{2M_{Pl}} \int dx^0 \frac{G_N m_1 m_2}{|\mathbf{x}_1 - \mathbf{x}_2|} \bar{h}_{00} \\
\text{Fig. (1.5)c} &= \frac{i}{M_{Pl}} \int dx^0 \left(\frac{3G_N m_1 m_2}{2|\mathbf{x}_1 - \mathbf{x}_2|} \bar{h}_{00} - \frac{1}{2} \sum_a m_a \mathbf{x}_{ai} \ddot{\mathbf{x}}_{aj} \bar{h}_{ij} \right).
\end{aligned} \tag{1.54}$$

Adding together the diagrams in fig. (1.5) with mirror images under particle exchange yields the radiation Lagrangian :

$$\begin{aligned}
L_{v^{5/2}} &= -\frac{\bar{h}_{00}}{2M_{Pl}} \left(\frac{1}{2} \sum_a m_a \mathbf{v}_a^2 - \frac{G_N m_1 m_2}{|\mathbf{x}_1 - \mathbf{x}_2|} \right) \\
&\quad - \frac{1}{2M_{Pl}} \epsilon_{ijk} \mathbf{L}_k \partial_j \bar{h}_{0i} + \frac{1}{2M_{Pl}} I_{ij} R_{0i0j}^{(1)}
\end{aligned} \tag{1.55}$$

where the Riemann tensor to linear order $R_{0i0j}^{(1)}$ is

$$R_{0i0j}^{(1)} = \frac{1}{2M_{Pl}} (\partial_0 \partial_i h_{0j} + \partial_0 \partial_j h_{0i} - \partial_0^2 h_{ij} - \partial_i \partial_j h_{00}) \tag{1.56}$$

At this order, \bar{h}_{00} and \bar{h}_{0i} couple respectively to the Newtonian gravitational energy of the bound system and the orbital angular momentum, both of which are constants of motion. Consequently, \bar{h}_{00} and \bar{h}_{0i} do not radiate. Only the Riemann tensor $R_{0i0j}^{(1)}$ coupled to the moment I_{ij} can lead to gravitational radiation.

To determine the power radiated in gravitational waves according to the optical theorem, we must calculate the imaginary part of the self-energy diagram in fig. (1.6).

$$\begin{aligned}
\text{Fig. (1.6)} &= \frac{1}{8M_{Pl}^2} \int dx_1^0 dx_2^0 I_{ij}(x_1^0) I_{kl}(x_2^0) \times \langle R_{0i0j} R_{0k0l} \rangle \\
&= -\frac{1}{80M_{Pl}^2} \int_k \frac{k_0^4}{k^2 + i\epsilon} |Q_{ij}(k_0)|^2
\end{aligned} \tag{1.57}$$

where the two-point function of the Riemann tensor is proportional to the projection operator $\frac{1}{2} (\delta_{ik} \delta_{jl} + \delta_{il} \delta_{jk} - \frac{2}{3} \delta_{ij} \delta_{kl})$ and $Q_{ij} = \sum_a m_a \mathbf{x}_{ai} \mathbf{x}_{aj}$ is the

quadrupole moment and $Q_{ij}(k_0)$ is its Fourier transform [41].

$$\text{Im}S_{eff} = -\frac{1}{80M_{Pl}^2} \int \frac{d^3\mathbf{k}}{(2\pi)^2 2|\mathbf{k}|} \mathbf{k}^4 |Q_{ij}(|\mathbf{k}|)|^2 \quad (1.58)$$

The integrand gives the differential graviton emission rate along the evolution of the system. Multiplying by $|\mathbf{k}|$ and integrating over all momenta leads to the total power radiated in gravitational waves

$$P = \frac{G_N}{5} \langle \ddot{Q}_{ij} \ddot{Q}_{ij} \rangle \quad (1.59)$$

We thus obtain quadrupole formula, the leading order power loss. Note that there are other approaches to calculating the quadrupole formula for a localized source, which make use of near, wave and far zones, see e.g. [44, 10].

For later reference, we recall the power formula evaluated for binaries in elliptical orbit around each other [45, 31],

$$P = \frac{32G_N^4 \mu^2 m^3}{5a^5} f(e) \quad (1.60)$$

with

$$f(e) = \frac{1}{(1-e^2)^{7/2}} \left(1 + \frac{73}{24}e^2 + \frac{37}{96}e^4 \right) \quad (1.61)$$

where e is the eccentricity of the orbit ($e = 0$ corresponds to circular orbits).

Chapter 2

Modified Gravity

Gravitational phenomena such as the expansion of the Universe, the formation of structure in the Universe, and the propagation of gravitational waves, are all believed to be governed by Einstein’s field equations. There are two issues, however, that prevent us from fully embracing general relativity. Firstly, general relativity is thought to be inadequate at the quantum level. Secondly, the need to introduce matter-energy components that can only be detected gravitationally may indicate a poor understanding of gravity at scales beyond the size of our solar system.

This chapter aims to provide a basis for constructing a theory of gravity. We discuss the tests that have shaped our understanding of gravity. Celestial bodies have guided us in our understanding of Nature and of gravity. Laser beams sent from the Earth and reflected back by mirrors on the Moon provide valuable information about how the Moon and the Earth fall towards the Sun. Careful monitoring of the Hulse-Taylor binary system for over twenty years revealed that they are orbiting closer and closer towards each other due to emission of gravitational radiation, in perfect agreement with the energy loss predicted by general relativity. These are just two of the many experiments that have been developed over the years to test theories of gravitation.

We start by reviewing the tests of the Equivalence Principles. We discuss the experimental bounds the foundational tests and the importance of metric theories of gravitation. The most relevant Solar System tests are presented. The [PPN](#) formalism, a milestone in testing theories of gravitation and the constraints on its parameters, is also reviewed. Gravitational radiation is a powerful tool in testing theories of gravitation since it also has the potential to test the strong-field regime of a theory. In discussing gravitational radiation, we only consider the weak-field regime and present the standard steps used to determine the radiation formula for a given theory of gravity. Cosmological tests are also possible but are not pursued in this manuscript.

We adopt here the definition of Modified Gravity of [7], “General relativity refers to a theory that simultaneously exhibits general covariance, universal couplings to all matter fields, as well as satisfying Einstein’s field equations. Modified Gravity then refers to any modification of these properties.” [Table 2.1](#)

FOUNDATIONS		
WEP	Eötvös [46]	$\eta \lesssim 0.3 \times 10^{-13}$
EEP	Hughes-Dever [47]	$n \leq 10^{-27} m$
SOLAR-SYSTEM TESTS		
Null-like	Deflection of Light [48]	$\theta \simeq (0.99992 \pm 0.00023) \times 1.75''$
	Shapiro Time Delay [49]	$\Delta t = (1.00001 \pm 0.00001) \Delta t_{GR}$
Time-like	Mercury Perihelion [50, 51]	$\Delta\omega \simeq 42.969'' \pm 0.052''$
	Nordtvedt Effect (SEP) [52]	$\eta = (-1.0 \pm 1.4) \times 10^{-13}$
PPN FORMALISM [10, 11]		
Parameter	Limit	Effect
$\beta^{PPN} - 1$	$(1.2 \pm 1.1) \times 10^{-4}$	Nordtvedt effect
$\gamma^{PPN} - 1$	$(2.1 \pm 2.3) \times 10^{-5}$	Shapiro time delay
ξ^{PPN}	10^{-3}	Ocean Tides [53, 10]
α_1^{PPN}	10^{-4}	Lunar laser ranging [54]
α_2^{PPN}	4×10^{-7}	Alignment of the Sun's spin axis with the ecliptic [55]
α_3^{PPN}	4×10^{-20}	Pulsar acceleration [56]
GRAVITATIONAL RADIATION		
Direct detection	Propagation speed Polarity	GWOs
Indirect detection	Binary pulsars	Hulse-Taylor Binary [57, 58] Double Binary [59]

Table 2.1: This table summarizes different ways of testing theories of gravity with experiment discussed in Chapter 2, coming from foundational considerations, solar system tests, the parametrized post-Newtonian formalism and gravitational radiation.

summarizes the tests that is presented in this Chapter.

2.1 Foundations

The equivalence principles are believed to be part of the foundations of a valid theory of gravity. A priori, the equivalence principles are not necessarily valid. We are foremost interested in what experiment can tell us about them. Doing so allows us to distinguish between observations that test the equivalence principles and observations that test theories of gravitation that satisfy them. Experiment indeed provides tight constraints on the **WEP** and the **EEP**. In this section, we review the most important of these experiments. Theories that obey the EEP are often referred to as ‘metric’ theories of gravity, and we explain why a valid theory of gravitation is expected to be a metric one.

The weak equivalence principle

The [WEP](#) is the least stringent of the equivalence principles. It must be shown that test particles follow the same trajectories in a gravitational field. Eötvös type experiments provide the strongest constraints on the [WEP](#). A torsion balance is used to determine the relative acceleration of two different materials toward distant astrophysical bodies. Given their small mass, they can be considered to be non-gravitating test particles of the gravitational field of the astrophysical body. Taking the materials to be beryllium and titanium, the tightest constraint on the relative difference in accelerations of the two bodies, a_1 and a_2 , is [46]

$$\eta = 2 \frac{|a_1 - a_2|}{|a_1 + a_2|} = (0.3 \pm 1.8) \times 10^{-13}. \quad (2.1)$$

In other words, for a theory to be considered a viable theory of gravity, the [WEP](#) must be satisfied up to the accuracy given by (2.1).

The Einstein equivalence principle

The [EEP](#) is the next most stringent of the equivalence principles but substantially more difficult to test. It must be shown that test particles follow the same trajectories, but also that special relativistic laws are valid in the rest frames of these particles. The Hughes-Drever experiment provides the most accurate and direct test of the [EEP](#). By looking for local spatial anisotropies in atomic spectral lines (in shape and separation), it tests whether gravitational fields beyond a single rank-2 tensor are allowed to couple directly to matter fields. [EEP](#) violating couplings to other rank-2 tensors cause spatial anisotropies that can be constrained by observing the spectral lines. The coupling n to a second metric, for instance, is constrained by the Hughes-Drever experiment to be [47]

$$n \lesssim 10^{-27} m, \quad (2.2)$$

where m is the mass of the particle. In order to be observationally viable, the coupling to the second metric must be very weak. The evidence provided by the Hughes-Drever experiment suggests that matter fields must be coupled to a single rank-2 tensor only. In this case, particles follow geodesics of this unique metric and special relativity can be recovered at any point so that the [EEP](#) is satisfied. These constraints do not apply to multiple rank-2 tensors that couple to matter through a linear combination $g_{\mu\nu} = \sum_I c_I h_{\mu\nu}^{(I)}$ where c_I are constants. In this case, the [EEP](#) is always satisfied.

There are also theoretical reasons to think the [EEP](#) is valid to high accuracy. The Schiff conjecture states that ‘*Any complete and self-consistent gravitational theory that obeys the [WEP](#) must also satisfy the [EEP](#)*’, although this is yet to be proven.

Theories that satisfy the [EEP](#) are referred to as “metric” theories of gravity. This is because a theory composed of a metric tensor that couples to matter defined on a differentiable manifold can be shown to have test particles that

follow geodesics of the metric space. Then for every point on the manifold, there is tangent plane which is taken to be Minkowski and thus special relativity is recovered. In other words, validity of the [EEP](#) is generally believed to imply that the gravitational theory is a metric one. The rest of this section is therefore devoted to testing metric theories of gravity.

2.2 Solar-System tests

We present here the constraints obtained by observational tests involving the solar system. For a metric theory of gravity to be valid, it must be compatible with all of these observations. The solar-system observations can be grouped into tests that involve either null trajectories or time-like trajectories. We first present the null trajectories tests: the deflection of light by the Sun and the Shapiro time-delay. We then present tests involving time-like trajectories: the anomalous perihelion precession of Mercury and the Nordtvedt effect.

2.2.1 Tests involving null trajectories

Light bending around the Sun. The deflection of light in space as it passes next to a massive object can be determined. In general relativity, this deflection angle θ of a photon's trajectory due to a mass M is given by

$$\theta = \frac{2M}{d}(1 + \cos\phi), \quad (2.3)$$

where d is the impact parameter, ϕ is the angle between the direction of the mass and the direction of the incoming photon as viewed by an observer. By noting the change in the position of the stars as they graze the Sun on the celestial sphere, it is possible to measure this deflection. Current measurements lead to [\[48\]](#)

$$\theta = (0.99992 \pm 0.00023) \times 1.75'', \quad (2.4)$$

The bending of light around the Sun is a gravitational lensing effect.

The Shapiro time-delay. When light grazes the Sun, not only is there a deflection in space, but there is also a deflection in time. In general relativity, this time delay corresponds to

$$\Delta t = 4M \ln \left(\frac{4r_1 r_2}{d^2} \right), \quad (2.5)$$

where d is the impact parameter, M is the mass of a heavy object, r_1 is the distance between the observer and the heavy object, and r_2 is the distance between a test object and the heavy object. For an observer on Earth, the approximate time delay for light grazing the Sun is given by

$$\Delta t \simeq 20 \left(12 - \ln \left[\left(\frac{d}{R_\odot} \right)^2 \left(\frac{au}{r_2} \right) \right] \right) \mu s, \quad (2.6)$$

where R_\odot is the radius of the Sun and au is an astronomical unit. In 2002, the Cassini spacecraft was used to measure the time-delay. Shifts in frequency

were measured in the radio waves to and from the spacecraft, while those signals traveled close to the Sun. The following constraint was obtained [49],

$$\Delta t = (1.00001 \pm 0.00001)\Delta t_{GR}. \quad (2.7)$$

where Δt_{GR} is the time-delay due to general relativity. In other words, a theory of gravitation must satisfy the time-delay within the accuracy of eq. (2.7).

2.2.2 Tests involving time-like trajectories

Perihelion precession of planets. According to Newtonian physics, the perihelion of a test particle orbiting an isolated point-like mass stays in a fixed position, relative to distant stars. In the solar system, however, the perihelion of the planet precesses. This precession can be explained by the fact that the planet-Sun system is not isolated, so other planets in the solar system perturb the orbit away from its idealized Newtonian orbit. Also, the planets are not test-particles, and the Sun's quadrupole moment also causes precession of the planets. Taking into account the precession due to the presence of other planets and the Sun's quadrupole moment, there still remains an anomalous precession in Mercury's orbit which cannot be explained by Newtonian physics (and visible matter). Experimentally, this precession amounts to [50]

$$42.94'' \pm 0.20'' \quad (2.8)$$

per century. More accurate measurements have been performed since then, see for example [60, 51].

In general relativity, this anomalous precession is estimated to be

$$\Delta\omega = \frac{6\pi M}{p} \simeq 42.98'', \quad (2.9)$$

per century, where M is the total mass of the two bodies, and p is the semi-latus rectum of the orbit. The contribution takes into account the correction to Newton's gravitational potential coming from general relativity. This prediction is compatible with observation (2.8). For a general theory of gravitation, these corrections in principle differ from general relativity, leading to a different prediction for $\Delta\omega$. Measurement of Mercury's perihelion precession therefore provides constraints for other theories of gravitation.

Nordtvedt effect. The Nordtvedt effect refers to the phenomenon whereby massive bodies fall at different rates, depending upon their gravitational self-energy, therefore violating the SEP. Every measurement of the Nordtvedt effect could potentially rule out general relativity as a valid theory of gravitation. So far, the best measurement of the Nordtvedt effect comes from the Earth-Moon system in the gravitational field of the Sun and can be viewed as a giant Eötvös torsion balance. Lunar laser ranging leads to the following constraint [52],

$$\eta = 2 \frac{|a_1 - a_2|}{|a_1 + a_2|} = (-1.0 \pm 1.4) \times 10^{-13}. \quad (2.10)$$

This result is consistent with general relativity and allows us to constrain other theories of gravity.

Frame-Dragging. Gravitomagnetism is the generation of gravitational fields by the rotation of a massive object. The space around the object would be dragged around with the rotation of the object. This effect is called the “Lense-Thirring” effect [61, 62]. The accuracy of experiments on this effect therefore places bounds on theories of gravitation. The accuracy as measured by LAGEOS is within the 5 – 10% [63], while Gravity Probe B is at around 15% [64].

2.3 Parametrized post-Newtonian formalism

Given the sheer quantity of alternative theories of gravity that have been proposed over the past century, tremendous work has been invested into constraining these theories in both the weak-field and strong field limits. Comparing theory with experiment via the PPN formalism is a powerful and efficient tool used to constrain candidate theories of gravitation in the weak-field limit. On one hand, experimentalists can collect data that constrain the parameters of the PPN formalism, called PPN parameters, without prior knowledge of the candidate theories. On the other hand, theorists can recast their theory in terms of these PPN parameters, which can then be compared with the experimental constraints. The PPN formalism has ruled out many theories of gravitation since its existence and points the way to the more viable candidates. For the purposes of this manuscript, we provide here an outline of the PPN formalism and refer the reader to [10, 65] for greater detail and for strong-field tests.

2.3.1 The method

The PPN formalism was devised as a way to compare theories of gravitation with each other and with experiment. It relies on first PN corrections which are corrections to Newton’s potential in the slow and weak-field limit. It describes the next-to-Newtonian order gravitational effects in terms of a standardized set of potentials and ten parameters. For a general metric theory of gravity, there are ten PPN parameters, α_1^{PPN} , α_2^{PPN} , α_3^{PPN} , β^{PPN} , γ^{PPN} , ζ_1^{PPN} , ζ_2^{PPN} , ζ_3^{PPN} , ζ_4^{PPN} , ξ^{PPN} . We determine the PPN parameters by solving the field equations with a perfect-fluid source in a standard coordinate gauge order-by-order.

The PPN formalism is a perturbative treatment of weak-field gravity, we therefore need a small expansion parameter. The small parameter is given by

$$U \sim v^2 \sim \frac{P}{\rho} \sim \Pi \sim O(2), \quad (2.11)$$

where U is the Newtonian potential, v is the 3-velocity of a fluid element, P is the pressure of the fluid, ρ is the rest-mass density and Π is the ratio of energy density to rest-mass density. Time derivatives relative to spatial derivatives have an order of smallness as well, ($c = 1$),

$$\frac{|\partial/\partial t|}{|\partial/\partial x|} \sim O(1). \quad (2.12)$$

In order to recover the Newtonian limit of a metric theory of gravity, for timelike particles coupled to the metric only, knowledge of g_{00} is required to $O(2)$. The [PN](#) limit for timelike particles requires knowledge of

$$\begin{aligned} g_{00} &\text{ to } O(4) \\ g_{0i} &\text{ to } O(3) \\ g_{ij} &\text{ to } O(2) \end{aligned} \tag{2.13}$$

Next, we must identify the different dynamical fields in the theory. The fields are then expanded perturbatively,

$$\begin{aligned} g_{00} &= 1 + h_{00}^{(2)} + h_{00}^{(4)} + O(6) \\ g_{0i} &= h_{0i}^{(3)} + O(5) \\ g_{ij} &= -\delta_{ij} + h_{ij}^{(2)} + O(4) \end{aligned} \tag{2.14}$$

If, for example, the theory contains an additional scalar field, then it is expanded as,

$$\phi = \phi_0 + \phi^{(2)} + \phi^{(4)} + O(6), \tag{2.15}$$

where ϕ_0 is the constant background value of ϕ . The same logic applies for additional vector or tensor fields in the theory. The energy-momentum tensor in the [PPN](#) formalism is taken to be that of a perfect fluid,

$$T^{\mu\nu} = (\rho + \rho\Pi + p)u^\mu u^\nu + pg^{\mu\nu} \tag{2.16}$$

The field equations can then be solved, order by order, by taking this expansion of the energy-momentum tensor and substituting the perturbed expressions for the dynamical fields. Once a gauge is chosen, there is still a gauge freedom that allows one to transform the metric into the ‘‘standard’’ [PN](#) gauge. In this gauge, the spatial part of the metric is diagonal and terms with time derivatives are removed. The solution to the field thus obtained is then compared with the standard [PPN](#) metric (the PPN superscript has been omitted from the PPN parameters to simplify notation):

$$\begin{aligned} g_{00} &= 1 - 2U + 2\beta U^2 + 2\xi U^2 + 2\xi G^2 \Phi_W - (2\gamma + 2 + \alpha_3 + \beta_1 - 2\xi)\Phi_1 \\ &\quad - 2(1 + 3\gamma - 2\beta + \beta_2 + \xi)\Phi_2 - 2(1 + \beta_3)\phi_3 + (\beta_1 - 2\xi)A \\ &\quad - 2(3\gamma + 3\beta_4 - 2\xi)\Phi_4 \\ g_{0i} &= \frac{1}{2}(3 + 4\gamma + \alpha_1 - \alpha_2 + \beta_1 - 2\xi)V_i + \frac{1}{2}(1 + \alpha_2 - \beta_1 + 2\xi)W_i \end{aligned} \tag{2.17}$$

$$g_{ij} = -(1 + 2\gamma U)\delta_{ij}$$

By comparison of the solution with the standard [PPN](#) metric, one can read off the [PPN](#) parameters. These parameters each represent different physical

phenomena. The Eddington-Robertson-Schiff parameters, β^{PPN} and γ^{PPN} , respectively characterize the nonlinearity and the spatial curvature produced by gravity. The parameters α_1^{PPN} and α_2^{PPN} characterize preferred frame effects. The Whitehead parameter ξ characterizes preferred-location effects. The remaining 5 parameters ζ_1^{PPN} , ζ_2^{PPN} , ζ_3^{PPN} , ζ_4^{PPN} and α_3^{PPN} are zero for semi-conservative theories, i.e. one derived from a covariant action principle.

The potentials are all of the form

$$F(x) = G_N \int d^3y \frac{\rho(y)f}{|x-y|}, \quad (2.18)$$

where G_N is the current value of Newton's constant, which we determine below in terms of G . The correspondences $F \mapsto f$ are given by

$$\begin{aligned} U &\mapsto 1 & \Phi_1 &\mapsto v_i v_i & \Phi_2 &\mapsto U & \Phi_3 &\mapsto \Pi & \Phi_4 &\mapsto p/\rho \\ \Phi_W &\mapsto \int d^3z \rho(z) \frac{(x-y)_j}{|x-y|^2} \left(\frac{(y-z)_j}{|x-z|} - \frac{(x-z)_j}{|y-z|} \right) & \mathcal{A} &\mapsto \frac{(v_i(x-y)_i)^2}{|x-y|^2} \\ V_i &\mapsto v^i & W_i &\mapsto \frac{v_j(x_j - y_j)(x^i - y^i)}{|x-y|^2}. \end{aligned} \quad (2.19)$$

Note that for U , $\Phi_{1,2,3,4}$, and V_i ,

$$F_{,ii} = -4\pi G_N \rho f. \quad (2.20)$$

We will also make use of the 'superpotential' χ :

$$\chi = -G_N \int d^3y \rho |x-y|, \quad (2.21)$$

which satisfies

$$\chi_{,ii} = -2U. \quad (2.22)$$

We also note the relation

$$\chi_{,i0} = V_i - W_i, \quad (2.23)$$

follows from the formula

$$\frac{\partial}{\partial t} \int d^3y \rho(\mathbf{y}, t) f(\mathbf{x}, \mathbf{y}) = \int d^3y \rho(\mathbf{y}, t) v^i(\mathbf{y}, t) \frac{\partial f}{\partial y^i} [1 + O(2)], \quad (2.24)$$

which, in turn, follows from the continuity equation for the fluid

$$\rho_{,0} + (\rho v^i)_{,i} = 0, \quad (2.25)$$

assumed to hold to $O(3)$.

These potentials encompass almost all known viable theories of gravity. The 'standard PPN gauge' is defined as the PN coordinate frame in which all dependence on $\chi_{,00}$ and $\chi_{,ij}$ has been removed from g_{00} and g_{ij} , respectively. This fixing determines the coordinate frame up to necessary order so that the standard form of the metric components is unambiguous.

The PPN parameters have been extensively tested by experiment [10, 11], see Table 2.1 for constraints on a selection of PPN parameters.

2.4 Gravitational radiation tests

The Hulse-Taylor binary pulsar PSR B1913+16 provided the first incontrovertible proof that gravitational waves exist. The binary system consists of a pulsar and a companion star. A pulsar is a rapidly spinning neutron star that sends out a beam of electromagnetic radiation that sweeps around and periodically ends up pointing in our direction. This signal has allowed scientists to determine many parameters that characterize the binary pulsar system, and more importantly, that their orbit is losing energy as time moves forward. Note also that a double-pulsar system provides another exciting laboratory with which gravity can be tested [59].

Figure 2.1 shows the cumulative shift in the periastron period in seconds for the binary star system PSR B1913+16 as the system loses energy by gravitational wave emission [1]. Experimental data coincides with radiation loss as predicted by general relativity to within 0.2%. Gravitational radiation is therefore not detected directly, but indirectly by how it affects the binary system. While this data is generally viewed as being an experimental confirmation of general relativity, it also provides a stringent test for other theories of gravitation.

As discussed in Section 1.3, general relativity predicts gravitational radiation which travels at the speed of light. It has two polarities: the ± 2 helicities in the language of quantum field theory; or the $+$ and \times modes in the language of relativists. To lowest order, the radiation in general relativity is quadrupolar. But the existence of gravitational radiation is a generic prediction of metric theories of gravitation. Some models predict additional modes to the quadrupolar one, such as monopolar and dipolar modes. The speeds at which they travel may be different than the speed of light. So detection of gravitational radiation alone is not enough to distinguish between various theories of gravitation, but the type of radiation could provide a powerful tool in validating (or ruling out) a candidate theory. Both indirect and direct detection of gravitational waves are potential tools for testing metric theories of gravitation.

2.4.1 Indirect detection

The effect of gravitational radiation on a system can be inferred, as illustrated by the Hulse-Taylor binary system. In general, we are interested in studying the back reaction of radiation emission on the source. It is assumed that the energy flux at infinity is balanced by an equal loss of mechanical energy which is apparent in the orbital decay of the system for a slowly moving and weak-field system. This assumption has been verified to a certain extent in general relativity, but it is assumed for generic metric theories of gravity. Here, we give an outline of the PN gravitational radiation formalism [9, 8, 10] used to determine the energy loss for a binary system in the context of a metric theory of gravity.

Before considering a generic metric theory of gravity, let's briefly recall an important conservation relation for general relativity. Eq. (1.23) tells us that the source term $\tau_{\mu\nu}$ is conserved,

$$\partial^\mu \tau_{\mu\nu} = 0 \tag{2.26}$$

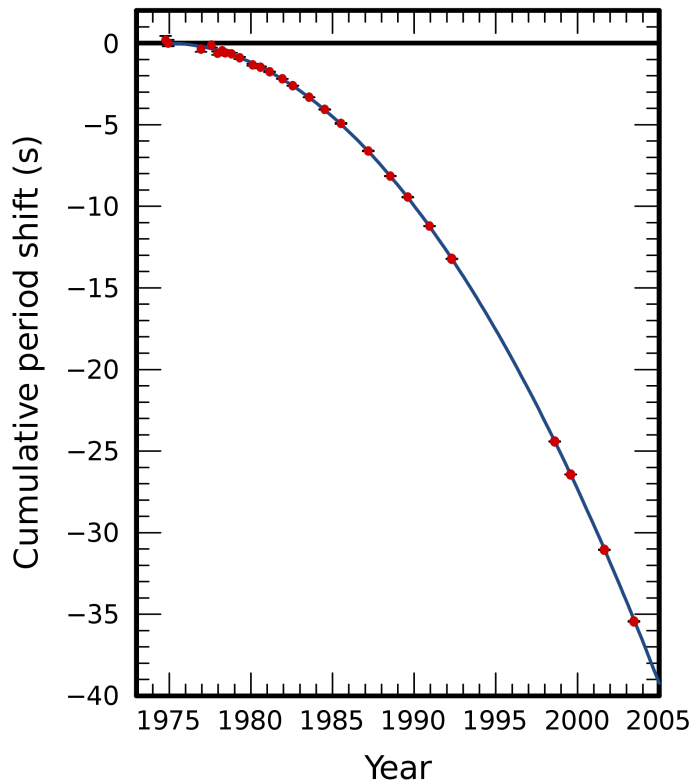


Figure 2.1: Red points are experimental data, and the blue line is the shift predicted by general relativity. Error bars are generally too small to be seen. Graph from [1].

where $\tau_{\mu\nu}$ reduces to the stress energy-momentum tensor $T_{\mu\nu}$ in flat spacetime [10]. The conservation relation allows us to define quantities P^μ ,

$$P^\mu \equiv \int_{\Sigma} \tau^{\mu 0} d^3x, \quad (2.27)$$

where integration is performed over a hypersurface Σ of constant t , where the boundary of integration is far from the source. These quantities P^μ are conserved for a localized source, modulo a flux of energy-momentum far from the source,

$$dP^\mu/dt = \int \partial_0 \tau^{\mu 0} d^3x = \int_{\partial\Sigma} \tau^{\mu j} d^2\sigma_j \quad (2.28)$$

Measured in asymptotically flat spacetime far from matter, P^0 and P^i correspond, respectively, to the total energy and the total momentum. It is also possible to define the total angular momentum, which is also conserved. The conservation relation (1.23) also leads to useful integral conservation relations, Eqs (1.38),

which we reproduce here,

$$\int d^3x \tau_{ij} = \frac{1}{2} \int d^3x \ddot{\tau}_{00} x^i x^j \quad (2.29a)$$

$$\int d^3x \dot{\tau}_{0i} x^j = - \int d^3x \tau_{ij}. \quad (2.29b)$$

$$\int d^3x \dot{\tau}_{00} x^i = - \int d^3x \tau_{i0}. \quad (2.29c)$$

Given that the wave-forms are written in terms of integrals of the source term, these integral conservation relations allow us to simplify the wave-forms. general relativity is called a ‘conservative’ metric theory of gravity, since total energy, total momentum and total angular momentum are conserved.

Unlike general relativity, the source term for generic metric theories of gravity is not generally conserved. However, a generic metric theory of gravity possesses another quantity called the ‘stress-energy complex’ $\mathfrak{T}_{\mu\nu}$ which is conserved $\partial^\mu \mathfrak{T}_{\mu\nu} = 0$. It is then possible to define the following conserved quantities,

$$P^\mu \equiv \int_{\Sigma} \mathfrak{T}^{\mu 0} d^3x, \quad (2.30)$$

modulo a flux term

$$dP^\mu / dt = \int \partial_0 \mathfrak{T}^{\mu 0} d^3x = \int_{\partial\Sigma} \mathfrak{T}^{\mu j} d^2\sigma_j \quad (2.31)$$

We also have integral conservation relations (valid in the near zone),

$$\int \dot{\mathfrak{T}}^{\mu 0} d^3x \equiv \dot{P}^0 = 0, \quad (2.32a)$$

$$\int \dot{\mathfrak{T}}^{00} x^j d^3x = P^j + 2 \int \mathfrak{T}^{[0j]} d^3x, \quad (2.32b)$$

$$\int \ddot{\mathfrak{T}}^{00} x^j x^k d^3x = 2 \int \mathfrak{T}^{(jk)} d^3x + 2 \int [\dot{\mathfrak{T}}^{[0j]} x^k + \dot{\mathfrak{T}}^{[0k]} x^j] d^3x, \quad (2.32c)$$

$$\int \dot{\mathfrak{T}}^{j0} \hat{\mathbf{r}} \cdot \mathbf{x} d^3x = \int \dot{\mathfrak{T}}^{jk} \hat{\mathbf{r}}_k d^3x. \quad (2.32d)$$

In complete analogy with general relativity, these conservation relations simplify the waveforms. Metric theories of gravity for which only total energy and total momentum are conserved are called ‘semiconservative’ theories.

Step 1. Select a (semiconservative) metric theory of gravity. Ensure that solar system tests are satisfied.

Step 2. Derive the gravitational wave equations. Expand the gravitational fields about their asymptotic values and express the field equations in the form of a wave equation

$$(c^{-2} \partial_0^2 - \Delta) \psi = -16\pi\tau, \quad (2.33)$$

where ψ is the field to linear order, c is the speed of propagation of the gravitational wave (see Section 1.3.4). The source term τ consists of matter, non-gravitational field stress energies and gravitational field perturbations of quadratic order and higher.

Step 3. Determine the energy loss rate dP^0/dt in terms of the linearized field ψ .

Step 4. Make a **PN** expansion of the source τ (see Section 2.3).

Step 5. Simplify ψ using integral conservations laws.

Step 6. Apply to binary systems. The bodies are taken to be smaller than the distance that separates them. Tidal interactions can be ignored and each body is considered to be static and spherical in its own rest-frame. From the energy balance assumption, the energy lost in radiation dE/dt corresponds to dP^0/dt .

Step 7. Determine the average energy loss over one orbit. The result is expressed as

$$\frac{dE}{dt} = -\left\langle \frac{\mu^2 m^2}{r^4} \frac{8}{15} (\kappa_1 \dot{v}^2 - \kappa_2 \dot{r}^2) \right\rangle. \quad (2.34)$$

The parameters κ_1 and κ_2 are called the ‘Peter-Mathews’ parameters, Eq. (2.34) generalizes the Peter-Mathews original result for the energy-loss in the context of general relativity, in which $\kappa_1 = 12$ and $\kappa_2 = 11$ [10, 45].

2.4.2 Direct detection

Gravitational wave observatories are in place or being built around the world. These observatories aim to detect gravitational waves directly, leading the way to the realm of gravitational wave astronomy. A positive detection has not yet been made, so the pursuit of direct detection continues. If we could detect gravitational radiation directly, however, then it would be possible to discriminate between different theories of gravitation by measuring their speed of propagation or their polarity.

Coalescing black holes are the most likely candidates for direct detection [66], although other sources of gravitational radiation could be detected, see [67] for a review of possible sources. In order to detect the gravitational wave signal, however, it must be filtered out from a huge amount of noise. This requires making a set of templates, and require high precision calculations in order to dig the signal out of the noise, thus the importance of **PN** physics.

Analytical methods have been developed to determine **PN** corrections to great accuracy for general relativity [32, 68]. Numerical Relativity is a complementary approach to calculating gravitational wave observables for coalescing black holes and other binaries with the help of supercomputers. This technique has been useful for comparison with analytical results, but also led to the predication of complementary phenomena. See [69] for an introduction.

2.5 Theoretical considerations

So far, we have seen the observations that have shaped our understanding of gravity. There are also theoretical motivations behind what constitutes a viable theory of gravity.

Ghosts

Ghosts arise from kinetic terms in the action with the wrong-sign, i.e. opposite of the gravity sector [70]. When this type of ghost is present, we can either accept the existence of negative norm states and abandon unitarity, or else accept that the energy eigenvalues of the ghost are negative [71]. Abandoning unitarity is disastrous since the quantum description falls apart. Accepting negative energies generate instabilities if it couples to other conventional fields, since the opposite sign means that the energy of the system described by the action is unbounded below. Methods have been developed to try to eliminate ghosts from a theory, by isolating them from the other fields, by making them heavy, etc. A theory devoid of ghosts, however, is generally much more manageable.

Theorems

In alternative theories of gravitation, Birkhoff's theorem of general relativity does not necessarily hold and so one must be cautious about expanding perturbations around Minkowski. While the no-hair theorem applies to general relativity, this is not necessarily the case for alternative theories of gravitation.

Next, Lovelock's theorem gives us clues on how to build a theory of modified gravity. Let the gravitational interaction depend on the metric tensor alone,

$$S = \int d^4x \mathcal{L}(g_{\mu\nu}). \quad (2.35)$$

If the action contains up to second order derivatives of $g_{\mu\nu}$, then variation with respect to the metric $dS/dg_{\mu\nu} = 0$ leads to the Euler-Lagrange expression

$$E^{\mu\nu}[\mathcal{L}] = \frac{d}{dx^\rho} \left[\frac{\partial \mathcal{L}}{\partial g_{\mu\nu,\rho}} - \frac{d}{dx^\lambda} \left(\frac{\partial \mathcal{L}}{\partial g_{\mu\nu,\rho\lambda}} \right) \right] - \frac{\partial \mathcal{L}}{\partial g_{\mu\nu}} \quad (2.36)$$

where the Euler-Lagrange equation is $E^{\mu\nu}[\mathcal{L}] = 0$.

Lovelock's Theorem: The only possible second-order Euler-Lagrange expression obtainable in a four dimensional space from a scalar density of the form $\mathcal{L} = \mathcal{L}(g_{\mu\nu})$ is

$$E^{\mu\nu} = \alpha\sqrt{-g} \left[R^{\mu\nu} - \frac{1}{2}g^{\mu\nu} R \right] + \lambda\sqrt{-g}g^{\mu\nu} \quad (2.37)$$

where α and λ are constants, and $R_{\mu\nu}$ and R are the Ricci tensor and scalar curvature, respectively.

According to Lovelock’s theorem, in order to build a metric theory of gravity with field equations that differ from the ones of general relativity, we must do at least one of the following things:

- Consider other fields, beyond or instead of the metric tensor.
- In the field equations, allow derivatives of the metric higher than order two .
- Allow spacetime dimensions to differ from four.
- Give up locality.

It is also possible to give up on either rank (2,0) tensor field equations, symmetry of the field equations under exchange of indices, or divergence-free field equations, but doing so means that the field equations can no longer be derived from an action principle by varying with respect to the metric. Modified theories of gravitation can therefore be classified into the following categories:

- Alternative Theories of Gravity with Extra Fields
- Higher Derivative and Non-Local Theories of Gravity
- Higher Dimensional Theories of Gravity

In what follows, we briefly discuss the Chameleon and Hořava gravity in the context of these possible modifications of gravity.

Alternative Theories of Gravity with Extra Fields

Scalar-Tensor Theories Scalar-tensor theories are extensions of general relativity that contain one or more fundamental scalars. Of the most well-known and experimentally viable candidate theories of gravity are scalar-tensor theories like Brans-Dicke theory, $f(R)$ theories [72], and multi-scalar tensor theories [21]. These types of scalar-tensor obey Lorentz invariance. $f(R)$ theory, a specific type of Brans-Dicke theory with parameter $\omega_{BD} = 0$, has been shown to be unviable but can be saved by introducing a ‘Chameleon’ mechanism [73, 72].

The scalar field which obeys this mechanism is called the Chameleon. The Chameleon was initially proposed as an alternative to Dark Matter [74, 75], but it has fine-tuning problems [76]. Despite this, the theory has the merits of being predictive so that it can be tested against experiment. The Chameleon’s hypothetical influence on electromagnetic phenomena is an example of how the Chameleon may be tested with experiment beyond the usual tests of gravity [77, 78].

Vector-Tensor Theories Another way to modify gravity with extra fields is to introduce a vector field. The Einstein-Æther or æ-theory is a special type of vector-tensor theory which consists of general relativity coupled to a dynamical vector field of unit norm called the æther [79, 80, 81]. The æther is a dynamical unit timelike vector field u^a which defines the preferred frame. Negative energy modes, aka ghosts, are avoided by constraining the æther to have a fixed

timelike magnitude. It is a diffeomorphism invariant theory of gravity that dynamically incorporates a preferred frame, thereby violating Lorentz symmetry but maintaining general covariance. The theory has been tested extensively, placing constraints on the free parameters of the theory [81]. The existence of this type of vector field is not as well motivated as scalar-tensor theories, but research in quantum gravity indicates that quantization is promising in æ-theory [82]. We mention the Einstein-Æther theory here since it is related to the low-energy limit of Hořava gravity [83].

Higher Derivative and Non-Local Theories of Gravity

Hořava gravity was initially proposed as UV complete theory of gravitation [16]. Hořava's proposal has several variants, and inconsistencies are present in the original formulation of the theory [84]. It was shown in [20] that a valid low-energy version of Hořava theory exists. This low-energy limit is called khronometric theory. Like æ-theory, khronometric theory also describes a diffeomorphism invariant theory with a unit timelike vector [18], but for which a preferred time-foliation is built into the theory. It is equivalent to a hypersurface orthogonal æther where only results that are insensitive to the transverse æther modes carry over to khronometric gravity [83, 20]. The validity of this theory needs to be tested against experiment, hence the work presented in Chapter 3.

High-energy versus low-energy modifications

In these attempts to modify gravity in the low-energy limit, one can often associate a high energy counterpart. Scalar-tensor theories, for example, are motivated by moduli fields that appear in higher dimensional approaches to gravity and quantum gravity, like string theory and branes. Khronometric theory, while valid as a low-energy theory in its own right, is motivated by a possible UV completion in the form of Hořava gravity. The point is that the categories listed in 2.5 are not rigidly enforced, but are often interlinked.

Chapter 3

Gravitational Radiation in Hořava gravity

General relativity continues to stubbornly agree with every observation related to it [65]. This would be extremely desirable if the theory could be merged with quantum mechanics in a straightforward way. Unfortunately, the current situation is far from this: the search for a consistent theory of quantum gravity remains elusive and there is no experimental guidance to shed light on it. Furthermore, the cosmological constant problem aside¹, the success of general relativity as a low-energy [EFT](#) points towards the Planck mass $M_P \approx 10^{19}$ GeV as the physical frontier where one expects to learn anything about quantum gravity. If the preceding arguments are realized in Nature, experimental information about quantum gravity will indeed be sparse in the foreseeable future.

More interesting for phenomenology are the proposals for [UV](#) completions of general relativity where the previous logic fails. These include models of gravitation with a low-energy cutoff beyond which general relativity ceases to be valid [85, 86]. If this cutoff scale is as low as the TeV, these proposals may have interesting phenomenology and may even be relevant for the resolution of the hierarchy problem. Another recent proposal in this category is Hořava gravity [16, 20]. This framework provides a candidate [UV](#) completion of general relativity, with effects that may permeate basically any gravitational experiment. It is on the implications of Hořava gravity for gravitational radiation that we pursue in this Chapter.

Essentially, Hořava's proposal consists of considering the existence of a preferred time-foliation of spacetime. Assuming the presence of this absolute structure, the general relativity Lagrangian can be supplemented by operators which render it power-counting renormalizable without destroying the unitarity of the theory [16]. The result is possibly a non-relativistic theory of quantum gravity [20] (in the sense that it is Lorentz-violating). The preferred foliation is in prin-

¹One may argue that the cosmological constant problem is a hint towards the actual theory of quantum gravity, and that a successful framework of quantum gravity should provide a mechanism to explain this phenomenological observation. We do not address this particular issue here.

ciple detectable at any energy scale, and it is not surprising that this approach (which is designed to cure the unsatisfactory behaviour of general relativity at distances of the order $M_P^{-1} \approx 10^{-33} \text{ cm}$) generically also modifies the theory at large distances² [20]. Among the different implementations of Hořava’s idea, we consider the so-called “healthy extension” [18]. This version possesses a stable Minkowski background where the issues about strong coupling appearing in other approaches are absent. Furthermore, variants of Hořava’s original proposal can be retrieved for a particular limit of this (generic and stable) case [18].

The low-energy (large-distance) sector of the theory is encoded into a scalar field φ , called³ the “khronon”, that characterizes the foliation structure and interacts with a metric field. We refer to this low-energy scalar-tensor theory as “khronometric” theory [20]. The extra scalar field φ turns out to be massless, and its presence modifies most of the predictions of general relativity, including the PPN parameters [20, 18, 88] and cosmological phenomena [89, 90]. These modifications differ from those of standard scalar-tensor theories [65, 10]. They are close, however, to the predictions of Einstein-aether theory (or æ-theory for short) [81]. This is not surprising since both theories incorporate a field whose expectation value violates Lorentz invariance (a unit timelike vector in the case of Einstein-aether, and φ in our case), and are otherwise generic. It can be shown that the khronon φ corresponds to the hypersurface-orthogonal mode of æ-theory, and many of the predictions of both theories are indeed identical [20, 83]. The PPN parameters derived from æ-theory and khronometric theory restrict the parameter space of those theories but are otherwise in agreement with current observations. Thus, both (low-energy) models represent interesting alternatives to general relativity, which, furthermore, have a high energy cutoff. The further advantage of khronometric theory is that beyond this energy cutoff there is a known UV completion, in the form of Hořava gravity.

The aim of this Chapter is to further constrain khronometric theory based on the loss of energy due to the emission of gravitational waves (GWs) from a binary self-gravitating system. This is a relevant test for gravitational theories given its sensitivity to the way gravity propagates (e.g. the degrees of freedom and corresponding properties), and also to the strong-field regime since known astrophysical sources of GWs tend to have strong gravitational self-energies [10, 32, 31]. The confirmation of general relativity’s famous quadrupole formula in the damping of a binary pulsar’s orbit is indeed one of its triumphs [57, 1]. Radiation tests have also been used in the past to constrain possible modifications of general relativity [65, 21, 26]. A priori for both æ-theory and khronometric theory, one expects this radiation formula to be modified due to a different speed of propagation of the tensor modes and the presence of new propagating fields. These modifications imply new ways to constrain the parameter space of the theory, independently of PPN and cosmological considerations. While the above expectations have been verified for æ-theory in the weak-field regime in [22], the constraints obtained are not final since the astrophysical systems for which radiation damping has been observed are not in the weak-field regime [65]. The incorporation of strong-field effects in the Einstein-aether began in

²A counterexample to this argument can be found in [87]. However, it is not clear how general relativity is recovered at large distances in this proposal.

³From Greek $\chi\rho\nu\nu\omicron\varsigma$ – time. The khronon is also known as the “T-field” [83].

[91].

We focus on the radiation formula in the post-Newtonian (weak field, slow-motion and weakly stressed [32]) regime of khronometric theory. This restriction is interesting for two reasons. First, we find deviations from general relativity’s quadrupole formula already at leading order. (This is similar to what happens in \mathfrak{a} -theory, as computed in [22].) Second, and from a purely pragmatic point of view, many of the formulae we present in this Chapter are useful for the phenomenologically relevant situation of compact sources. First results relevant for the study of gravitational radiation from these systems include the black hole solutions derived in [92, 93], and those for neutron stars in \mathfrak{a} -theory [94]. The use of binary pulsar observations to constraint Hořava gravity was suggested in [95].

To extract information about the damping of the orbit of a binary self-gravitating system from the emission of GWs, we take advantage of the fact that khronometric theory is semi-conservative (in the language of [10]). Then, for the bound system there exists a conserved energy that decreases due to the emission of gravitational radiation. By computing the energy flux at infinity, we can derive the flux of energy lost by the binary. Under the assumption that this energy is extracted entirely from the orbital motion of the binary, the subsequent damping of the orbits can be computed using Kepler’s third law. This assumption has been tested to lowest order in general relativity [31], and is plausible for khronometric theory.

This Chapter presents original work done in collaboration with Blas [25]. It is structured as follows. In Sec. 3.1, we define the action for khronometric theory and the equations of motion relevant for low-energy phenomenology. Sec. 3.2 is devoted to the linearized equations for the fields far away from the source (far-zone). In Sec. 3.4, we study the conserved properties of the source relevant for the PN calculation. We derive the explicit expressions for the different waveforms, up to and including the first PN order corrections in Sec. 3.5. In Sec. 3.7, we determine the formula for the average power loss in GWs. This formula is evaluated for a Newtonian system of two point-masses in Sec. 3.8, where the Peters-Mathews parameters for khronometric theory are derived. We summarize our results and conclude in Sec. 3.10. Section 3.3 contains a derivation of the PPN parameters for our model. Section 3.9 compares the monopole contribution, or lack thereof, in both khronometric theory and \mathfrak{a} -theory for a particular choice of parameters. Finally, Section 3.6 provides a summary of the notion of energy relevant for our study.

3.1 Action for khronometric theory at low energies

As outlined in the introduction, Hořava gravity is based on the existence of an absolute time foliation of spacetime. This allows for the general relativity Lagrangian to be supplemented with higher dimensional operators that render the theory power-counting renormalizable [16]. These operators are suppressed by a scale M_* whose magnitude is constrained by various phenomenological tests.

The most stringent of these tests comes from absence of deviations from Newton's law at short distances [20] which implies that $M_* \gtrsim (10 \mu m)^{-1} \sim 10^{14}$ Hz [65, 20]. Thus, these higher dimensional operators are irrelevant for the binary systems of interest⁴ and we neglect them in the following. The presence of a preferred foliation also has consequences at energy scales below M_* . Indeed, at low-energies new operators appear (compared to general relativity) that are compatible with the group of gauge invariance preserving the preferred foliation, i.e. the foliation-preserving diffeomorphism [16, 20]. Renormalization group arguments imply that these relevant operators should be added to the general relativity action, which has been done in the Stückelberg (or covariant) formulation of the theory in [20, 19]. In this formulation, the preferred-time foliation corresponds to the expectation value of a scalar field φ called the “khronon”. This field is such that the normal to the surfaces of constant field is timelike,

$$\partial_\mu \varphi \partial^\mu \varphi > 0. \quad (3.1)$$

The action of the theory is invariant under diffeomorphisms, and Lorentz invariance is broken by condition (3.1) in a spontaneous way. Also, the action must be endowed with invariance under field reparametrizations

$$\varphi \mapsto f(\varphi), \quad (3.2)$$

which follows from our requirement of a preferred time-foliation as opposed to a preferred time. It corresponds to the time reparametrization invariance of the theory in the original formulation of [16]. The invariance under the transformations (3.2) is readily implemented by making the action depend on φ through the combination

$$u_\mu \equiv \frac{\partial_\mu \varphi}{\sqrt{\partial_\rho \varphi \partial^\rho \varphi}}. \quad (3.3)$$

Clearly, u_μ is non-singular whenever condition (3.1) is satisfied. Notice also that u_μ is a unit timelike vector.

The low-energy action for the healthy extension of Hořava gravity corresponds to the most general action describing the coupling of φ with a metric field $g_{\mu\nu}$ at low-energies and compatible with the aforementioned invariances [20]. It is given by

$$S = -\frac{M_b^2}{2} \int d^4x \sqrt{-g} \left[R + K^{\mu\nu}{}_{\sigma\rho} \nabla_\mu u^\sigma \nabla_\nu u^\rho \right] + S_m, \quad (3.4)$$

where M_b is an arbitrary mass parameter to be related to the Planck mass,

$$K^{\mu\nu}{}_{\sigma\rho} = \beta \delta_\rho^\mu \delta_\sigma^\nu + \lambda \delta_\sigma^\mu \delta_\rho^\nu + \alpha u^\mu u^\nu g_{\sigma\rho}, \quad (3.5)$$

and α , β and λ are free dimensionless constants⁵. We also introduce a term S_m in Eq. (3.4) representing the matter component of the theory. We assume that

⁴As an example, the famous PSR 1913+16 binary pulsar has a characteristic frequency of 10^2 Hz [65]. We assume that the speed of propagation of all the modes is similar to the speed of light. We comment on this assumption when we derive the energy-loss formula in Sec. 3.7.

⁵Note that the parameter λ corresponds to λ' in the notations of [20]. It also differs from the λ defined in [16].

matter is universally coupled to the metric $g_{\mu\nu}$, which enforces the weak equivalence principle [65]. This action defines what we call “khronometric theory”. For later convenience, we introduce

$$S_\chi \equiv -\frac{M_b^2}{2} \int d^4x \sqrt{-g} K^{\mu\nu}{}_{\sigma\rho} \nabla_\nu u^\rho \nabla_\mu u^\sigma = -\frac{M_b^2}{2} \int d^4x \sqrt{-g} K^\mu{}_\sigma \nabla_\mu u^\sigma,$$

where

$$K^\mu{}_\sigma \equiv K^{\mu\nu}{}_{\sigma\rho} \nabla_\nu u^\rho = K^{\nu\mu}{}_{\rho\sigma} \nabla_\nu u^\rho.$$

is used to compactify notation.

Khronometric theory can be considered on its own as an alternative to general relativity with an extra scalar field, independently of quantum gravity motivations. This approach is similar to the way Einstein-æther theories are constructed. The only difference is that the vector u_μ is taken to be a generic timelike vector in æ-theory [81], meaning that it has more degrees of freedom than in the khronometric case. It also implies an extra term in the generic action with respect to Eq. (3.4). This extra term can be absorbed by the ones in action (3.4) for hypersurface orthogonal vectors, i.e. whenever u_μ satisfies Eq. (3.3). Khronometric theory and æ-theory share the nice feature of having a high energy cutoff. The advantage of the former is that a UV completion in the form of Hořava gravity is known.

Let the khronon and matter energy-momentum tensors be, respectively,

$$T_{\mu\nu}^\chi \equiv \frac{2}{\sqrt{-g}} \frac{\delta S_\chi}{\delta g^{\mu\nu}}, \quad T_{\mu\nu}^m \equiv \frac{2}{\sqrt{-g}} \frac{\delta S_m}{\delta g^{\mu\nu}}.$$

The explicit expression for $T_{\mu\nu}^\chi$ reads

$$\begin{aligned} M_b^{-2} T_{\mu\nu}^\chi &= -\nabla_\rho \left(K_{(\mu\nu)} u^\rho + K^\rho{}_{(\mu} u_{\nu)} - K_{(\mu}{}^\rho u_{\nu)} \right) + \frac{1}{2} g_{\mu\nu} K^\rho{}_\sigma \nabla_\rho u^\sigma \\ &\quad + \alpha a_\mu a_\nu + 2\nabla_\rho K^\rho{}_{(\mu} u_{\nu)} - u_\mu u_\nu u^\sigma \nabla_\rho K^\rho{}_\sigma - 2\alpha a_\sigma u_{(\mu} \nabla_{\nu)} u^\sigma + \alpha a^\rho a_\rho u_\mu u_\nu, \end{aligned}$$

where we have introduced the notation

$$a_\mu \equiv u^\rho \nabla_\rho u_\mu.$$

The equations of motion derived from varying the action with respect to the metric are

$$\mathcal{Q}_{\mu\nu} \equiv G_{\mu\nu} - M_b^{-2} (T_{\mu\nu}^\chi + T_{\mu\nu}^m) = 0. \quad (3.6)$$

The equation of motion for the khronon field is

$$\mathcal{Q}_\chi \equiv \nabla_\mu J^\mu \equiv \nabla_\mu \left(\frac{1}{\sqrt{X}} \mathcal{P}^{\mu\nu} [\nabla_\sigma K^\sigma{}_\nu - \alpha a_\sigma \nabla_\nu u^\sigma] \right) = 0, \quad (3.7)$$

where

$$\mathcal{P}^{\mu\nu} \equiv (g^{\mu\nu} - u^\mu u^\nu). \quad (3.8)$$

As usual, this equation follows from the covariant conservation of the khronon energy-momentum tensor. That it can be represented as the conservation of a current is a consequence of the invariance of the theory under reparametrizations of the khronon given by Eq. (3.2) [19].

3.2 Equations of motion in the far-zone

The physical system of interest for radiation damping consists of an isolated self-gravitating astrophysical source. By this we mean that there is a region of spacetime surrounding the source where the fields acquire their background values plus small perturbations. Thus, there exists a coordinate frame where the metric in this region satisfies⁶,

$$g_{\mu\nu} = \eta_{\mu\nu} + h_{\mu\nu},$$

with $|h_{\mu\nu}| \ll 1$. For the khronon field, we fix the parametrization invariance (3.2) by working with a time coordinate corresponding to the background of the field. Thus, we expand it as

$$\varphi = t + \chi,$$

where $|\chi| \ll t$. It is easy to verify that the background fields are indeed solutions of the equations of motion (3.6) in the absence of matter. To derive the flux of energy lost by this system, it is enough to understand the behavior of the fields produced by the isolated source in this region where they are weak. This is so because the energy carried by GWs is radiated away and eventually permeates the “weak-field” zone. We can extract the power radiated by integrating the flux of energy over a sphere surrounding the source at a particular time after the emission. This calculation is further simplified in the region far away from the source due to the applicability of the both the “weak-field” and “far-zone” approximations of section 1.3.4.

To derive the equations governing the perturbations $h_{\mu\nu}$ and χ , we split Eq. (3.6) and Eq. (3.7) into linear and non-linear parts as follows

$$\bar{G}_{\mu\nu} - M_b^{-2} \bar{T}_{\mu\nu}^{\chi} = M_b^{-2} \tau_{\mu\nu}, \quad \bar{Q}_{\chi} = -\mathcal{Q}_{\chi}^{NL}. \quad (3.9)$$

The expression for $\tau_{\mu\nu}$ reads

$$\tau_{\mu\nu} = T_{\mu\nu}^m + (T_{\mu\nu}^{\chi})^{NL} - M_b^2 G_{\mu\nu}^{NL}. \quad (3.10)$$

This separation into linear and non-linear parts allows us to solve for $h_{\mu\nu}$ and χ perturbatively in M_b^{-2} . The terms $\tau_{\mu\nu}$ and \mathcal{Q}_{χ}^{NL} can be interpreted to be source terms for the linear equations at different orders in M_b^{-2} . They include contributions from both matter and non-linear gravitational fields of lower order.

The linearized khronon energy-momentum tensor satisfies the following conservation laws

$$\partial^{\mu} \bar{T}_{\mu i}^{\chi} = 0, \quad \partial^{\mu} \bar{T}_{\mu 0}^{\chi} = M_b^2 \bar{Q}_{\chi}. \quad (3.11)$$

It follows from the invariance of the linearized theory under linear diffeomorphisms. Next, from the transverse properties of the $\bar{G}_{\mu\nu}$ and when the equations of motion are imposed, one finds

$$\partial^{\mu} (T_{\mu\nu}^m + T_{\mu\nu}^{\chi} - M_b^2 G_{\mu\nu}^{NL}) = 0.$$

Together with Eq. (3.11), this yields the following conservation equations for the source tensor $\tau_{\mu\nu}$

$$\partial^{\mu} \tau_{\mu\nu} = -\partial^{\mu} \bar{T}_{\mu\nu}^{\chi} = -M_b^2 \delta_{\nu}^0 \bar{Q}_{\chi} \quad (3.12)$$

which is of particular importance in Sec. 3.4 and beyond.

⁶In this section, Greek indices are manipulated with the Minkowski metric.

3.2.1 Wave equations

We saw in Section 1.3.4 that it was useful to decompose the gravitational perturbations into irreducible representations of $SO(3)$ of Eq. (1.24), which we reproduce here,

$$\begin{aligned} h_{00} &= 2\phi, & h_{0i} &= -\frac{\partial_i}{\sqrt{\Delta}}B + V_i, \\ h_{ij} &= t_{ij} + 2\partial_{(i}F_{j)} + 2\frac{\partial_i\partial_j}{\Delta}E + 2\left(\delta_{ij} - \frac{\partial_i\partial_j}{\Delta}\right)\psi, \end{aligned} \quad (3.13)$$

where $t_{ii} = \partial_i t_{ij} = \partial_i V_i = \partial_j F_j = 0$.

Tensors

To single out the tensorial part of the equations of motion as written in Eq. (3.9), we reintroduce the transverse-traceless projector $P_{ij,kr}$ and the transverse projector P_{ij} of Eq. (1.25). Applying the projector $P_{ij,kr}$ to \mathcal{Q}_{kr} yields

$$P_{ij,kr}\mathcal{Q}_{kr} = \frac{1}{2}P_{ij,kr}\left[\beta\ddot{h}_{kr} - (\partial_0^2 - \Delta)h_{kr} - 2M_b^{-2}\tau_{kr}\right],$$

leading to the wave equation for the tensor modes

$$(c_t^{-2}\partial_0^2 - \Delta)t_{ij} = -2M_b^{-2}P_{ij,ks}\tau_{ks}, \quad (3.14)$$

with $c_t^2 = 1/(1 - \beta)$ representing the speed of propagation of the tensor polarizations. This coincides with the results of æ-theory [37].

Vectors and Scalars

Consider now the vectorial part of the equations. Contrary to æ-theory [22, 37] this sector does not contain any propagating polarizations. Indeed, one finds

$$\begin{aligned} P_{ij}\mathcal{Q}_{0j} &= \frac{(1 - \beta)}{2}\Delta(V_i - \dot{F}_i) - M_b^{-2}P_{ij}\tau_{j0} = 0, \\ P_{ik}\partial_j\mathcal{Q}_{kj} &= \frac{(1 - \beta)}{2}\Delta(\dot{V}_i - \ddot{F}_i) - M_b^{-2}P_{ik}\partial_j\tau_{kj} = 0. \end{aligned} \quad (3.15)$$

The first equation represents a constraint and its time derivative yields the second equation (which follows from gauge invariance). For definiteness, we choose to work in the gauge

$$F_i = 0, \quad (3.16)$$

which completely fixes the gauge freedom in the vector sector.

Scalars

The scalar sector of the theory is different from general relativity. In particular, it includes an extra degree of freedom. We choose to work in the gauge

$$\chi = B = 0, \quad (3.17)$$

which completely fixes the gauge in the scalar sector. The choices (3.16) and (3.17) are referred to as the “unitary gauge”. In this gauge, the non-redundant equations of motion derived from (3.6) and (3.7) are

$$\alpha\Delta\phi = 2\Delta\psi - M_b^{-2}\tau_{00}, \quad (3.18a)$$

$$(\beta + \lambda)\Delta\dot{E} = -2(\lambda + 1)\Delta\dot{\psi} + M_b^{-2}\partial_i\tau_{0i}, \quad (3.18b)$$

$$(c_s^{-2}\partial_0^2 - \Delta)\psi = \frac{\alpha M_b^{-2}}{2(\alpha - 2)} \left(\frac{2}{\alpha}\tau_{00} + \tau_{ii} - \frac{(2 + \beta + 3\lambda)}{(\beta + \lambda)} \frac{\partial_i\partial_j}{\Delta}\tau_{ij} \right). \quad (3.18c)$$

The speed of propagation of the scalar perturbation is given by

$$c_s^2 = \frac{(\alpha - 2)(\beta + \lambda)}{\alpha(\beta - 1)(2 + \beta + 3\lambda)}, \quad (3.19)$$

which coincides with the scalar mode of æ-theory [37].

In comparison to the propagating degrees of freedom in general relativity, Eq. (1.32), we find that khronometric theory has 3 physical propagating degrees of freedom, 4 gauge degrees of freedom and 4 physical non-propagating components. We see that khronometric theory involves two speeds of propagation, the tensor and the scalar speeds c_t and c_s . We assume that the system is slowly moving with respect to both speeds which are considered to be of the same order, $c_t \sim c_s \sim 1$. Thus, for a typical velocity $v \sim \omega R$ of the source, the sum in Eq. (1.37) represents a well-defined expansion in the small parameter,

$$v \ll 1,$$

i.e. it is a PN expansion, cf. Eq. (1.22). In other words, every time derivative in the near zone represents an extra $O(v)$.

3.3 Post-Newtonian expressions

The PPN formalism is a valuable tool for comparing theories of gravitation with each other and with experiment in the weak, non-relativistic limit [10]. In this section, we briefly present the steps involved in the PPN calculation for khronometric theory (see also [20]) following the procedure described in Section 2.3. The final result are the parameters (all the other PPN parameters cancel)

$$\begin{aligned} \beta^{PPN} &= \gamma^{PPN} = 1, \\ \alpha_1^{PPN} &= \frac{4(\alpha - 2\beta)}{\beta - 1}, \\ \alpha_2^{PPN} &= \frac{(\alpha - 2\beta)(-\beta(3 + \beta + 3\lambda) - \lambda + \alpha[1 + \beta + 2\lambda])}{(\alpha - 2)(\beta - 1)(\beta + \lambda)}. \end{aligned} \quad (3.20)$$

They coincide with results in [20] in the limit of small parameters. The non-zero parameters α_1^{PPN} and α_2^{PPN} indicate that khronometric theory violates Lorentz invariance. These same two parameters are non-vanishing for æ-theory, although the dependence on the parameters α , β and λ is different. In both theories, however, the relationship between α_1^{PPN} and α_2^{PPN} is the same

$$\alpha_2^{PPN} = \frac{\alpha_1^{PPN}}{2} - \frac{(2\beta - \alpha)(3\lambda + \beta + \alpha)}{(\lambda + \beta)(2 - \alpha)}.$$

To compute the previous results we closely follow [10, 96] to which we refer the reader for further details. The source is assumed to be a fluid with a covariantly conserved energy-momentum tensor

$$T^{\mu\nu} = (\rho + \rho\Pi + p)v^\mu v^\nu - pg^{\mu\nu},$$

where v^μ is the four velocity of the source, ρ the rest mass energy density, Π the internal energy density and p the isotropic pressure of the fluid. We are interested in matter sources that are weakly self-gravitating, slowly moving⁷ and weakly stressed. These are known as PN sources [32] and satisfy (1.22).

In what follows, recall that the different fields have the following expansion,

$$\begin{aligned} g_{00} &= 1 + O(v^2) + O(v^4), & g_{0i} &= O(v^3), \\ g_{ij} &= -\delta_{ij} + O(v^2), & \chi &= O(v^2) + O(v^3). \end{aligned} \quad (3.21)$$

Also, we use the following potentials

$$F(x) = G_N \int d^3y \frac{\rho(y)f}{|x-y|},$$

where we introduce

$$G_N \equiv \frac{1}{4\pi M_b^2(2-\alpha)}, \quad r_{12}^i \equiv x_1^i - x_2^i. \quad (3.22)$$

and the correspondence $F \mapsto f$ is given by

$$\begin{aligned} U &\mapsto 1, & \Phi_1 &\mapsto v_i v_i, & \Phi_2 &\mapsto U, & \Phi_3 &\mapsto \Pi, & \Phi_4 &\mapsto p/\rho, \\ V_i^{PPN} &\mapsto v^i, & W_i^{PPN} &\mapsto \frac{v_j(x_j - y_j)(x^i - y^i)}{|x-y|^2}. \end{aligned}$$

The steps to take are:

1. Solve g_{00} to order $O(v^2)$. For this we use the 00 component of Eq. (3.6) to $O(v^2)$, which yields⁸

$$\Delta^2 h_{00} = 8\pi G_N \rho.$$

2. Solve g_{ij} to $O(v^2)$. Following [96], we choose the gauge conditions

$$\partial_i^2 h_{ij} = -\frac{1}{2} \left(\partial_i^2 h_{00} - \partial_i^2 h_{kk} \right). \quad \partial_i^3 h_{0i} = \Gamma \partial_0^2 h_{00}.$$

The arbitrary constant Γ will be chosen to write the result in the PPN gauge. Then from the ij component of Eq. (3.6) to $O(v^2)$, we find

$$\Delta^2 h_{ij} = 8\pi G_N \rho \delta_{ij}.$$

⁷For theories with modes propagating at different speeds, this means that the typical velocity v of the source is small with respect to all of them.

⁸We use a number over the field to keep track of the order in v .

3. Solve χ to $O(v^3)$. The khronon equation of motion (3.7) to leading order is given by

$$\left(\Delta \chi^3 - \Gamma \partial_0^2 h_{00} \right) = -\frac{(3\lambda + \alpha + \beta)}{2(\lambda + \beta)} \partial_0^2 h_{00},$$

4. Solve g_{0i} to $O(v^3)$. In our gauge, the $0i$ component of Eq. (3.6) to $O(v^3)$ yields

$$\Delta h_{0i}^3 = \frac{8\pi G_N \rho v_i (\alpha - 2) - [-2 + \alpha + \Gamma(1 - \beta)] \partial_0^2 h_{00}}{\beta - 1}.$$

5. Solve g_{00} to $O(v^4)$. From the 00 component of Eq. (3.6) to $O(v^4)$, we find

$$\begin{aligned} \Delta h_{00}^4 &= \partial_i^2 h_{00} \partial_i^2 h_{00} - h_{00} \Delta h_{00}^2 - 4\Delta \Phi_1 + 4\Delta \Phi_2 - 2\Delta \Phi_3 - 6\Delta \Phi_4 \\ &+ \frac{(-\alpha^2 + 2\beta(3 + \beta - 2\Gamma) + 2(3 + 3\beta - 2\Gamma)\lambda + 2\alpha(\beta(\Gamma - 1) + (\Gamma - 3)\lambda))}{(\alpha - 2)(\beta + \lambda)} \Delta \partial_0^2 H, \end{aligned}$$

where $H = -G_N \int d^3y \rho |x - y|$ is known as the superpotential.

6. To go to the PPN gauge, we choose Γ that cancels the term depending on H in the previous equation [10].

Putting everything together, we have (to desired order)

$$\begin{aligned} g_{00}^{PPN} &= 1 - 2U + 2U^2 - 4\Phi_1 - 4\Phi_2 - 2\Phi_3 - 6\Phi_4 = 1 + \Delta H, \\ g_{ij}^{PPN} &= -(1 + 2U)\delta_{ij} = \delta_{ij}(-1 + \Delta H), \\ g_{0i}^{PPN} &= \frac{1}{2}(7 + \alpha_1^{PPN} - \alpha_2^{PPN})V_i^{PPN} + \frac{1}{2}(1 + \alpha_2^{PPN})W_i^{PPN}, \\ \chi^{PPN} &= \frac{(\alpha - 2\beta)(2 + \beta + 3\lambda)\dot{H}}{2(\alpha - 2)(\beta + \lambda)}, \end{aligned}$$

which, compared to the generic PPN metric (see for example, Eq. (A.11) of [96]) implies that deviations from the PPN parameters vanish except for the ones cited in (3.20).

The PN metric in the unitary gauge of Eqs. (3.16) and (3.17) is easily derived from these PPN expressions. It suffices to go from the PPN gauge to the unitary gauge via a diffeomorphism $\delta x^\mu = \xi^\mu$ satisfying

$$\xi^0 = -\frac{(\alpha - 2\beta)(2 + \beta + 3\lambda)\dot{H}}{2(\alpha - 2)(\beta + \lambda)}, \quad \xi^i = \frac{(\alpha + \beta + 3\lambda)\partial_i H}{2(\beta + \lambda)}.$$

This leads to the following PN metric in the unitary gauge

$$\begin{aligned} g_{00} &= 1 + \Delta H + O(v^4), \\ g_{ij} &= \delta_{ij}(-1 + \Delta H) - \frac{(\alpha + \beta + 3\lambda)}{\beta + \lambda} \partial_j \partial_i H + O(v^4), \\ g_{0i} &= \frac{1}{4}(8 + \alpha_1^{PPN})(V_i^{PPN} + W_i^{PPN}) + O(v^4), \\ \chi &= O(v^4). \end{aligned} \tag{3.23}$$

3.4 The source: conservation properties

The source terms for the equations (3.14), (3.15) and (3.18) are expressed in terms of the pseudo-tensor $\tau_{\mu\nu}$. In order to find solutions to the Poisson and wave equations in the far-zone, we use the method already described in Section 1.3.4. Specifically, Eqs. (1.37) and (1.34) indicate that we need to evaluate various integrals of $\tau_{\mu\nu}$. In what follows, we present results that are relevant for simplifying those integrals (and therefore the wave forms that appear in Sec. 3.5) and include leading PN corrections.

From Eq. (3.12), one can establish the useful integral conservation laws,

$$\int d^3x \tau_{ij} = \frac{1}{2} \int d^3x \ddot{\tau}_{00} x^i x^j - \frac{1}{2} \int d^3x \partial^\mu \dot{\tau}_{\mu 0} x^i x^j. \quad (3.24a)$$

$$\int d^3x \dot{\tau}_{0i} x^j = - \int d^3x \tau_{ij}. \quad (3.24b)$$

$$\int d^3x \dot{\tau}_{00} x^i = - \int d^3x \tau_{i0} + \int d^3x \partial^\mu \tau_{\mu 0} x^i. \quad (3.24c)$$

In deriving the previous equations, we assume that all the boundary integrals cancel (the corrections to this assumption are negligible at large r). The difference with respect to the general relativity integral conservation laws is the presence of the terms proportional to $\partial^\mu \tau_{\mu 0}$ coming from the non-conservation of $\tau_{\mu\nu}$, Eq. (3.12). Remember that the current τ_{i0} is conserved for khronometric theory. Naively one expects $\partial^\mu \tau_{\mu 0}$ to contribute to order as low as $O(v^3)$. To see that this is not the case, we notice that Eqs. (3.24) can be simplified by writing the equation of motion (3.7) as an equation for a conserved current (which corresponds to the Noether current related to the invariance of the theory under reparametrizations of φ , Eq. (3.2)),

$$\partial_\mu (\sqrt{-g} J^\mu) = 0. \quad (3.25)$$

Furthermore, in the unitary gauge, $\varphi = t$ and $J^0 = 0$ (see Appendix D of [20]). Since J^i is linear in perturbations, we find that

$$\bar{Q}_\chi = -\partial_i (\sqrt{-g} J^i)^{NL}. \quad (3.26)$$

Thus,

$$\partial^\mu \tau_{0\mu} = M_b^2 \partial_i (\sqrt{-g} J^i)^{NL} \sim O(v^5), \quad (3.27)$$

and the dipolar corrections turn out to be high in PN order. In particular, at order $O(v^5)$ only the Eq. (3.24c) is modified with respect to general relativity. A straightforward but tedious calculation using the PN metric displayed in Eq. (3.23) yields

$$\int d^3x \partial^\mu \tau_{0\mu} x^i = \frac{1}{2} \int dx \rho [(\alpha_1^{PPN} - \alpha_2^{PPN}) V_i^{PPN} + \alpha_2^{PPN} W_i^{PPN}] + O(v^6), \quad (3.28)$$

where α_1^{PPN} and α_2^{PPN} are given in Eq.(3.20).

These constants are the PPN parameters related to the violation of Lorentz invariance of the theory (see Section 3.3). In the limit of small parameters they

coincide with those found in [20]. The potentials V_i^{PPN} and W_i^{PPN} are also defined in Section 3.3. Finally, the form of the Eq. (3.28) is identical to the one found for æ-theory [91].

The previous formulae (3.24) and (3.28) can also be derived by relating the pseudo-tensor $\tau_{\mu\nu}$ to a conserved (but asymmetric) object. Indeed, from Eqs. (3.12) and (3.7) it is evident that

$$\mathfrak{T}_{\mu\nu} \equiv \tau_{\mu\nu} + M_b^2 \delta_\mu^0 \eta_{\nu\rho} \bar{J}^\rho$$

satisfies

$$\partial^\nu \mathfrak{T}_{\mu\nu} = 0.$$

This object has a contribution linear in the fields. To build a quadratic conserved pseudo-tensor it is enough to add the conserved current found in (3.25) and consider the object

$$\mathfrak{T}_{\mu\nu}^q \equiv \tau_{\mu\nu} + M_b^2 \delta_\mu^0 \eta_{\nu\rho} (\bar{J}^\rho - \sqrt{-g} J^\rho) = \tau_{\mu\nu} - M_b^2 \delta_\mu^0 \eta_{\nu\rho} (\sqrt{-g} J^\rho)^{NL}.$$

The resulting integral conservation laws for this object are then identical to the ones found in [10, 91]. The existence of this conserved quadratic current is a generic consequence of the theory being *semi-conservative*, as discussed in Section 2.4. This conserved current satisfies

$$\mathfrak{T}_{0i}^q - \mathfrak{T}_{i0}^q = M_b^2 (\sqrt{-g} J^i)^{NL}.$$

Then, one can use the Eq. (4.103) in [10] to compute (3.27). Even if this method may save a lot of computations, it is inconvenient since the result in [10] is derived in the PPN gauge, whereas we are interested in the result in the unitary gauge (3.28).

3.5 Wave forms in the far-zone

We are now ready to compute the explicit form of the wave solutions in the far-zone, which we do consistently up to $O(v^6)$ in the PN approximation. For the tensor and vector modes, the solutions of Eqs. (3.14), (3.15), (1.37) and (3.24) are (in the gauge $F_i = 0$)

$$t_{ij}(t, x) = -\frac{1}{4\pi M_b^2 r} \hat{\mathbf{P}}_{ij,ks} \ddot{Q}_{ks}(t - r/c_t) - \frac{1}{2\pi M_b^2 c_t r} \hat{\mathbf{P}}_{ij,ks} \hat{\mathbf{r}}^a \dot{S}_{ks,a}(t - r/c_t) + O(v^6), \quad (3.29a)$$

$$V_i(t, x) = -\frac{c_t^2}{2\pi M_b^2} \left(\frac{1}{r} \int d^3 \tilde{x} P_{ij} \tau_{j0}(t, \tilde{x}) \right), \quad (3.29b)$$

where

$$Q(t)_{ij} \equiv I(t)_{ij} - \frac{1}{3} \delta_{ij} I_{kk}(t), \quad I_{ij}(t) \equiv \int d\tilde{x} \tau_{00}(t, \tilde{x}) \tilde{x}^i \tilde{x}^j, \\ S_{ks,a}(t) \equiv \int d^3 \tilde{x} \tau_{ks}(t, \tilde{x}) \tilde{x}^a.$$

The quantity Q_{ij} represents the quadrupole of τ_{00} , I_{ij} is its second mass moment and I_{kk} its monopole. Note that in the far-zone, the transverse projector $P_{ij} \equiv \delta_{ij} - \frac{\partial_i \partial_j}{\Delta}$ (see Eq. (1.25)) can be substituted by the transverse part of the algebraic projector,

$$\hat{\mathbf{P}}_{ij} \equiv \delta_{ij} - \hat{\mathbf{r}}^i \hat{\mathbf{r}}^j.$$

This substitution is valid up to $O(R/r)$ terms. The object $\hat{\mathbf{P}}_{ij,ks}$ is defined as

$$\hat{\mathbf{P}}_{ij,kr} \equiv \hat{\mathbf{P}}_{ik} \hat{\mathbf{P}}_{jr} - \frac{1}{2} \hat{\mathbf{P}}_{ij} \hat{\mathbf{P}}_{kr}.$$

Anticipating the results of Sec. 3.7, we notice that the energy-loss formula depends on the time derivative of the fields. For the vector part, the previous expression yields

$$\dot{h}_{0i} = \dot{V}_i = -\frac{c_t^2}{2\pi M_b^2} \left(\frac{1}{r} \int d^3 \tilde{x} P_{ij} \dot{\tau}_{j0}(t, \tilde{x}) \right). \quad (3.30)$$

From the conservation law (3.12), this term can be expressed as the integration over the boundary of the transverse component of the source, which cancels away from the source, and we can neglect the vector perturbations altogether.

Concerning the scalar field, from the wave equation (3.18c) one finds

$$\begin{aligned} \psi = & \frac{\alpha}{8\pi(\alpha-2)M_b^2 r} \left(\frac{3}{2} [Z-1] \hat{\mathbf{r}}^i \hat{\mathbf{r}}^j \ddot{Q}_{ij}(t-r/c_s) + \frac{1}{2} Z \ddot{I}_{kk}(t-r/c_s) \right. \\ & + \frac{2}{c_s \alpha} \hat{\mathbf{r}}^i \int d^3 \tilde{x} \dot{\tau}_{00}(t-r/c_s, \tilde{x}) \tilde{x}^i + \frac{1}{3c_s^3 \alpha} \hat{\mathbf{r}}^i \hat{\mathbf{r}}^j \hat{\mathbf{r}}^k \int d^3 \tilde{x} \ddot{\tau}_{00}(t-r/c_s, \tilde{x}) \tilde{x}^i \tilde{x}^j \tilde{x}^k \\ & \left. + \frac{1}{c_s} \hat{\mathbf{r}}^a \dot{S}_{kk,a}(t-r/c_s) - \frac{(2+\beta+3\lambda)}{c_s(\beta+\lambda)} \hat{\mathbf{r}}^i \hat{\mathbf{r}}^j \hat{\mathbf{r}}^k \dot{S}_{ij,k}(t-r/c_s) \right) + O(v^6), \end{aligned} \quad (3.31)$$

where

$$Z \equiv \frac{(\beta-1)(\alpha_1^{PPN} - 2\alpha_2^{PPN})}{3(\alpha-2\beta)}. \quad (3.32)$$

Notice that the conservation law $\dot{\tau}_{00} = \partial_i(\tau_{0i} + \bar{J}_i)$ has been used to show that the first moment of τ_{00} is constant in time and therefore ignored in (3.31). From the results in the previous section, we see that the modification to the general relativity results appear at order $O(v^4)$. Notice also that it follows from (3.28) and the constancy of the integral of τ_{i0} that the dipolar contribution in (3.31) is $O(v^5)$ and suppressed by the PPN parameters. Finally, the quadrupole terms in the tensor and scalar sectors differ slightly, as they depend on different retarded times. For the remaining scalar fields ϕ and E , from Eqs. (3.18) one finds

$$\phi = \frac{2}{\alpha} \psi + \frac{1}{4\pi M_b^2 \alpha r} \int d^3 \tilde{x} \tau_{00}, \quad \dot{E} = -\frac{2(\lambda+1)}{\beta+\lambda} \dot{\psi}. \quad (3.33)$$

3.6 Notion of energy for an asymptotically flat spacetime

The definition of the energy carried by gravity waves is non-trivial (see [97] for a review on the concepts of energy and momentum in general relativity). For

the problem at hand, we follow the procedure of [91] (see also [98]) and use the notion of energy for asymptotically flat spacetimes derived in [99]. Given an isolated source, we can compute the time variation of this notion of energy by performing an integral of the flux in the far-zone, which we idealize as being infinitely far away from the source. We associate this energy loss to the energy carried away by gravitational radiation. As shown in [99, 100], this alternative approach is equivalent to the one based on pseudo-tensors used in standard computations of energy loss due to gravitational radiation [10, 31, 38].

To characterize the energy carried away from a system by GWs, we use a method different from the standard technique defined in terms of the Landau-Lifshitz or related pseudotensors [10, 31, 38, 97]. Here, instead of computing the energy carried by GWs, we derive the loss of energy of the isolated system during the process of gravitational radiation. This resembles the definition of energy loss by the time variation of the Bondi-Sachs mass [34, 97]. However, we will use a different notion of conserved energy that, to our knowledge, was first used in the context of GWs in [22]. This energy is well-defined for asymptotically flat spacetimes satisfying the boundary conditions (3.50), which we use to define isolated sources. Its conservation follows from the invariance of the asymptotic solution under time translations and it reduces to the standard notion of energy for flat spacetime [99] (see also [101, 102]). Since the method is not standard, this section is devoted to presenting a succinct summary.

Given a Lagrangian density $L(\Phi)$ depending on some dynamical fields Φ , we define its associated 4-form (we present the 3 + 1 case) as

$$\mathbf{L}(\Phi) = L(\Phi)d^4x.$$

Using the product rule, the first variation of the previous form following from the variation $\delta\Phi$ can be expressed as,

$$\delta\mathbf{L}(\Phi) = \mathbf{E}_\Phi\delta\Phi + d\Theta_L(\Phi, \delta\Phi),$$

where $\mathbf{E}_\Phi = 0$ are the equations of motion of the theory. If the variation $\delta\Phi$ is a diffeomorphism generated by a vector field ξ , the previous variation should correspond to the action of this transformation over $\mathbf{L}(\Phi)$,

$$\delta_\xi\mathbf{L}(\Phi) = d(i_\xi\mathbf{L}),$$

where $i_\xi\mathbf{L}$ refers to the contraction of the form \mathbf{L} with the vector field ξ . Define the Noether current 3-form associated to ξ and $L(\Phi)$ as

$$\mathbf{J}_L \equiv \Theta_L(\Phi, \delta_\xi\Phi) - i_\xi\mathbf{L}. \quad (3.34)$$

This form is clearly closed when the equations of motion are satisfied. In practice, to find the components of the 3-form Θ_L , notice that it is dual to a 1-form. In components

$$\Theta_{L\mu\nu\rho} = \epsilon_{\alpha\mu\nu\rho}\Theta_L^\alpha,$$

where the index of Θ_L^α is risen with the metric $g^{\mu\nu}$ and $\epsilon_{\alpha\mu\nu\rho}$ are the components of the Levi-Civita 4-form defined for the metric $g_{\mu\nu}$. From this definition it follows that

$$d\Theta_L = \sqrt{-g}\nabla_\mu\Theta_L^\mu d^4x = \partial_\mu(\sqrt{-g}\Theta_L^\mu)d^4x, \quad (3.35)$$

from which one can easily identify the components of Θ_L .

To associate the flux generated by ξ to a Hamiltonian evolution from an initial hypersurface Σ , one must assume [99, 102] that in the boundary of the initial hypersurface, denoted by $\partial\Sigma$, it is possible to find a 3-form \mathbf{B}_L such that

$$\delta \int_{\partial\Sigma} i_\xi \mathbf{B}_L = \int_{\partial\Sigma} i_\xi \Theta_L.$$

If such a current exists, the flux generated by ξ corresponds to the orbits generated by the Hamiltonian

$$H_\xi \equiv \int_{\Sigma} \mathbf{J}_L - \int_{\partial\Sigma} i_\xi B_L. \quad (3.36)$$

Finally, since \mathbf{J}_L is closed when the equations of motion are satisfied, it follows that locally $\mathbf{J}_L = d\mathbf{Q}_L$. Thus, when the equations of motion hold, H_ξ can be written as a pure boundary term,

$$H_\xi = \int_{\partial\Sigma} (\mathbf{Q}_L - i_\xi B_L). \quad (3.37)$$

To define a canonical notion of energy, we shall now assume that ξ is an asymptotic time translation, with components $\xi^\mu \rightarrow \delta_0^\mu$ and that the asymptotic conditions on the dynamical fields have been specified in such a way that the surface integrals appearing in Eq. (3.37) approach a finite limit. The Hamiltonian then corresponds to the generator of time evolution. We define the canonical energy at a hypersurface slice of constant time Σ_t to be [99]

$$\mathcal{E}_L = \int_{S_t^2} (\mathbf{Q}_L - i_{\delta_0^\mu} B_L), \quad (3.38)$$

where S_t^2 represents the boundary sphere at the boundary of Σ_t . Whenever \mathcal{E}_L is well-defined, it is a conserved quantity, and we can remove the t label in S_t^2 .

We now apply the previous formalism to our action (3.4). The hypersurface of constant time corresponds to a sheet of the preferred foliation. Even if not necessary, it is convenient to work with an action for which

$$\int_{S^2} i_\xi \Theta_L = 0. \quad (3.39)$$

This equation is not satisfied for the Einstein-Hilbert action part of (3.4) (see e.g. Eq. (87) in [99]). As explained in [99], the existence of a background metric $\eta_{\mu\nu}$ makes it possible to build a covariant action (which is required to get a conserved current (3.34)) equivalent to Einstein-Hilbert and satisfying (3.39). Indeed, let us write $g_{\mu\nu} = \eta_{\mu\nu} + h_{\mu\nu}$ and consider $h_{\mu\nu}$ and $\eta_{\mu\nu}$ as independent dynamical fields. We can then add a boundary term invariant under diffeomorphisms to the action (3.4) to yield

$$S' \equiv S + \frac{M_0^2}{2} \int d^4x (\sqrt{-g} ((\Gamma_{\mu\nu}^\alpha - \bar{\Gamma}_{\mu\nu}^\alpha) g^{\mu\nu} - (\Gamma_{\mu\nu}^\mu - \bar{\Gamma}_{\mu\nu}^\mu) g^{\nu\alpha}))_{,\alpha} \equiv \int d^4x L', \quad (3.40)$$

where $\bar{\Gamma}_{\sigma\nu}^{\mu}$ refers to the connection compatible with the background metric $\eta_{\mu\nu}$. The part corresponding to general relativity reads

$$S'_{\Gamma\Gamma} = -\frac{M_0^2}{2} \int d^4x [\sqrt{-g}g^{\mu\rho} (\Gamma_{\rho\nu}^{\alpha}\Gamma_{\alpha\mu}^{\nu} - \Gamma_{\alpha\nu}^{\nu}\Gamma_{\mu\rho}^{\alpha}) + (\sqrt{-g} (\bar{\Gamma}_{\mu\nu}^{\alpha}g^{\mu\nu} - \bar{\Gamma}_{\mu\nu}^{\mu}g^{\nu\alpha}))_{,\alpha}]. \quad (3.41)$$

The equations of motion derived from varying the previous action with respect to $h_{\mu\nu}$ and $\eta_{\mu\nu}$ are the same, as these fields appear only in the combination $g_{\mu\nu}$, except in the boundary term. As a consequence, $\eta_{\mu\nu}$ can be considered to be Minkowski, and we can assume that the equations of motion fix $h_{\mu\nu}$.

For the computation of $\mathbf{J}_{\Gamma\Gamma}$ corresponding to the action (3.41) and the vector field ∂_t , with components δ_0^μ , we first notice that ∂_t is a Killing vector of $\eta_{\mu\nu}$,

$$\delta_{\partial_t}\eta_{\mu\nu} = 2\bar{\nabla}_{(\mu}\eta_{\nu)\alpha}\delta_0^\alpha = 0,$$

and the boundary term in Eq. (3.41) does not contribute to $\mathbf{J}_{\Gamma\Gamma}$. For the first term one finds the corresponding current

$$\Theta_{\Gamma\Gamma}^\nu = \frac{M_0^2}{4} \left(\Gamma_{\mu\alpha}^\nu (g^{\mu\alpha}g^{\rho\sigma}\delta g_{\rho\sigma} - 2g^{\mu\rho}g^{\alpha\tau}\delta g_{\tau\rho}) + g^{\nu\alpha} (2\Gamma_{\sigma\beta}^\beta g^{\rho\sigma}\delta g_{\rho\alpha} - \Gamma_{\alpha\beta}^\beta g^{\rho\sigma}\delta g_{\rho\sigma}) \right). \quad (3.42)$$

This term is linear in the connection and does not depend on the derivative of $\delta g_{\mu\nu}$. To construct the conserved current, we use

$$\delta_{\partial_t}g_{\mu\nu} = 2\nabla_{(\mu}g_{\nu)\alpha}\delta_0^\alpha = 2g_{\alpha(\mu}\Gamma_{\nu)0}^\alpha,$$

Thus, under the assumption that the fields fall-off at large distances as (3.50), the current (3.42) vanishes asymptotically as $O(r^{-4})$, which means that its contribution to (3.39) cancels. Indeed the cancellation of the contribution to (3.39) holds in the more general situation where one considers variations $\delta g_{\mu\nu}$ which do not change the asymptotic behaviour (3.50). Finally, the energy $\mathcal{E}_{\Gamma\Gamma}$ derived from Eq. (3.41) coincides with the ADM mass which also agrees with the energy derived from the Landau-Lifshitz pseudotensor [99, 100].

The term S_χ in the action (3.4) yields a current

$$\Theta_\chi^\nu = -M_b^2 \left[(\alpha a_\sigma \nabla_\mu u^\sigma - \nabla_\rho K^\rho_\mu) \frac{\mathcal{P}^{\nu\mu}}{\sqrt{X}} \delta\chi + K^{\nu\rho} \frac{\mathcal{P}_\rho^\alpha}{\sqrt{X}} \partial_\alpha \delta\chi - \frac{1}{2} ([K^{\nu\alpha} + K^{\alpha\nu}] u^\sigma - K^{\alpha\sigma} u^\nu - u^\alpha u^\sigma u_\rho K^{\nu\rho}) \delta g_{\alpha\sigma} \right]. \quad (3.43)$$

Remember that the invariance under diffeomorphisms is non-linearly realized⁹ on χ

$$\delta_\xi \chi = \xi^0 + \xi^\mu \partial_\mu \chi.$$

From Eq. (3.50) this means that $\delta_{\partial_t} \chi \sim O(1)$. Similarly $u_\alpha = \frac{\delta_{\alpha 0}}{\sqrt{g^{00}}} \sim \delta_{\alpha 0} + O(1/r)$. Thus, $\Theta_\chi^\nu \sim O(r^{-3})$, which means that the contribution of this term to (3.39) cancels.

⁹We could also work with the field φ for which $\delta_\xi \varphi = \xi^\mu \partial_\mu \varphi$.

Finally, we find that the conserved energy (3.36) for the action (3.40) inside a constant time hypersurface Σ_t is given by

$$\mathcal{E} = \int_{\Sigma_t} d^3x \sqrt{-g} \mathcal{J}_{S'}^0, \quad (3.44)$$

with $\mathcal{J}_{S'}^0$ representing the coordinates of the 1-form dual to the corresponding 3-form, Eq. (3.34),

$$\mathcal{J}_{S'}^\nu \equiv (\Theta_{\Gamma}^\nu + \Theta_\chi^\nu) - \delta_0^\nu L'. \quad (3.45)$$

The contribution from the khronon action is simplified once one considers the equation of motion for χ . Indeed, Θ_χ^ν in Eq. (3.43) includes a term

$$(\alpha a_\sigma \nabla_\mu u^\sigma - \nabla_\rho K^\rho{}_\mu) \frac{\mathcal{P}^{\nu\mu}}{\sqrt{X}} = J^\nu, \quad (3.46)$$

where J^ν is defined in (3.7). In the unitary gauge, this current is purely spatial, which means that this term does not contribute to (3.44).

We are eventually interested in the flux of energy loss through GWs, so we want to compute the quantity,

$$\dot{\mathcal{E}} = \int_\Sigma d^3x \sqrt{-g} \dot{\mathcal{J}}_{S'}^0 = - \oint_{S_\infty^2} d\Omega \sqrt{-g} r^2 \hat{\mathbf{r}}^i \mathcal{J}_{S'}^i, \quad (3.47)$$

where we have used the fact that the current $\mathcal{J}_{S'}^\mu$ is conserved on-shell, which is a consequence of \mathbf{J} being closed and (3.35). The final ingredient is to evaluate $\mathcal{J}_{S'}^i$. From Eq. (3.42),

$$\Theta_{\Gamma}^i = \frac{M_b^2}{4} \dot{h}_{\alpha\beta} [\eta^{\alpha\beta} (\partial^\rho h_\rho^i - \partial^i h_\sigma^\sigma) - 2\partial^\alpha h^{\beta i} + \partial^i h^{\alpha\beta} + \eta^{\beta i} \partial^\alpha h_\sigma^\sigma] + O(h^3). \quad (3.48)$$

For the khronon terms, we find that at quadratic order in the unitary gauge

$$\Theta_\chi^i = M_b^2 \left[\bar{K}^{(\alpha i)} (\bar{\Gamma}_{\alpha 0}^0 + \eta_{\alpha\rho} \bar{\Gamma}_{00}^\rho) - \bar{K}^{i0} \bar{\Gamma}_{00}^0 \right]. \quad (3.49)$$

From this expression it is clear that the notion of energy (3.44) is not well defined for spacetimes with radiation at infinity satisfying conditions (3.51). This is an unphysical divergence, which is regularized for a flux of energy of finite duration [101]. For our purposes, it is enough to notice that the time variation (3.47) (and hence the flux) is well defined for these boundary conditions. Also, only the part of the integral quadratic in perturbations does not vanish, which implies that the previous expressions are enough to compute the flux of energy at infinity. The steps to go from the previous formula to the final result (3.53) are explained in the next section, Sec. 3.7.

3.7 Energy-loss formulae for post-Newtonian systems

In deriving the energy-loss formula, we make the following assumptions. We start by assuming that our system consists of an asymptotically Minkowski

spacetime at early times, with the following fall-off properties in the unitary gauge,

$$g_{\mu\nu} = \eta_{\mu\nu} + O(1/r), \quad \partial_\alpha g_{\mu\nu} = O(1/r^2), \quad \chi = 0. \quad (3.50)$$

As for the matter fields, we assume that they vanish asymptotically to ensure that there are no boundary integral contributions. The previous conditions allow us to define a convenient notion of conserved energy \mathcal{E} , Eq. (3.44), as the conserved charge associated to the invariance of the asymptotic solution under asymptotic time translations¹⁰. To compute the flux of gravitational radiation, we consider the moment of time when the emitted GWs are already at spatial infinity, which means that the fall-off properties of the fields change to

$$h_w \sim O(1/r), \quad \dot{h}_w \sim \omega O(1/r), \quad \partial_r h_w \sim \omega/c_s O(1/r). \quad (3.51)$$

The quantity \mathcal{E} with these boundary conditions is in general divergent. Nevertheless, its change due to the radiation emitted during a finite interval of time is well-defined [101]. We focus on computing the time variation of \mathcal{E} , Eq. (3.47). As shown in Section 3.6, $\dot{\mathcal{E}}$ is finite for conditions (3.51) and only has contributions that are quadratic in the fields.

We also consider the time average of the quantity $\dot{\mathcal{E}}$ over several periods of the source, $\langle \dot{\mathcal{E}} \rangle$. The final averaged energy-loss formula is a standard observable in GW experiments (including the binary system of interest, where the observed damping of the orbits occurs after several periods) and the final expression is simplified since total time derivatives vanish when integrated.

The final expression is further simplified after one takes into account the following considerations. From the form of the solution of the tensor modes, Eq. (3.29a), and of the field ψ , Eq. (3.31), then in the far-zone these fields satisfy the equation

$$c_\sigma \partial_i \sigma = -\hat{\mathbf{r}}^i \dot{\sigma}, \quad (3.52)$$

for the corresponding speeds of propagation. Remember also that in the far-zone, the tensor modes t_{ij} are transverse with respect to the algebraic projector $\hat{\mathbf{r}}^i t_{ij} = 0$. For the vector part, we already showed that it does not contribute to $\langle \dot{\mathcal{E}} \rangle$, as its time derivative cancels, cf. Eq. (3.30). Similarly, the fields E and ϕ always appear under a time or a space derivative. Thus, we notice that the dependence on the source appearing in Eq. (3.33) will be either higher order in R/r for the space derivatives (and therefore negligible), or of the form

$$\int d^3 \tilde{x} \dot{\tau}_{00} = -M_b^2 \int d^3 \tilde{x} \bar{Q}_\chi = M_b^2 \int d^3 \tilde{x} \partial_i (\sqrt{-g} J^i)^{NL} = 0.$$

So, only the ψ contribution for E and ϕ is non-zero, and therefore these fields satisfy relation (3.52). In fact, the latter relation is also satisfied by the scalar part of h_{ij} .

The previous considerations (and some algebra presented in the Section 3.6) yield the final result for the rate of energy loss of the system,

$$\langle \dot{\mathcal{E}} \rangle = -\frac{M_b^2}{4} \oint_{S_\infty^2} d\Omega r^2 \left\langle \frac{1}{c_t} \dot{t}_{ij} \dot{t}_{ij} - \frac{8(\alpha-2)}{\alpha c_s} \dot{\psi} \dot{\psi} \right\rangle. \quad (3.53)$$

¹⁰Even if this symmetry is broken by the background for the field φ , it is still a symmetry due to the reparametrization invariance of the theory (3.2).

Whereas the radiation emitted in the tensor modes always decreases the energy of the system, the behaviour of the emitted scalar modes depends on the parameter α . We see that the emitted energy is positive for the range $0 < \alpha < 2$, as expected since these values are also required for the stability of the Minkowski background (absence of ghosts) [18].

Up to this point, we have consistently worked to first PN order (which corresponds to and includes $O(v^5)$ in the wave-forms). Given the time derivatives in Eq. (3.53), substitution of the waveforms (3.29a) and (3.31) yields the energy loss of the system from gravitational radiation up to and including $O(v^{12})$, although the leading order of the expression is $O(v^{10})$. To simplify what follows, we therefore focus on Newtonian sources and the corrections at this order. Substituting the waveforms to lowest PN order in the previous expressions and performing the angular integrals, we find the energy-loss formula¹¹

$$\langle \dot{\mathcal{E}} \rangle = -\frac{1}{8\pi M_b^2} \left\langle \frac{\mathcal{A}}{5} \ddot{Q}_{ij} \ddot{Q}_{ij} + \mathcal{B} \dot{I} \dot{I} \right\rangle, \quad (3.54)$$

where (recall Eq. (3.32))

$$\mathcal{A} \equiv \frac{1}{c_t} - \frac{3\alpha(Z-1)^2}{2c_s(\alpha-2)}, \quad \mathcal{B} = -\frac{\alpha Z^2}{4c_s(\alpha-2)}.$$

The final expression, Eq. (3.54), differs from the general relativity result in two ways: the coefficient corresponding to the quadrupole depends on the parameters of the model; there is a monopole contribution already at this first Newtonian order. This is similar to the formula derived for æ-theory¹² [91]. Let us note something quite remarkable in the context of the khronometric theory that we are studying. All of the Solar System tests are passed in the limit $|\alpha_1^{PPN}| \ll 1$, $|\alpha_2^{PPN}| \ll 1$, see Table 2.1, which can be achieved by the single requirement $|\alpha - 2\beta| \ll 1$, cf. (3.20). In this limit, $Z = 1$, the dipole term (3.28) cancels and the monopole contribution in Eq. (3.54) is still present. This last result contrasts with the æ-theory case for which there is only a modified quadrupole (in the equivalent limit). This discontinuity between the two theories is discussed in Section 3.9.

3.8 Energy loss by a Newtonian binary system

To complete the calculation, the power-loss formula (3.54) must be supplemented by the equations of motion of the system to desired PN order. We content ourselves with a 2-body Newtonian system composed of point-masses m_1 and m_2 . The matter action is then given by

$$S^m = -\sum_{A=1}^2 \int m_A ds_A, \quad (3.55)$$

¹¹In this final formula, we compute the quadrupole and monopole terms at a time when radiation from both the tensor and scalar modes simultaneously reaches the boundary of the isolated system. For different speeds of propagation c_t and c_s , the discrepancy in emission time is irrelevant for stationary production of GWs.

¹²For the monopole and quadrupole contributions, the definition of Z in [91] differs from Eq. (3.32) by a factor of two. We attribute this difference to a typo in [91].

where ds_A represents the proper-time of the A -th particle. A priori, m_A depends on the khronon field. Since we are only interested in the Newtonian system, it is enough to Taylor expand the mass around its background value and use only the leading order contribution, hence m_A is taken to be constant. Using the preferred time as the affine parameter, the energy-momentum tensor derived from (3.55) is

$$T_{\mu\nu}^m = \frac{1}{\sqrt{-g}} \sum_{A=1}^2 \frac{m_A u_{A\mu} u_{A\nu}}{\sqrt{g_{\rho\sigma} u_A^\rho u_A^\sigma}} \delta^{(3)}(x^k - x_A^k(t)),$$

where the A -th body follows the trajectory $x_A^k(t)$ with four-velocity u_A^μ . At Newtonian order this yields

$$\ddot{I}_{ij}(t - r/c_\sigma) = \partial_0^2 \sum_{A=1}^2 m_A x_A^i(t - r/c_\sigma) x_A^j(t - r/c_\sigma).$$

We evaluate this at very late times as explained in the previous section. Next, from the geodesic equation derived from (3.55), we find Newton's law

$$\ddot{x}_1^i = -G_N \frac{m_2}{r_{12}^2} \hat{\mathbf{r}}_{12}^i, \quad \ddot{x}_2^i = G_N \frac{m_1}{r_{12}^2} \hat{\mathbf{r}}_{12}^i,$$

where we introduce

$$r_{12}^i \equiv x_1^i - x_2^i. \quad (3.56)$$

As usual in binary systems, it is convenient to define the problem in terms of the relative distances and the position of the center of mass $x_{CM} \equiv \frac{m_1 x_1 + m_2 x_2}{m_1 + m_2}$. Finally, assuming¹³ that the system is at rest with respect to the preferred frame (so that $\dot{x}_{CM} = 0$) we get

$$\ddot{I}_{ij}(t - r/c) = -\frac{2G_N \mu M}{r_{12}^2} \left(4\hat{\mathbf{r}}_{12}^{(i} v^{j)} - 3\hat{\mathbf{r}}_{12}^i \hat{\mathbf{r}}_{12}^j \dot{r}_{12} \right).$$

with $\mu \equiv m_1 m_2 / M$, $M \equiv m_1 + m_2$ and $v^i \equiv \dot{r}_{12}^i$ is related to the expansion parameter v . Thus, the loss of energy in gravitational radiation for a Newtonian binary system is given by

$$\langle \dot{\mathcal{E}} \rangle = -\frac{1}{\pi M_b^2} \left(\frac{G_N M \mu}{r_{12}^2} \right)^2 \left\langle \frac{1}{15} \mathcal{A} (12v^2 - 11\dot{r}_{12}^2) + \frac{\mathcal{B}}{2} \dot{r}_{12}^2 \right\rangle, \quad (3.57)$$

from which we deduce the Peters-Mathews parameters, already discussed in Section 2.4,

$$\kappa_1 = 12(1 - \alpha/2)\mathcal{A}, \quad \kappa_2 = (1 - \alpha/2) \left(11\mathcal{A} - \frac{15}{2}\mathcal{B} \right).$$

Once the energy loss for the binary system is known, one can use Kepler's third law to relate it to the damping of the orbit. The expression for the change of the orbit's period for generic Peter-Mathews parameters in terms of other orbital parameters of the system can be found in [103].

¹³ Corrections to this assumption are considered as higher order in the PN expansion.

In general relativity, the previous analysis suffices to predict the radiation damping of binary systems for compact (relativistic) sources, like the PSR1913+16 [10]. This is because the structure of the compact stars of the binary does not influence the orbit in general relativity (this is called the ‘effacing principle’ which is a consequence of the strong equivalence principle). This is certainly not true for most alternative theories of gravity. Thus, to yield concrete predictions about the radiation damping of systems with highly relativistic sources (sources with large self-energies), one must first understand the behaviour of the fields beyond the PN approximation. One can then use Eq. (3.54) to derive the energy loss resulting in a change of the orbit (at corresponding PN order). For scalar-tensor theories, the final result is a test of the strong-field regime [104, 43, 105]. For \mathfrak{x} -theory, the first steps were performed in [91] based on the stellar solutions of [94] and using the effective field theory methods of [23, 106, 107, 108]

It is beyond the scope of this Chapter to derive the radiation damping of these realistic systems (including relativistic self-gravitating objects) for khronometric theory. In any case, we do not expect the new corrections to cancel the ones we have already derived for the Newtonian source, and thus we find it appropriate to use Eq. (3.57) to set order of magnitude bounds on the free parameters of the khronometric action (3.4). Current data on the radiation damping of the Hulse-Taylor binary system agrees with general relativity up to a level slightly better than one part in one hundred [65, 1]. This means that the formula (3.57) should agree with general relativity to $O(10^{-2})$, which finally implies the bound (for the case where α , β and λ are of the same order)

$$\alpha \sim \beta \sim \lambda \lesssim 10^{-2}. \quad (3.58)$$

The previous bound is less stringent than the bounds coming from the PPN analysis [20, 10],

$$|\alpha_1^{PPN}| \lesssim 10^{-4}, \quad |\alpha_2^{PPN}| \lesssim 10^{-7}.$$

As can be directly seen from Eq. (3.20), the PPN bounds are automatically satisfied in the limit $\alpha = 2\beta$. In this limit, $Z = 1$, and our expression (3.58) yields the most stringent bound for the theory. Notice in particular that it constrains the propagation speeds to be close to $c = 1$. Another constraint in this limit comes from the difference between G_N as derived in (3.56) and the value for Newton’s constant appearing in Friedmann’s equation, G_c [18]. The value of G_c is constrained by nucleosynthesis and satisfies $\left| \frac{G_N}{G_c} - 1 \right| \leq 0.13$ [109], which, in terms of the parameters in the action (3.4), implies the estimate $\alpha, \beta, \lambda \lesssim 0.1$ [18]. Also, we should ensure the absence of gravitational Cherenkov radiation, which implies $c_t^2 \geq 1$ and $c_s^2 \geq 1$ (this means that a particle moving through the aether does not radiate¹⁴). Notice that the speeds are superluminal, which does not pose a threat to Lorentz violating theories as long as causality is maintained [17].

¹⁴We thank D. Levkov and S. Sibiryakov for pointing this out to us.

3.9 The Einstein-aether and the monopole

The Einstein-Aether with metric $g_{\mu\nu}$ and æther u^μ is defined by the following action

$$S = -\frac{M^2}{2} \int d^4x \sqrt{-g} \left[R + \tilde{K}^{\mu\nu}{}_{\sigma\rho} \nabla_\mu u^\sigma \nabla_\nu u^\rho + \lambda(u^a u_a - 1) \right]. \quad (3.59)$$

where R is the Ricci scalar, the tensor $\tilde{K}^{\mu\nu}{}_{\sigma\rho}$ is given by

$$\tilde{K}^{\mu\nu}{}_{\sigma\rho} \nabla_\mu \equiv c_1 g_{\sigma\rho}^{\mu\nu} + c_2 \delta_\sigma^\mu \delta_\rho^\nu + c_3 \delta_\rho^\mu \delta_\sigma^\nu + c_4 u^\mu u^\nu g_{\sigma\rho} \quad (3.60)$$

and the c_i are dimensionless coupling constants. The æther is imposed to be timelike of unit norm, so the term proportional to λ enforces this constraint and λ is a Lagrange multiplier. In the weak-field, slow-motion limit, æ-theory reduces to Newtonian gravity, where the constant M is related to Planck's mass M_P by

$$M_P \equiv M \left(1 - \frac{c_{14}}{2} \right) \quad (3.61)$$

where $c_{14} = c_1 + c_4$. The PPN parameters of æ-theory coincide with those of general relativity, with the exception of α_1 and α_2 which are nonzero for æ-theory. In particular, the nonzero parameters of æ-theory are given by the following:

$$\begin{aligned} \beta &= \gamma = 1 \\ \alpha_1 &= \frac{-8(c_3^2 + c_1 c_4)}{2c_1 - c_1^2 + c_3^2} \\ \alpha_2 &= \frac{\alpha_1}{2} - \frac{(c_1 + 2c_3 - c_4)(2c_1 + 3c_2 + c_3 + c_4)}{(c_1 + c_2 + c_3)(2 - c_{14})} \end{aligned} \quad (3.62)$$

In both khronometric and Einstein-aether theories, we compare the monopole contribution to the energy-loss formula in the limit for which the PPN parameters are identical to general relativity.

The free parameters of khronometric theory are α , β and λ and those of the Einstein-aether [81] are c_i for $i = 1, \dots, 4$. We have the correspondence¹⁵ $c_1 = 0$, $c_2 = \lambda$, $c_3 = \beta$ and $c_4 = \alpha$. Notice that one less parameter is needed to define khronometric theory. This is because the action of a hypersurface orthogonal aether (which is equivalent to khronometric theory [20]) contains a term that can be absorbed by the others, reducing the number of independent terms from four down to three [83].

Comparing the results of this Chapter and the work presented in [22], we see that the waveforms for the spin-0 and spin-2 modes are essentially identical. The main difference comes from the expression for Z of Eq. (3.32). Let \tilde{Z} be the equivalent expression in æ-theory,

$$\tilde{Z} \equiv \frac{(c_{13} - 1)(\tilde{\alpha}_1^{PPN} - 2\tilde{\alpha}_2^{PPN})}{3(c_{14} - 2c_{13})}, \quad (3.63)$$

¹⁵Recall that we are using the mostly minus signature. The mostly plus signature is used in [22] and leads to a different correspondence between the parameters.

where $\tilde{\alpha}_1^{PPN}$, $\tilde{\alpha}_2^{PPN}$ are the Lorentz violating PPN parameters in \mathfrak{a} -theory and $c_{ij} = c_i + c_j$. Then the khronometric expression for Z is precisely \tilde{Z} , but with $c_1 = 0$.

The limit $\alpha_1^{PPN} = \alpha_2^{PPN} = 0$ in khronometric theory can be achieved by setting $\alpha = 2\beta$ and leads to $Z = 1$. By inspection of the energy-loss formula (3.54), we see that the monopole is proportional to Z and therefore persists in this limit. In generic \mathfrak{a} -theory, the equivalent limit that sets the PPN parameters of Eq. (3.62) to general relativity is given by

$$c_2 = \frac{-2c_1^2 - c_1c_3 + c_3^2}{3c_1}, \quad c_4 = -\frac{c_3^2}{c_1} \quad (3.64)$$

and leads to $\tilde{Z} = 0$. The corresponding monopole is proportional to \tilde{Z} and subsequently vanishes in this limit. Therefore, the values of Z and \tilde{Z} explain the presence or absence of the monopole in the limit when the PPN parameters are identical to those of general relativity.

It is natural to ask if \tilde{Z} can be tweaked so that \mathfrak{a} -theory has a monopole when $\tilde{\alpha}_1^{PPN} = \tilde{\alpha}_2^{PPN} = 0$. A first possibility would be to consider the limit that resembles khronometric theory, namely $c_1 = 0$ and $c_4 = 2c_3$. This leads to $\tilde{Z} = 1$, like in khronometric theory, indicating that a monopole may be possible. However, requiring only $c_1 = 0$ implies that $\alpha_1^{PPN} = 8$, which clearly violates constraints on α_1^{PPN} . One could try to set $c_1 = 0$ and $c_3 = 0$ to get $\alpha_1^{PPN} = 0$, but this case of \mathfrak{a} -theory has yet to be studied [81], but anyway results in vanishing propagation speeds for the tensor and vector sectors of the theory. Alternatively, one may try to make the denominator in (3.63) vanish to retrieve a finite limit. Setting $c_{14} = 2c_{13}$ yields $\tilde{Z} = 1$. However, the second condition in (3.64) implies $c_1 = c_3 = c_4 = 0$, which is a singular limit for \mathfrak{a} -theory.

3.10 Discussion

Our aim has been to study the radiation loss from an isolated source in the PN approximation for khronometric theory. This theory is an interesting alternative to general relativity with a high energy cutoff and for which a UV completion may be possible in the form of Hořava gravity. It is also very similar to \mathfrak{a} -theory, as in both cases there is a preferred time coordinate. The difference is that khronometric theory has only one extra scalar degree of freedom, the khronon, whereas \mathfrak{a} -theory relies on a timelike unit dynamical vector leading to three extra degrees of freedom, consisting of one scalar and one vector field.

For arbitrary parameters, we have shown in Eq. (3.54) that the formula controlling the power loss of the system (which may be related to the change of the orbital period of a binary source) is modified with respect to general relativity already at lowest, Newtonian, order. In particular, the quadrupole contribution differs from general relativity, partly due to the different speeds of propagation of the tensor modes in both theories. Furthermore, there is also an extra monopole contribution at this order. The monopole at leading order in khronometric theory contrasts with the usual situation in other scalar-tensor theories [21]. At higher order, there are other modifications, including the dipole term

(3.28). Quite remarkably, in the phenomenologically interesting limit where all PPN parameters coincide with general relativity (which corresponds to the limit $\alpha = 2\beta$ for our parameters), the monopole is still present, and its strength is proportional to the parameters appearing in the action of the theory, Eq. (3.4). These results for khronometric theory are similar to those of æ-theory, modulo vector propagating degrees of freedom that are absent for the khronometric case. There is a key difference, however, since æ-theory only has a modified quadrupole to lowest order in the equivalent limit.

This chapter has been devoted to PN sources. These types of sources do not correspond to the ones found in the binary systems of interest, which are compact and characterized by strong gravitational fields. Despite this, we have evaluated the energy-loss formula for the simplest possible system: a Newtonian binary. Doing so provides an order of magnitude estimate on the parameters of the theory (as we do not expect corrections due to strong-fields to cancel the modifications apparent in the power loss formula). Thus, our results are relevant for constraining the case $\alpha = 2\beta$. In this case, requiring the rate of radiation damping to be close to general relativity sets constraints on this parameters of order $O(10^{-2})$. These constraints represent the strongest phenomenological bounds for this particular choice of parameters and are relevant for the cosmological implications of the theory, including the recently suggested model of dark-energy [110].

Sources with strong self-energies is left for future research and can be treated in our theory in the same way as scalar-tensor theories [104, 43, 105]: a phenomenon of “scalarization” modifies the orbit of these sources as compared with the post-Newtonian ones. It would also be interesting to consider our results in the parametrized post-Einsteinian framework introduced in [111] (see also [112] for the binary pulsar constraints for this framework). Finally, the consequences of alternatives theories of gravity for experiments of direct detection of GWs have been recently discussed, see e.g. [65, 113]. We hope to extend this works to khronometric theories in the future.

Chapter 4

Effective field theory analysis of general relativity

While general relativity is one of the most successful theories of our time, it is typically viewed as an effective field theory, valid below some energy scale known as the cutoff, but unreliable at energies above. In effective field theory, the effect of quantum processes at arbitrarily high energies contribute to what is observed at low energies. These high energy processes renormalize the coupling constants of the theory. While physicists today are searching for ways to complete general relativity at high energies with some quantum theory of gravity, it is not necessary to know the full quantum theory in order to make meaningful predictions, as long as the system of study is well below the cutoff. This is precisely what Goldberger and Rothstein do in determining post-Newtonian corrections for the problem of gravitating bodies. In particular, their method takes a low speed limit of general relativity to describe gravitating bodies. Based on their effective field theory method, we propose a way to measure deviations from general relativity with Solar System and gravitational radiation tests.

First of all, we adopt a phenomenological approach to general relativity. To understand what we mean by this statement, consider perturbations of the metric around Minkowski $g_{\mu\nu} = \eta_{\mu\nu} + \kappa h_{\mu\nu}$, where κ characterizes the gravitational coupling. Then the Einstein-Hilbert action is

$$S_{EH} = -2\frac{1}{\kappa^2} \int d^4x \sqrt{g} R(x) \quad (4.1)$$

$$\rightarrow -2\frac{1}{\kappa^2} \int d^4x [c_2(\partial h)^2 + c_3 h(\partial h)^2 + c_4 h^2(\partial h)^2 \dots] \quad (4.2)$$

where we have ignored the tensor structure for the sake of illustration. From the theoretical point of view of general relativity, this structure is fixed by definition of the Einstein-Hilbert action. The coefficients c_n are given by $c_n = \kappa^n$ for $n \geq 2$. In general relativity, the coupling κ is taken to be of order of the inverse Planck's mass¹ $\kappa \equiv 1/M_{Pl} \equiv (32\pi G_N)^{1/2}$ and is already defined by the theory.

¹In this chapter, we use the definition of Planck's mass given in [23]

From the phenomenological point of view of a gauge theory, we could start from the expanded action (4.2) and determine the coefficients by experiment, the way coupling constants are determined experimentally in the Standard Model. In this chapter, we adopt this experimental approach and propose to measure the coefficients c_3 and c_4 based on EFT methods. The terms proportional to $h(\partial h)^2$ and $h^2(\partial h)^2$ describe the trilinear and quartic self-interactions respectively. In this sense, we propose an EFT way to test the non-linear structure of general relativity. This is similar in spirit to the search of deviations from the standard model, in which the triple and quartic gauge boson couplings were measured at LEP2 and at the Tevatron [114, 115, 116]

As discussed in Section 1.4, the effective field theory method of Goldberger and Rothstein [23] presents a way to calculate PN corrections to gravitational wave observables from n-body systems. Recall that the method, called NRGR, is an effective field theory of interacting massive bodies under the influence of gravity as described by Einstein’s relativity. It is ‘non-relativistic’ because the bodies being studied move at speeds v much smaller than the speed of light. Essentially, the gravitational field is described by the Einstein-Hilbert action while the interaction of the massive bodies is described by point-particles moving along their respective worldlines. After untangling the long and short wavelength physics, the post-Newtonian corrections are represented by Feynman diagrams which can be organized in powers of v ($c = 1$). NRGR tells us that binary systems probe both the radiative sector of the theory, through the emission of gravitational radiation, and the bound system, through the non-linearities intrinsic to general relativity which are already present in the conservative part of the Lagrangian. In the language of field-theory, these non-linearities can be traced to the non-abelian vertices of the theory, such as the three- and four-graviton vertices. It is therefore natural to ask whether we can extract a measurement of these vertices from binary pulsars or from future observations of coalescing binaries at interferometers.

Given NRGR, we propose a way to measure these coefficients by observing binary systems and their post-Newtonian dynamics. Practically, this is done by allowing the coefficients c_3 and c_4 to be arbitrary. We then calculate gravitational wave observables with these arbitrary coefficients using NRGR and deduce their values from the Solar System and gravitational radiation tests of Chapter 2. Taking for example the three-graviton vertex, we parametrize deviation from the usual general relativity value by β_3 so that we recover general relativity when $\beta_3 = 0$. The coefficient c_3 and parameter β_3 are then related by $c_3 = (1 + \beta_3)/M_{Pl}^3$. Next, we rederive the gravitational wave observables with these modified coefficients i.e. β_3 is introduced as a ‘tag’ that allows us to track deviation from its general relativity value throughout the computations. The same technique is applied to c_4 , for the four-graviton vertex, where deviation from its general relativity value is parametrized by β_4 .

Assumed in our approach is that general relativity is the correct effective field theory. From a theoretical point of view, β_3 and β_4 are strictly zero. From an experimental point of view, β_3 and β_4 are to be determined by measurement. Although they are expected to be extremely small, β_3 and β_4 are nonzero due to the nature of experimental error. It then becomes possible to compare experimental data to determine which tests provide the most stringent constraints.

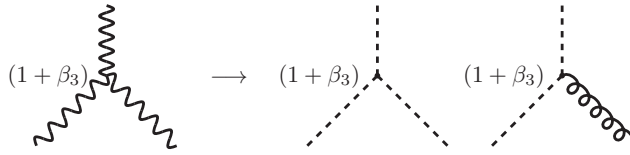


Figure 4.1: Experimental bound on the three-graviton vertex parametrized by a small deviation β_3 from the general relativity value in the de Donder gauge. Wiggly lines, dashed lines and curly lines respectively represent $h_{\mu\nu}$, potential gravitons $H_{\mathbf{k}\mu\nu}$ and radiation gravitons $\bar{h}_{\mu\nu}$.

This chapter is organized as follows. In Section 4.1, we analyze the three-graviton vertex in detail. Notably, we explain how to measure deviations of the three-graviton vertex from the bound system and from the radiative system. We also provide measurements from lunar-laser ranging, from the Hulse-Taylor binary and provide estimates for future interferometers. We also show that lunar laser ranging provides a better bound on deviations from general relativity than what can be expected at interferometers. In Section 4.2, we briefly discuss the four-graviton vertex. In Section 4.3, we discuss our method and compare it with other approaches to testing theories of gravitation. In particular, we discuss what it means to allow β_3 and β_4 to deviate from their standard general relativity values from a theoretical point of view. We point out that our method is a phenomenological one and we compare it with the PPN formalism [11]. It is also important to note that we propose a method that tests for small deformations of general relativity, where perturbation theory is appropriate, although we do not attempt to construct an underlying quantum theory of gravity that gives rise to these deviations.

4.1 Measuring the three-graviton vertex

The effective field theory approach NRGR offers a way to visualize PN corrections with Feynman diagrams. We see immediately from figures (1.4) and (1.5) that the three-graviton vertex can already be probed by experiment: it contributes to the bound system at 1PN and to leading order in the radiative sector of general relativity. The method described above amounts to multiplying the three-graviton vertex by a factor $(1 + \beta_3)$.

In this section, we calculate the effect of β_3 on the EIH Lagrangian, the radiation formula and the phase. We compare these results with experimental data. From the deformed Einstein-Infeld-Hoffmann Lagrangian, we obtain a bound of $|\beta_3| < 2 \times 10^{-4}$ from Lunar laser ranging. From the deformed quadrupole formula, we obtain $\beta_3 = (4.0 \pm 6.4) \times 10^{-4}$ from the Hulse-Taylor binary, which is slightly worse but still comparable to the bound from Lunar laser ranging. Finally, we show that study of the phase at interferometers is not competitive with the previous bounds due to degeneracy with spin.

4.1.1 The modified bound system

Allowing for a small deviation in the three-graviton vertex affects the HHH and $HH\bar{h}$ vertices². Following the NRGR procedure with nonzero β_3 , we get an additional contribution to the EIH Lagrangian of eq. (1.52), proportional to β_3 ,

$$L_{cons}^{\beta_3} = L_{EIH} - \beta_3 \frac{G_N^2 m_1 m_2 (m_1 + m_2)}{r^2} \quad (4.3)$$

Let's compare this result with the Lagrangian whose equations of motion are the same as the equations of motion of a test particle in the PPN metric. In Section 2.3 on the PPN formalism, we were presented with the most general PPN metric. A metric theory where all of the PPN parameters vanish except for the Eddington parameters $\beta^{PPN} = \gamma^{PPN} = 1$, to 1PN, is given by

$$\begin{aligned} g_{00} &= 1 - 2U + 2\beta^{PPN}U^2 \\ g_{0i} &= \frac{1}{2}(4\gamma^{PPN} + 3)V_i \\ g_{ij} &= -(1 + 2\gamma^{PPN}U)\delta_{ij} \end{aligned} \quad (4.4)$$

Recall that this metric is generated by a source, treated as a perfect fluid with density $\rho(\mathbf{x})$ and velocity field $v(\mathbf{x})$. The terms U and V_i are generalized potentials defined over a fluid source defined in eq. (2.18). The PPN parameters, notably the Eddington parameters, have been extensively probed by experiment, see Table 2.1. Writing $\beta^{PPN} = 1 + \bar{\beta}$ and $\gamma^{PPN} = 1 + \bar{\gamma}$, the experimental bounds are

$$\bar{\gamma} = (2.1 \pm 2.3) \times 10^{-5} \quad (4.5)$$

from the Doppler tracking of the Cassini spacecraft, and

$$4\bar{\beta} - \bar{\gamma} = (4.4 \pm 4.5) \times 10^{-4} \quad (4.6)$$

from lunar laser ranging due to the Nordtvedt effect [65]. In general metric theories of gravity, the Earth and the Moon fall towards the Sun with slightly different accelerations due to their gravitational self-energy and is monitored by measuring the Earth-Moon distance by sending laser light to retroreflectors set on the moon during the Apollo program. The perihelion shift of Mercury, on the other hand, provides the bound $\bar{\beta} \leq 3 \times 10^{-3}$ [117].

In the PPN formalism, the 1PN correction to Newton's potential (for semi-conservative theories without preferred frame effects i.e. such that the following PPN parameters vanish $\alpha_1 \equiv \alpha_2 \equiv \xi \equiv \zeta_1 \equiv \zeta_2 \equiv \zeta_3 \equiv \zeta_4 \equiv 0$, see eq. (6.80) of [10]) is given by

$$\begin{aligned} L_{PPN} &= \frac{1}{8} \sum_a m_a \mathbf{v}_a^4 + \frac{G_N m_1 m_2}{2|\mathbf{x}_1 - \mathbf{x}_2|} \times \\ &\quad \left((2\gamma_{PPN} + 1)(\mathbf{v}_1^2 + \mathbf{v}_2^2) - (4\gamma_{PPN} + 3)\mathbf{v}_1 \cdot \mathbf{v}_2 - \frac{(\mathbf{x}_{12} \cdot \mathbf{v}_1)(\mathbf{x}_{12} \cdot \mathbf{v}_2)}{|\mathbf{x}_1 - \mathbf{x}_2|^2} \right. \\ &\quad \left. - (2\beta_{PPN} - 1) \frac{G_N(m_1 + m_2)}{|\mathbf{x}_1 - \mathbf{x}_2|} \right) \end{aligned} \quad (4.7)$$

²Recall from Section 1.4 that H and h represent potential and radiation gravitons respectively.

Comparing L_{PPN} of eq.(4.7) and $L_{cons}^{\beta_3}$ of eq.(4.3), we see that β_3 and the Eddington parameter β^{PPN} are related to each other by $\beta^{PPN} = 1 + \beta_3$. Note that this comparison makes sense since both β^{PPN} and β_3 are gauge invariant and are therefore observables: they have been defined with respect to a specific gauge, respectively the standard PPN gauge and the de Donder gauge. In other words, experimental bounds on the three-graviton vertex from experiment are translated into

$$|\beta_3| < 3 \times 10^{-3} \quad (4.8)$$

from the perihelion of Mercury, and

$$|\beta_3| < 2 \times 10^{-4} \quad (4.9)$$

(at 68%c.l.) from lunar laser ranging. We conclude here that lunar laser ranging provides the best bound on β_3 when probing the conservative sector of the theory.

4.1.2 The modified power radiated

Following the NRRG procedure with nonzero β_3 for determining the radiation, we get the following effective radiation Lagrangian

$$L_{rad}^{\beta_3} = \frac{1}{2M_{Pl}} (Q_{ij}R_{0i0j} + qR_{0i0i} + \beta_3(3Vh_{00} + Z_{ij}h_{ij})) \quad (4.10)$$

where as usual, $Q_{ij} = \sum_a m_a x_{ai} x_{aj}$ is the quadrupole moment of the source and we define

$$\begin{aligned} q &= \frac{1}{3} \sum_a m_a x_a^2 \\ V(r) &= \frac{G_N m_1 m_2}{r} \\ Z_{ij}(r) &= \frac{G_N m_1 m_2 r_i r_j}{r^3} \end{aligned} \quad (4.11)$$

where $r = |\mathbf{x}_1 - \mathbf{x}_2|$. The terms proportional to β_3 are induced by the modification of the three-graviton vertex. We have omitted the terms in h_{00} and h_{0i} since, as we know from (1.55), these are coupled to conserved quantities and therefore do not radiate.

We then calculate the imaginary part of the self-energy diagram in fig. (1.6) with L_{rad} to get the power radiated. In our case, we compute the imaginary part of

$$- \frac{i}{8M_{Pl}^2} \sum_{a,b=1}^4 \int dt_1 dt_2 I_{ij}^a(t_1) I_{kl}^b(t_2) \langle S_{ij}^a(t_1) S_{kl}^b(t_2) \rangle \quad (4.12)$$

where $I_{ij}^a = (Q_{ij}, q\delta_{ij}, \beta_3 V\delta_{ij}, \beta_3 Z_{ij})$ depends on the matter variables and $S_{ij}^a = (R_{0i0j}, R_{0i0j}, \delta_{ij}h_{00}, h_{ij})$ on the gravitational field. The P_{Qq} contribution vanishes identically since Q_{ij} is traceless. P_{qq} vanishes as well since $\delta_{ij}\delta_{kl}$ contracted with the two-point function $\langle R_{0i0j} R_{0k0l} \rangle \sim \delta_{ik}\delta_{jl} + \delta_{il}\delta_{jk} - \frac{2}{3}\delta_{ij}\delta_{kl}$ gives zero. Similarly, the contributions

from QV, qZ and VZ vanish as well. The contributions VV and ZZ are of order β_3^2 and can be neglected. We are left with

$$\begin{aligned} P_{QQ} &= \frac{G_N}{5} \langle \ddot{Q}_{ij} \ddot{Q}_{ij} \rangle \\ P_{QZ} &= -2\beta_3 G_N \langle \ddot{Q}_{ij} \dot{Z}_{ij} \rangle \\ P_{qV} &= -6\beta_3 G_N \langle \dot{q} \dot{V} \rangle \end{aligned} \quad (4.13)$$

P_{QQ} is the usual quadrupole formula obtained in relativity, while the new contributions coming from β_3 are P_{QZ} and P_{qV} .

Using the Keplerian equations of motion for an elliptic orbit of eccentricity e we get

$$\begin{aligned} P_{QQ} &= \frac{32G_N^4 \mu^2 m^3}{5a^5} f(e) \\ P_{QZ} &= \beta_3 \frac{32G_N^4 \mu^2 m^3}{5a^5 (1-e^2)^{7/2}} \left(\frac{5}{2} + \frac{175}{24} e^2 + \frac{85}{96} e^4 \right) \\ P_{qV} &= -\beta_3 \frac{32G_N^4 \mu^2 m^3}{5a^5 (1-e^2)^{7/2}} \left(\frac{5}{16} e^2 + \frac{5}{64} e^4 \right) \end{aligned} \quad (4.14)$$

where $f(e)$ was found in Eq. (1.61) for general relativity. For a Keplerian orbit of a binary system, the orbital energy of the system $E = \frac{1}{2} \mu (\dot{r}^2 + r^2 \dot{\psi}^2) - G_N \mu m / r$ (in the center of mass) is related to its period P_b by

$$P_b \propto (-E)^{-3/2} \quad (4.15)$$

therefore the evolution of the orbital period is

$$\frac{\dot{P}_b}{P_b} = -\frac{3}{2} \frac{\dot{E}}{E} \quad (4.16)$$

Combining this with the energy-balance equation $\dot{E} = -P$ and the total power radiated when $\beta_3 \neq 0$ of eq. (4.14)

$$\frac{\dot{P}_b}{P_b} = -\frac{96}{5} G_N^{5/3} \nu m^{5/3} \left(\frac{P_b}{2\pi} \right)^{-8/3} (f(e) + \beta_3 g(e)) \quad (4.17)$$

where $f(e)$ is the general relativity result (??) and

$$g(e) = \frac{1}{(1-e^2)^{7/2}} \left(\frac{5}{2} + \frac{335}{48} e^2 + \frac{155}{192} e^4 \right) \quad (4.18)$$

is the extra contribution proportional to β_3 . The masses of the two compact stars depend on two observables: the periastron shift ω and the Einstein time delay γ_E . In particular, the periastron shift fixes the total mass m of the system, while the Einstein time delay measures a combination of the masses (see e.g. eqns (6.56) and (6.93) of ref. [31]). Using $L_{cons}^{\beta_3}$ of eq. (4.3) and repeating the computation of the periastron shift ω , we find

$$\omega_{\beta_3} = \left(1 - \frac{\beta_3}{3} \right) \omega_{GR} \quad (4.19)$$

while the Einstein time delay remains unchanged since it is unaffected by the post-Keplerian parameters. Therefore, when $\beta_3 \neq 0$, the true value of the total mass m in eq. (4.17) is instead

$$m_{\beta_3} = \left(1 + \frac{\beta_3}{2}\right) m_{GR} \quad (4.20)$$

Similarly, the symmetric mass ratio becomes

$$\nu_{\beta_3} = (1 + w\beta_3) \nu_{GR} \quad (4.21)$$

where

$$w = \frac{\kappa}{3} \frac{\sqrt{1+4\kappa} - 2}{\sqrt{1+4\kappa}} \frac{1}{(1+4\kappa)^{1/2} - (1+\kappa)} \quad (4.22)$$

and

$$\kappa = \frac{\gamma}{e} \left(\frac{2\pi}{P_b}\right)^{1/3} (G_N m_{GR})^{-2/3} \quad (4.23)$$

Putting everything together, we find that the ratio between the \dot{P}_b for $\beta_3 \neq 0$ and its GR value is

$$\frac{\dot{P}_b^{\beta_3}}{\dot{P}_b^{GR}} = 1 + \beta_3 \tilde{g}(e) \quad (4.24)$$

to linear order in β_3 with

$$\tilde{g}(e) = \frac{g(e)}{f(e)} + \frac{5}{6} + w \quad (4.25)$$

The term $g(e)/f(e)$ comes from the effect of β_3 on the radiative sector of the theory whereas the term $(5/6) + w$ comes from its effect on the conservative sector, i.e. the mass determination. Inserting the numerical values for the Hulse-Taylor pulsar, we obtain $\tilde{g}(e) \simeq 3.21$, with a dominant contribution of $g(e)/f(e) \simeq 2.38$ coming from the radiative sector of the theory. For this binary pulsar, after correcting for the Doppler shift due to the relative velocity between us and the pulsar induced by the differential rotation of the Galaxy, the ratio between the observed value \dot{P}_b^{obs} and the GR prediction \dot{P}_b^{GR} is

$$\dot{P}_b^{obs}/\dot{P}_b^{GR} = 1.0013(21). \quad (4.26)$$

Interpreting this as a measurement of β_3 , we finally get

$$3.21\beta_3 = 0.0013(21), \quad (4.27)$$

which translates into

$$\beta_3 = (4.0 \pm 6.4) \times 10^{-4}, \quad (4.28)$$

so the experimental bound on the three-graviton vertex is consistent with the general relativity prediction to within 0.1%. This bound is slightly worse but still comparable to the one from lunar laser ranging, eq. (4.9). The bound obtained in (4.28), however, is obtained by probing the radiative sector of general relativity while the bound obtained from lunar laser ranging probes only the

conservative sector. For the double pulsar [118], we find $\tilde{g}(e) \simeq 3.3$. Since \dot{P}_b for the double pulsar is presently measured with an accuracy of about 1.4%, we get a larger bound compared to eq. (4.28). However, further monitoring³ of this system is expected to bring the error on \dot{P}_b down to the order of 0.1%.

4.1.3 The modified phase

We now compare these results with what can be expected from the detection of a binary coalescence at gravitational wave interferometers. In this case, one can determine the physical parameters of the inspiralling bodies by performing matched filtering of theoretical waveform templates. In the matched filtering method, any difference in the time behavior between the actual signal and the theoretical template model will eventually cause the two to go out of phase, with a consequent drop in the signal-to-noise ratio (SNR). The introduction of β_3 affects the template, and in particular the accumulated phase

$$\phi = 2\pi \int_{t_{\min}}^{t_{\max}} f(t) dt, \quad (4.29)$$

where $f(t)$ is the time-varying frequency of the source, and the subscript min (max) denotes the values when the signal enters (leaves) the detector bandwidth. Thus, in principle, detection of a gravitational wave signal from coalescing binaries could be translated into a measurement of the three-graviton vertex. In this section we investigate the accuracy of such a determination.

With respect to the timing of binary pulsars, there are at least three important qualitative differences that affect the accuracy at which these systems can test the non-linearities of general relativity. First, coalescing compact binaries in the last stage of the coalescence reach values of $v/c \sim 1/3$, and are therefore much more relativistic than binary pulsars, which rather have $v/c \sim 10^{-3}$. Second, the leading Newtonian result for ϕ is of order $(v/c)^{-5}$ so it is much larger than one, and to get the phase with a precision $\Delta\phi \ll 1$, as needed by interferometers, all the corrections at least up to $O(v^6/c^6)$ to the Newtonian result must be included, so higher-order corrections are important even if they are numerically small relative to the leading term. In other words, even if PN corrections are suppressed by powers of v/c with respect to the leading term, they can be probed up to high order because what matters for gravitational wave interferometers is the overall value of the PN corrections to the phase, and not their value relative to the large Newtonian term. These two considerations should suggest that interferometers are much more sensitive than pulsar timing to the non-linearities of general relativity.

On the other hand, for binary pulsars we can measure not only the decay of the orbital period due to gravitational wave emission, but also several other Keplerian observables that provide a determination of the geometry of the orbit, as well as post-Keplerian observables, such as the periastron shift and the Einstein time delay, which fix the masses of the stars in the binary system. This

³Our method has been recently used by Kramer et al. using more recent (still unpublished) data from the double pulsar. The result provides a more stringent bound on β_3 by a factor of approximately two (M. Kramer, personal communication).

is not the case for the detection of coalescences at interferometers. With interferometers, the parameters that determine the waveform, such as the masses and spins of the stars, must be determined from the phase of the gravitational wave itself, and one must then carefully investigate the degeneracies between the determination of β_3 and the determination of the masses and spins of the stars. This effect clearly goes in the direction of degrading the accuracy of parameter reconstruction at gravitational wave interferometers, with respect to binary pulsar timing, so in the end it is not obvious a priori which of the two, gravitational wave interferometers or binary pulsar timing, is more sensitive to the non-linearities of general relativity. In the rest of this section, we show that binary pulsar timing is indeed more sensitive.

The phase

Gravitational wave interferometers are sensitive to the accumulated phase of binary coalescences defined by

$$\phi = 2\pi \int_{t_{min}}^{t_{max}} f(t) dt \quad (4.30)$$

where $f(t)$ is the orbital frequency of the source and the signal stays in the detector band-width during a time t with $t_{min} \leq t \leq t_{max}$. In this section, we calculate the phase with PN corrections for a binary system in a circular orbit for general relativity.

The back-reaction of gravitational wave emission on the source can be computed from energy balance equation

$$P = -\dot{E} \quad (4.31)$$

where P is the power emitted and E is the energy of the bound system. Start by defining the gauge invariant quantity

$$x \equiv v^2 \equiv (G_N m \omega_s)^{2/3}, \quad (4.32)$$

where G_N is Newton's constant, $m = \sum_a m_a$ is the total mass of the bodies constituting the binary system and ω_s is the orbital frequency which is related to the orbital radius by $\omega_s^2 = Gm/R$. The PN expansions of P and E in terms of x are

$$\begin{aligned} E &= E_0 x (c_0 + c_1 x + c_2 x^2 + \dots) \\ P &= P_0 x^5 (d_0 + d_1 x + d_{\frac{3}{2}} x^{3/2} + d_2 x^2 + \dots) \end{aligned} \quad (4.33)$$

where for relativity, the values for the coefficients c_i and d_i , are [119]

$$E_0 = -\frac{\mu}{2}, \quad c_0 = 1, \quad c_1 = -\frac{3}{4} - \frac{\nu}{12}, \quad c_2 = \left(-\frac{27}{8} + \frac{19}{8}\nu - \frac{1}{24}\nu^2 \right), \quad (4.34)$$

$$\begin{aligned} P_0 &= \frac{32\nu^2}{5G}, \quad d_0 = 1, \quad d_1 = -\frac{1247}{336} - \frac{35}{12}\nu, \\ d_{\frac{3}{2}} &= 4\pi d_2 = -\frac{44711}{9072} + \frac{9271}{504}\nu + \frac{65}{18}\nu^2. \end{aligned} \quad (4.35)$$

$\mu \equiv m_1 m_2 / m$ is the reduced mass of the system and $\nu \equiv \mu / m$ is the dimensionless mass ratio. Plugging (4.33) into (4.31), we obtain

$$\dot{x} = -\frac{P_0 d_0}{E_0} x^5 \left[1 + \frac{d_1 - 2d_0 c_1}{d_0} x + \dots \right], \quad (4.36)$$

which can be solved perturbatively ($E_0 < 0, P_0 > 0$). We introduce a new time parameter $\Theta = \frac{P_0 b_0}{64 E_0} |t_c - t|$, where t_c is the time of coalescence. Using Θ , $d\phi/dt = \omega_s$, and the values in (4.34), we obtain the standard result

$$\phi = -\frac{\Theta^{5/8}}{\nu} \left(1 + a_1(\nu) \Theta^{-1/4} + a_2 \Theta^{-3/8} + \dots \right). \quad (4.37)$$

with

$$\begin{aligned} a_1(\nu) &= \frac{3715}{8064} + \frac{55}{96} \nu \\ a_2 &= -\frac{3\pi}{4} \end{aligned} \quad (4.38)$$

β_3 contribution to the phase

Setting $\beta_3 \neq 0$, we repeat the above computation of the orbital phase for a circularized orbit. The phase of the binary system is affected by the modified power emission due to β_3 . In rederiving the phase, the coefficient P_0 of (4.34) is replaced by the total power emitted as described by (4.14) for circular orbits ($e = 0$). We get

$$P_0^{\beta_3} = P_0 (1 + b_0 \beta_3 + \dots) \quad (4.39)$$

with $b_0 = 5/2$. To 1.5PN order and neglecting spin, the phase with $\beta_3 \neq 0$ is of the form

$$\phi = -\frac{\Theta^{5/8}}{\nu} \left[(1 + b_0 \beta_3) + a_1(\nu)(1 + b_1 \beta_3) \Theta^{-1/4} + a_2(1 + b_2 \beta_3) \Theta^{-3/8} \right] \quad (4.40)$$

with

$$\Theta = \frac{\nu |t_c - t|}{5 G_N m} (1 - b_0 \beta_3) \quad (4.41)$$

where Θ is the new β_3 -dependent time parameter; a_1, a_2 are respectively the 1PN and 1.5PN prediction in GR found in (4.37); and b_1, b_2 respectively parametrize the 1PN and 1.5PN correction due to β_3 for which, for our purposes, we estimate to be of order $\mathcal{O}(1)$.

We find that β_3 modifies the orbital phase $\phi(t)$ already at 0PN (i.e. Newtonian) level. To linear order in β_3 , eq. (4.40) is just

$$\phi^{0\text{PN}} = -\frac{\Theta^{5/8}}{\nu} (1 + b_0 \beta_3). \quad (4.42)$$

Combining the factors ν and m which enter in the definition of Θ with the explicit factor $1/\nu$ in eq. (4.42) we recover the well-know result that the Newtonian phase depends on the masses of the stars only through the chirp mass

$M_c = \nu^{3/5}m$. From eq. (4.42) we immediately understand the crucial role that degeneracies have for interferometers. In fact, since M_c is determined from eq. (4.42) itself, using only the 0PN phase, it is impossible to detect the deviation from the prediction of general relativity induced by β_3 . A non-zero value of β_3 would simply induce an error in the determination of M_c .

The same happens at 1PN level. In fact, at 1PN order and with $\beta_3 \neq 0$ the phase has the form

$$\phi^{\text{1PN}} = -\frac{\Theta^{5/8}}{\nu} \left[(1 + b_0\beta_3) + a_1(\nu)(1 + b_1\beta_3)\Theta^{-1/4} \right], \quad (4.43)$$

where, as before, $b_0 = -5/2$ is the 0PN correction proportional to β_3 , while $a_1(\nu)$ is the 1PN general relativity prediction [32, 31], and b_1 (which is possibly ν -dependent) parametrizes the 1PN correction due to β_3 . (For simplicity, we only write the term linear in β_3 explicitly, since $|\beta_3|$ is much smaller than one, but all our considerations below can be trivially generalized to terms quadratic in β_3 , just by allowing the function $b_1(\nu)$ to depend also on β_3). In general we expect b_1 to be $O(1)$, and we will see below that for our purposes this estimate is sufficient.

Using M_c and ν as independent mass variables, in place of m_1 and m_2 , we see that while the effect of β_3 on the 0PN phase can be reabsorbed into M_c , its effect on the 1PN phase can be reabsorbed into a rescaling of ν . Observe that, in the detection of a single coalescence event, gravitational wave interferometers do not measure the functional dependence of ν of the 1PN phase, but only its numerical value for the actual value of ν of that binary system, so we cannot infer the presence of a term proportional to β_3 from the fact that it changes the functional form of the ν -dependence from the one obtained by $a_1(\nu)$ in eq. (4.38). Thus, even at 1PN order, it is impossible to detect the deviations from general relativity induced by β_3 . A non-zero β_3 would simply induce an error on the determination of M_c and ν , i.e. on the masses of the two stars.

We then examine the situation at 1.5PN order. Let us at first neglect the spin of the two stars. Then the 1.5PN phase with $\beta_3 \neq 0$ has the generic form

$$\begin{aligned} \phi^{\text{1.5PN}} = & -\frac{\Theta^{5/8}}{\nu} \left[(1 + b_0\beta_3) + a_1(\nu)(1 + b_1\beta_3)\Theta^{-1/4} \right. \\ & \left. + a_2(1 + b_2\beta_3)\Theta^{-3/8} \right], \end{aligned} \quad (4.44)$$

where $a_2 = -3\pi/4$ is the 1.5PN general relativity prediction and b_2 is the (possibly ν -dependent) 1.5PN correction due to β_3 . Again, we will not need its exact value, and we will simply make the natural assumption that it is $O(1)$.

However, for the purpose of determining β_3 , neglecting spin is not correct. Indeed, at 1.5PN order the spin of the bodies enters through the spin-orbit coupling, and the evolution of the gravitational wave frequency f with time is given by [120]

$$\frac{df}{dt} = \frac{96}{5}\pi^{8/3}M_c^{5/3}f^{11/3} \left[1 - \frac{24}{5}a_1(\nu)x + (4\pi - \beta_{\text{LS}})x^{3/2} \right], \quad (4.45)$$

where $x = (\pi M f)^{2/3}$, while β_{LS} describes the spin-orbit coupling and is given by

$$\beta_{\text{LS}} = \frac{1}{12} \sum_{a=1}^2 \left[113 \frac{m_a^2}{M^2} + 75\nu \right] \hat{\mathbf{L}} \cdot \boldsymbol{\chi}_a, \quad (4.46)$$

where \mathbf{L} is the orbital angular momentum, $\boldsymbol{\chi}_a = \mathbf{S}_a/m_a^2$ and \mathbf{S}_a is the spin of the a -th body. In principle β_{LS} evolves with time because of the precession of \mathbf{L} , \mathbf{S}_1 and \mathbf{S}_2 . However, it turns out that in practice it is almost conserved, and can be treated as a constant [66]. Integration of eq. (4.45) then shows that, in the 1.5PN phase, β_{LS} is exactly degenerate with β_3 in eq. (4.44). Furthermore, observe that β_{LS} , depending on the spin configuration, can reach a maximum value of about 8.5 [66] (and its maximum value remains large even in the limit $\nu \rightarrow 0$), while β_3 is already bound by laser ranging at the level of 2×10^{-4} and by pulsar timing at the level of 10^{-3} (which tests the radiative sector, as do gravitational wave interferometers). Thus, the effect of β_3 at 1.5PN is simply reabsorbed into a (very small) shift of β_{LS} .

At 2PN order β_3 is degenerate with the parameter σ that describes the spin-spin interaction

$$\begin{aligned} \sigma &= \frac{\nu}{48} [721(\hat{\mathbf{L}} \cdot \boldsymbol{\chi}_1) - 247\boldsymbol{\chi}_1 \cdot \boldsymbol{\chi}_2(\hat{\mathbf{L}} \cdot \boldsymbol{\chi}_2)] \\ &+ \frac{1}{96} \sum_{a=1}^2 \frac{m_a^2}{M^2} [719(\hat{\mathbf{L}} \cdot \boldsymbol{\chi}_a)^2 - 233\boldsymbol{\chi}_a^2]. \end{aligned} \quad (4.47)$$

The first term is the one which is usually quoted in the literature, first computed in [120] (see also [121, 122]). The term in the second line, computed recently in [123], is however of the same order, and must be included.

The first term is proportional to ν , and reaches a maximum value $\sigma_{\text{max}}(\nu) \simeq 10\nu$. In a coalescence with very small value of ν , this term is therefore suppressed; e.g. in an extreme mass-ratio inspiral (EMRI) event at LISA where a BH of mass $m_1 = 10M_\odot$ falls into a supermassive BH with $m_2 = 10^6 M_\odot$, one has $\nu = 10^{-5}$ and the term in the first line has a maximum value $\sim 10^{-4}$. If this standard term gave the full answer, a value of β_3 in excess of this value could therefore give an effect that cannot be ascribed to σ . However, the presence of the new term recently computed in [123] spoils this reasoning, since it is not proportional to ν . The conclusion is that, just as with β_{SL} at 1.5PN order, the effect of β_3 at 2PN order is just reabsorbed into a small redefinition of σ , and therefore simply induces an error in the reconstruction of the spin configuration (observe also that fixing β_{LS} does not allow us to fix the spin combinations that appear in σ .)

More generally, the phase of gravitational waves emitted during the coalescence of compact binaries [124, 114], up to 3.5PN, has the form

$$\Psi(f) = 2\pi f t_c - \Phi_c + \sum_{k=0}^7 [\psi_k + \psi_{kl} \ln f] f^{(k-5)/3} \quad (4.48)$$

where f is the gravitational wave frequency, and t_c and Φ_c are the time and the phase at merger. The seven non-zero coefficients ψ_k with $k = 0, 2, 3, \dots, 7$ and the two non-zero coefficients ψ_{kl} with $k = 5, 6$ are known from the PN

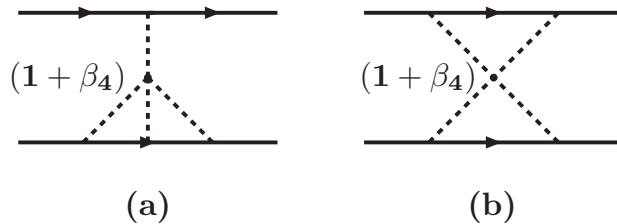


Figure 4.2: The diagrams that contribute to the conservative dynamics, which are affected by a modification of the four-graviton vertex.

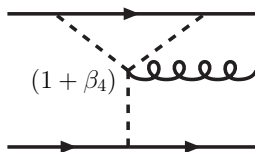


Figure 4.3: The diagram that contributes to the radiative dynamics, which is affected by a modification of the four-graviton vertex.

expansion, in terms of the two masses m_1 and m_2 . One could in principle investigate the effect of β_3 on higher-order coefficients, such as the 2.5PN term ψ_5 and the 3PN term ψ_6 in (4.48), which at LISA could have been measured with a precision of order 10^{-2} [124]. Unfortunately, it is difficult to translate them into bounds on β_3 because at 2.5PN order one finds that β_3 is degenerate with a different combination of spin and orbital variables, which is not fixed by the 1.5PN spin-orbit term (see Table II of ref. [125]), while at 3PN order the spin contribution is not yet known. The conclusion is therefore that interferometers cannot measure the three- and higher-order graviton vertex, since the effect of a modified vertex is simply reabsorbed into the determination of the masses and spin of the binary system. The conclusion that interferometers are not competitive with pulsar timing for measuring deviations from general relativity was also reached in Ref. [126], although in a different context. In fact, Ref. [126] was concerned with multiscalar-tensor theories, whose leading-order effect is the introduction of a term corresponding to dipole radiation (a “minus one”-PN term).

4.2 The four-graviton vertex

We now examine what can be said about the four-graviton vertex, parametrized by β_4 . In the conservative part of the Lagrangian, β_4 contributes through the diagrams of Fig. 4.2. However, these contributions only affect the equations of motion at 2PN order, so there is no hope of detecting it in solar system experiments, where the velocities at play are very small. For the same reason, no significant bound can be obtained from binary pulsars; from a simple order of magnitude estimate we find that the Hulse-Taylor pulsar can only give a limit

$\beta_4 < O(10)$, which is not significant.

At gravitational wave interferometers, β_4 enters into the phase for the first time at 1PN order, through the diagram in Fig. 4.3. However, it suffers exactly the same degeneracy issues as β_3 , so it cannot be measured to interesting accuracy at present or future interferometers, at least with the technique discussed here. Note however that we have worked in the restricted PN approximation, in which only the harmonic at twice the source frequency is retained. Higher-order harmonics however break degeneracies between various parameters in the template [127], and it would be interesting to investigate whether their inclusion in the analysis allows one to put a bound on β_3 and β_4 from binary coalescences.

4.3 The method

In this section, we discuss what it means to allow the vertices to deviate from their standard general relativity values. We emphasize that our way of “tagging” the vertices with β_3 and β_4 is a phenomenological parametrization. We explain how this parametrization is similar to the PPN parametrization. It is different, however, from other approaches that test gravity within the framework of a more fundamental theory that could give rise to deviations from general relativity.

Let us start by clarifying the meaning of introducing β_3 and β_4 . In ordinary general relativity, with $\beta_{3,4} = 0$, coordinate transformation invariance ensures that the negative norm states decouple. After gauge fixing (in the De Donder gauge for instance), the kinetic terms for all of the ten components of the metric are invertible, but four of them have the wrong sign, i.e. they give rise to negative norm states. In the De Donder gauge the six positive-norm states that diagonalize the kinetic term are

$$\tilde{h}_{ij} \equiv h_{ij} + \frac{1}{2}\delta_{ij}(h_{00} - \delta^{lm}h_{lm}), \quad (4.49)$$

while the four “wrong-sign” components are given by the spatial vector h_{0i} and by the scalar

$$\tilde{h}_N \equiv h_{00} - \delta^{lm}h_{lm}. \quad (4.50)$$

In standard general relativity, the existence of these negative-norm states do not create difficulties because they are coupled to four integrals of motion (energy, and the three components of angular momentum), so they cannot be produced. In contrast, the remaining six “healthy” components couple to the source multipole moments. As discussed in Section 1.3.3, after complete gauge fixing one finds that among the six positive-norm states, four obey Poisson-like equations, so they do not radiate (even though they are non-radiative physical degrees of freedom), while the remaining two are the radiative degrees of freedom representing gravitational waves.

Allowing $\beta_3 \neq 0$ has the effect that the negative norm state \tilde{h}_N now couples, already at lowest order, to a non conserved quantity, namely to a combination of the Newtonian kinetic and potential energy of the binary system. This means that, in general, a modification of general relativity in which we just change the strength of the three-graviton vertex cannot be taken as a fundamental

field theory, neither at the quantum level, nor even at the classical level, since the negative-norm state contributes to the classical radiated power (a related concern is that, for $\beta_3 \neq 0$, the energy-momentum tensor is in general not conserved). A consistent classical and quantum field theory could in principle emerge from a simultaneous modification of all the vertices of the theory, such as the three-, four- and higher-order graviton vertices, together with a related modification of the graviton-matter couplings. As a trivial example, an overall rescaling of the gauge coupling in a Yang-Mills theory, or of Newton's constant in general relativity, results in a combined modification of all the vertices, but obviously introduces no pathology. In any case, our approach to the problem is purely phenomenological. We introduce β_3 and β_4 simply as “tags” that allow us to track the contribution of the three- and four-graviton vertices throughout the computations. As long as $|\beta_3| \ll 1$ and $|\beta_4| \ll 1$, the corrections that they induce to the radiated power are small compared to the standard general relativity result, so the total radiated power is given by the general relativity result plus a small correction, and in particular the total radiation emitted is positive. At this phenomenological level the introduction of modified vertices is therefore acceptable, and provides a simple and, most importantly, gauge invariant manner of quantifying how well different observations constrain the non-linear sector of general relativity, in a way which is intrinsic to general relativity itself, without reference to any other specific field theory.

A second issue is whether a modification of the vertices of this form (typically with β_3, β_4 , etc. not independent, but related to each other by some consistency conditions) could emerge from a plausible and consistent extension of general relativity. Actually, a typical UV completion of general relativity at an energy scale Λ will rather generate corrections to the vertices that are suppressed by inverse powers of Λ , so it would give rise to an energy dependent β_3 , e.g. $\beta_3 = E^2/\Lambda^2$, which furthermore, at the energy scales that we are considering and for any sensible choice of Λ , would be utterly negligible. Still, let us remark that this kind of behavior is not a theorem. It assumes the UV-IR decoupling typical of effective field theories, and one can exhibit counterexamples. For instance, in non-commutative Yang-Mills theories there is a UV-IR mixing, such that low-energy processes receive contributions from loops where very massive particles are running, and these contributions are independent of the mass of these particles [128]. Anyway, again our aim here has not been to test any given consistent extension of general relativity, but rather provide a simple and phenomenologically consistent way of quantifying how well various experiments can test the non-linearities of general relativity, and quantify how the results of different experiments compare among themselves.

It is also interesting to observe that, even when β_3 and β_4 are non-zero, the graviton remains massless at the classical level, since β_3 and β_4 affect interaction terms, but not the kinetic term. The breaking of diffeomorphism invariance induced by β_3 and β_4 could in principle generate a graviton mass at the one-loop level. However, even if we are using the language of quantum field theory, in the end we are only interested in the classical theory, since quantum loops are suppressed by powers of \hbar/L , where L is the angular momentum of the system, so they are completely negligible for a macroscopic system.⁴

⁴At the quantum level, if a mass is generated, it will be power divergent with the cutoff,

Our aim has been to quantify how well the non-linearities of general relativity can be tested by various existing or planned experiments/observations. Historically, there have been several approaches to this problem and, basically, one can identify two complementary strategies. The first is to develop a purely phenomenological approach in which deviations from general relativity are expressed in terms of a number of parameters, without enquiring at first whether such a deformation of general relativity can emerge from a fundamental theory.

An example of such an approach is the **PPN** formalism of Section 2.3. general relativity corresponds to $\beta^{PPN} = 1$ and $\gamma^{PPN} = 1$. More phenomenological parameters can be introduced by working at higher PN orders, see [11]. One then investigates how deviations of β^{PPN} and γ^{PPN} from their general relativity values affect various experiments. To get the bounds of equations (4.5),(4.6), we do not need to know the fundamental theory that gives rise to values of β^{PPN} and γ^{PPN} that differ from their general relativity values. However, it is interesting to see that consistent field theories exist that give rise to values of β^{PPN} and γ^{PPN} different from one. For instance, a Brans-Dicke theory with parameter ω_{BD} gives $\beta^{PPN} = 1$ and $\gamma^{PPN} = (1 + \omega_{BD})/(2 + \omega_{BD})$, with the general relativity value $\gamma^{PPN} = 1$ recovered for $\omega_{BD} \rightarrow \infty$, while more general tensor-scalar theories can produce both $\gamma^{PPN} \neq 1$ and $\beta^{PPN} \neq 1$. However, in the **PPN** approach, one can also explore other possibilities, such as **PPN** parameters that correspond to preferred-frame effects or to violation of the conservation of total momentum. It is also important to observe that the parameters β^{PPN} and γ^{PPN} are gauge-invariant, and are therefore observables, because they have been defined with respect to a specific gauge, namely the standard **PPN** gauge in which the metric takes the form (4.4).

In this sense, our effective field theory approach is similar to the **PPN** parametrization. We quantify how well general relativity performs with respect to experiments of relativistic gravity by studying how much these experiments constrain the values of the non-abelian vertices of the theory, in particular the three- and four-graviton vertices. After choosing a gauge (the De Donder gauge, corresponding to harmonic coordinates) we multiply the three-graviton vertex by a factor $(1 + \beta_3)$ and the four-graviton vertex by a factor $(1 + \beta_4)$, with constants β_3 and β_4 . For $\beta_3 = \beta_4 = 0$ we recover general relativity. Observe that, since β_3 and β_4 are defined with respect to a given gauge choice, they are gauge-invariant by definition. This is in fact the same logic used to define in a gauge-invariant manner the **PPN** parameters β^{PPN} and γ^{PPN} . Our method differs from the **PPN** approach, however, in that the **PPN** formalism can be adapted to test metric theories of gravity in general whereas the effective field theory approach proposed in this Chapter only tests general relativity.

A complementary approach to the problem is to study a specific class of field-theoretical extensions of general relativity. A typical example is provided by multiscalar-tensor theories, motivated by quantum completions of general relativity like string theory. These have been studied in detail and compared with

and will have to be fine tuned order by order in perturbation theory. However, the fact that quantum divergences have to be subtracted order by order is a generic problem of the standard quantum extension of general relativity, independently of β_3 . In any case, again, our approach is purely phenomenological, and the introduction of β_3 and β_4 is simply a tool for tracking a specific contribution to the computation.

experimental tests of relativistic gravity in refs. [129, 21, 130, 131, 132, 43, 126]. First of all, this approach has the advantage that one is testing a specific and well-defined fundamental theory. Secondly, an experimental bound on the parameters of a given scalar-tensor theory, such as for instance the bound $\omega_{\text{BD}} > 40000$ on the parameter ω_{BD} of Brans-Dicke theory obtained from the tracking of the Cassini spacecraft [49] is, strictly speaking, a statement about that particular extension of general relativity and not about general relativity itself.

4.4 Discussion

We have proposed to quantify the accuracy to which various experiments probe the non-linearities of general relativity, by translating their results into measurements of the non-abelian vertices of the theory, such as the three-graviton vertex and the four-graviton vertex. This is similar in spirit to tests of the Standard Model of particle physics, where the non-abelian vertices involving three and four gauge bosons have been measured at LEP and at the Tevatron.

We have shown that, at a phenomenological level, this can be done by introducing parameters β_3 and β_4 that quantify deviations from the general relativity prediction of the three- and four-graviton vertices, respectively. We have found that, in the conservative sector of the theory, i.e. as long as one neglects the emission of gravitational radiation at infinity, the introduction of β_3 at 1PN order is phenomenologically equivalent to the introduction of a parameter $\beta^{\text{PPN}} = 1 + \beta_3$ in the parametrized PN formalism. Strong bounds on β_3 therefore come from solar system experiments, and most notably from lunar laser ranging, providing a measurement at the 0.02% level.

The modification of the three-graviton vertex however also affects the radiative sector of the theory, and we have found that the timing of the Hulse-Taylor pulsar gives a bound on β_3 at the 0.1% level, not far from the one obtained from lunar laser ranging. Conceptually, however, the two bounds have different meanings, since lunar laser ranging only probes the conservative sector of the theory, while pulsar timing is also sensitive to the radiative sector.

We have then studied the results that could be obtained from the detection of coalescences at interferometers, and we have found that, even if β_3 already modifies the gravitational wave phase at the Newtonian level and β_4 at 1PN order, their effect can always be reabsorbed into other parameters in the template, such as the mass and spin of the two bodies so, rather than detecting a deviation from the general relativity prediction, one would simply make a small error in the estimation of these parameters.

Chapter 5

Effective Field Theory Analysis of the Chameleon

Scalar-tensor theories have been alternatives of general relativity [133, 134] for over half a century. Today, many alternative theories of gravitation are scalar-tensor theories in some form or another. Since there is no experimental evidence of long-range “fifth” forces, there are basically two ways for a scalar to exist in Nature while maintaining the absence of an extra force. This scalar field should be either weakly coupled to matter, or massive enough for its interactions to be effectively short-ranged. A massless scalar field that couples to ordinary matter with gravitational strength would lead to a violation of the equivalence principle.

A standard way to maintain a long-ranged force due to an extra scalar field is to suppress its coupling to matter. The task is not straightforward, however, since scalar fields tend to couple to matter with gravitational strength, see [135, 136] for ideas based on symmetry principles to suppress scalar couplings. Otherwise, the presence of light scalar fields, or *moduli*, with run-away potentials is suggested by higher dimension gravity, like supergravity [137]. Stabilizing them by giving them a mass turns out to be difficult and has only been achieved in specific constructions [138].

The chameleon was originally suggested in a cosmological context and has been exploited as a quintessential field to give a description of dark energy [74, 75]. The chameleon mechanism was proposed to suppress long-range interactions mediated by a scalar field, the chameleon, while allowing its fundamental dimensionless coupling to ordinary matter be of order unity. The mechanism consists of giving the scalar field a mass that depends on local matter density. The scalar is called the ‘chameleon’ for its ability to evade detection in environments of different density. In theory, the chameleon acquires a large enough mass in the neighbourhood of experiments (high density), allowing it to escape detection and searches for violation of the equivalence principle. It remains effectively massless in almost empty space (low density), for instance in interplanetary space, so that it can propagate to astrophysical or cosmological distances.

We focus our attention on a theoretical issue that is phenomenologically relevant for the chameleon whenever third or higher order non-derivative self-interactions of scalar fields are taken into account. Self-interactions have already been considered, either by taking into account the ϕ^4 self-interaction [139, 140] (where ϕ denotes the scalar field) or by considering a specific type of potential [141, 142]. We show that qualitatively different results are obtained if ϕ^3 interactions are taken into account, as derived in [143], even if such modifications are quantitatively negligible for most ranges of parameter values. Our analysis is an application of the effective field theory methods, called non-relativistic general relativity NRGR [23], originally proposed for Einstein gravity.

This chapter is organized as follows. In sec. 5.1, we present the chameleon action, derive the chameleon equation of motion and show that its dynamics can be rewritten in terms of an effective potential. We then derive static and spherically symmetric solutions in the thin- and thick-shell approximations. We close the section by pointing out reason to question the linear approximation that is used in deriving chameleon solutions. In sec. 5.2, we analyze the effect of self-interactions on the chameleon mediated potential for a generic choice of parameters, showing that it may *grow* over astrophysical distances, although for solar-system values of the physical parameters, self-interactions have no phenomenological consequence. We finally conclude in sec. 5.3.

5.1 The chameleon in brief

The chameleon scalar-field is defined by the following action $S = S_{EH} + S_\phi + S_m$ with

$$\begin{aligned} S_{EH} &= \frac{M_{Pl}^2}{2} \int d^4x \sqrt{-g} R, \\ S_\phi &= - \int d^4x \sqrt{-g} \left(\frac{1}{2} \partial_\mu \phi \partial^\mu \phi - V(\phi) \right), \\ S_m &= \int d^4x \sqrt{-g} \mathcal{L}_m \left(\psi^{(i)}, g_{\mu\nu}^{(i)} \right) \end{aligned} \quad (5.1)$$

where $g_{\mu\nu}$ is the metric with signature $(-, +, +, +)$, with determinant g , R is the Ricci scalar, and $M_{Pl}^2 = 8\pi G_N$ is the reduced Planck's mass and G_N is Newton's constant. The scalar-field ϕ is known as the chameleon. It is coupled to matter fields $\psi^{(i)}$ via the modified metric $g_{\mu\nu}^{(i)} \equiv e^{2\beta_i \phi / M_{Pl}} g_{\mu\nu}$, where the superscript i denotes different particles species and β_i are dimensionless coupling constants, allowing a different coupling for each species. We choose the potential $V(\phi)$ to be an inverse power-law of the form

$$V(\phi) = M^4 (M/\phi)^\alpha, \quad (5.2)$$

where α is positive and M is the mass scale of the problem which may be much smaller than the reduced Planck's mass $M_{Pl} \equiv (8\pi G_N)^{-1/2} \simeq 2.4 \cdot 10^{18} \text{GeV}$. The specific form of the potential, however, is not crucial but the chameleon mechanism requires it to be a decreasing function without a minimum [76]. Qualitatively similar potentials appear in supergravity compactifications inspired by superstring constructions [144].

5.1.1 The chameleon equation of motion

Varying the action with respect to ϕ yields the chameleon equation of motion

$$\nabla^2\phi = V_{,\phi}(\phi) - \sum_i \frac{\beta_i}{M_{Pl}} e^{4\beta_i\phi/M_{Pl}} g_{(i)}^{\mu\nu} T_{\mu\nu}^{(i)} \quad (5.3)$$

where $T_{\mu\nu}^{(i)} \equiv (-2/\sqrt{-g^{(i)}})\delta\mathcal{L}_m/\delta g_{(i)}^{\mu\nu}$ is the stress-energy tensor for the i th species of matter. The chameleon couples to the trace of the energy momentum tensor of matter $T^{(i)} \equiv g^{\mu\nu}T_{\mu\nu}^{(i)}$. For non relativistic matter, one has $T^{(i)} \simeq -\tilde{\rho}_i$, where $\tilde{\rho}_i$ is the energy density in the Jordan frame for the i -th particle species. To simplify the analysis, we only consider natural couplings to matter of order unity for all species in which case it is enough to consider only one particle species so we drop the i index i.e. $\beta_i \sim \beta \sim 1$. It is also convenient to define $\tilde{\rho} = \rho e^{-3\beta\phi/M_{Pl}}$ so that ρ is conserved in the Einstein frame and is independent of ϕ . Then the equation of motion can be rewritten in terms of an effective potential

$$\nabla^2\phi = V_{eff,\phi}(\phi) \quad (5.4)$$

where $V_{eff,\phi}(\phi)$ is the effective potential given by

$$V_{eff}(\phi) = V(\phi) + \rho e^{\beta\phi/M_{Pl}} = M^4 \left(\frac{M}{\phi}\right)^\alpha + \rho e^{\beta\phi/M_{Pl}}. \quad (5.5)$$

In other words, the dynamics of the scalar field are not solely governed by the potential $V(\phi)$ but on the effective potential $V_{eff,\phi}(\phi)$ which explicitly depends on the matter density ρ .

5.1.2 The chameleon mass and non-linear couplings

We want to Taylor expand the effective potential around the minimum value of the chameleon $\bar{\phi}$, which is given by $V_{eff,\phi}(\bar{\phi}) = 0$, leading to

$$\bar{\phi} \simeq M \left(\frac{\alpha M_{Pl} M^3}{\beta \rho}\right)^{1/(\alpha+1)}. \quad (5.6)$$

We are interested in parameters for which $\bar{\phi} < M_{Pl}$, which is the case if M and ρ satisfy

$$M < \left(\frac{\beta}{\alpha} M_{Pl}^\alpha \rho\right)^{\frac{1}{\alpha+4}}. \quad (5.7)$$

For example, by eq. (5.7), the numerical values $\rho = 1\text{g/cm}^3 \simeq (5 \cdot 10^{-2}\text{MeV})^4$, $\alpha = 2$ give a mass of $M < 3$ TeV.

Taylor expanding the effective potential around its minimum $\bar{\phi}$ yields

$$V_{eff}(\phi) = \frac{m_\phi^2}{2} (\phi - \bar{\phi})^2 + \frac{g_3 M}{3!} (\phi - \bar{\phi})^3 + \frac{\lambda}{4!} (\phi - \bar{\phi})^4 + \sum_{n>4} \frac{g_n}{n! M^{n-4}} (\phi - \bar{\phi})^n, \quad (5.8)$$

where the following ρ -dependent parameters have been defined: the mass m_ϕ , the dimensionless trilinear coupling g_3 , the quartic coupling $g_4 \equiv \lambda$ and the generic dimensionless n-linear coupling g_n . These coefficients of the Taylor expansion depend on the local mass density and are given by

$$\begin{aligned} m_\phi^2 &\simeq (\alpha + 1) M^2 \left(\frac{\beta \rho}{M^3 M_{Pl}} \right)^{\frac{\alpha+2}{\alpha+1}} \exp(\beta \bar{\phi}/M_{Pl}), \\ g_3 &\simeq -(\alpha + 1)(\alpha + 2) \left(\frac{\beta \rho}{M^3 M_{Pl}} \right)^{\frac{\alpha+3}{\alpha+1}} \exp(\beta \bar{\phi}/M_{Pl}), \\ \lambda &\simeq (\alpha + 1)(\alpha + 2)(\alpha + 3) \left(\frac{\beta \rho}{M^3 M_{Pl}} \right)^{\frac{\alpha+4}{\alpha+1}} \exp(\beta \bar{\phi}/M_{Pl}). \end{aligned} \quad (5.9)$$

For later reference g_n is given by

$$g_n = (-1)^n \frac{(\alpha + n - 1)!}{\alpha!} \left(\frac{M}{\bar{\phi}} \right)^{\alpha+n}, \quad (5.10)$$

where the factor involving the exponential of $\bar{\phi}$ has been neglected. We will see in sec. 5.2 that the interactions with $n \geq 5$ are of negligible phenomenological impact.

5.1.3 The chameleon profile

Now we discuss the chameleon static solution for extended bodies like the bodies that compose our solar-system. Following [75, 142, 76], we discuss the “thin-shell” and “thick-shell” solutions for spherically symmetric massive bodies in the weak-field limit. The thin-shell solution eq. (5.14) encompasses the relevant physics for extended bodies.

Consider a spherically symmetric body of density ρ_b , radius R and total mass M_b , surrounded by an environment of density ρ_∞ . Let $g_{\mu\nu} = \eta_{\mu\nu}$. Then the chameleon equation of motion (5.4) in terms of spherical coordinates becomes

$$\phi'' + \frac{2}{r} \phi' = V_{eff,\phi}(\phi) \quad (5.11)$$

In what follows, let m_b, m_∞ respectively denote the value of m_ϕ inside and outside the body. Similarly, let ϕ_b, ϕ_∞ respectively denote the value of the chameleon at the minimum of the effective potential, $\bar{\phi}$, when $\rho = \rho_0$ and $\rho = \rho_\infty$. A solution of the chameleon equation of motion is also referred to as the chameleon profile or the chameleon potential.

Let us start with the external solution ($r > R$). As a first approximation of the long range behaviour of the chameleon in the presence of massive bodies, we linearize (5.11) by keeping only the quadratic term in the potential expansion (5.8). The chameleon equation of motion becomes

$$\phi'' + \frac{2}{r} \phi' - m_\infty^2 (\phi - \phi_\infty) = 0, \quad (5.12)$$

The solution to the linearised equation (5.12) with boundary conditions $\phi \rightarrow \phi_\infty$ as $r \rightarrow \infty$ leads to

$$\phi(r > R) = B \frac{e^{-m_\infty(r-R)}}{r} + \phi_\infty, \quad (5.13)$$

where B is a dimensionless constant. This external solution is indeed a Yukawa potential of interaction range, or Compton wavelength, $\lambda = m_\infty^{-1}$ which characterizes the chameleon. In particular, we consider the case in which the environment outside the body is endowed with such a small density that the Compton wavelength of the chameleon is much greater than the length scales of interest ($m_\infty r \ll 1$).

The thin-shell and thick-shell solutions are found by solving for the chameleon inside the massive body, under specific approximations, and smoothly matching the internal and external solutions at the boundary $r = R$.

The thin-shell solution

The thin-shell approximation supposes that the Compton wavelength of the chameleon inside the body is much smaller than the body $m_b R \gg 1$. The solutions to the linearized equation (5.12) inside and outside the body are respectively

$$\begin{aligned}\phi(r < R) &= A \frac{\sinh(m_b r)}{r} + \phi_b, \\ \phi(r > R) &= B \frac{e^{-m_\infty(r-R)}}{r} + \phi_\infty,\end{aligned}\tag{5.14}$$

where the integration constants are fixed by requiring the solution and its derivative to continuously match at the boundary $r = R$, giving the constants

$$\begin{aligned}A &= \left[\frac{1 + m_\infty R}{m_b R \coth(m_b R) + m_\infty R} \right] \frac{R(\phi_\infty - \phi_b)}{\sinh(m_b R)}, \\ B &= \left[\frac{m_b R \coth(m_b R) - 1}{m_b R \coth(m_b R) + m_\infty R} \right] R(\phi_b - \phi_\infty).\end{aligned}\tag{5.15}$$

The solution outside the body can be rewritten as

$$\phi(r > R) \simeq -\frac{\beta_{eff}}{4\pi M_{Pl}} \frac{M_b e^{-m_\infty(r-R)}}{r} + \phi_\infty \quad m_b R \gg 1,\tag{5.16}$$

and

$$\beta_{eff} = \frac{3\phi_\infty M_{Pl}}{\rho_b R^2}.\tag{5.17}$$

When $m_b R \gg 1$, the chameleon ϕ is close to the minimum inside most of the body and only at the boundary of the body (where the densities suddenly change) does a *thin shell* contribute to the overall chameleon field. This is the case for extended bodies, like the planets and our sun within the solar system. Given that the chameleon mass m_∞ outside of the body is generally tiny, the thin-shell solution eq.(5.16), is analogous to the standard Newtonian potential when $\beta_{eff} = 1$. So the suppression of the chameleon coupling is conveniently parameterized by β_{eff} . For instance, approximating the earth by a sphere of radius 6.4×10^6 m with homogeneous density $\rho_\oplus \simeq 5.5$ g/cm³ immersed in the galactic medium composed of baryonic gas with density $\rho_G \simeq 10^{-24}$ g/cm³, and assuming that $M = 1$ eV and $\alpha = \beta = 1$, then the effective coupling evaluates to $\beta_{eff} \simeq 5 \times 10^{-3}$

	$\rho(\text{g/cm}^3)$	$m_\phi(\text{eV})$	λ_C (m)	$-g_3$	λ	ϕ/M
Earth	5.5	1.4×10^{-6}	0.14	6.4×10^{-16}	2.6×10^{-19}	9.8×10^3
Atmosphere	1.3×10^{-3}	2.8×10^{-9}	72	3.6×10^{-23}	2.2×10^{-28}	6.4×10^5
Interplanetary Space	10^{-24}	4×10^{-25}	5×10^{17}	2×10^{-65}	4×10^{-81}	2×10^{16}

Table 5.1: Value of the parameters for different densities ($\alpha = \beta = 1$, $M = 1\text{eV}$). For comparison, $1\text{pc} \simeq 3 \times 10^{16}\text{m}$.

Setting $M = 1\text{ eV}$ and $\alpha = \beta = 1$, typical values of the coupling constants (5.9) are summarized in tab. 5.1 for the earth, the atmosphere and interplanetary space. These values illustrate how the parameters of the chameleon vary depending on the density of the surrounding environment. In particular, for a relatively dense region like inside the earth, the chameleon is much more massive than in interplanetary space.

The thin-shell solution (5.14) has the beneficial effect of suppressing the otherwise phenomenologically dangerous coupling to matter, but it does so in a non-universal manner. The chameleon couples to matter not only through the total mass of the body, but also through parameters such as the radius of the massive body. This peculiar coupling leads to violation of the equivalence principle, even in its weak form.

The thick-shell solution

The thick-shell approximation supposes that the Compton wavelength of the chameleon inside the body is larger than the body itself $m_b R < 1$. When $\phi(r) > \phi_b$ inside the massive body (i.e. $r < R$), the effective potential can be approximated by its increasing branch leading to the approximate equation of motion

$$\phi'' + \frac{2}{r}\phi' + \frac{\beta\rho}{M_{Pl}} = 0. \quad (5.18)$$

Retaining the approximate form (5.12) of the equation of motion *outside* the massive body of total mass M_b leads to the solution

$$\begin{aligned} \phi(r < R) &= -\frac{\beta\rho_b r^2}{6M_{Pl}} + \text{const}, \\ \phi(r > R) &= \frac{\beta}{4\pi M_{Pl}} \frac{M_b e^{-m_\infty(r-R)}}{r} + \phi_\infty. \end{aligned} \quad (5.19)$$

This profile is a self-consistent solution for $\phi(r < R) > \phi_b$ and has been named the *thick shell* solution, occurring for $m_b R < 1$, but is irrelevant for our analysis of extended astrophysical bodies.

5.1.4 A threat from chameleon self-couplings

A non-trivial assumption has been made in the above analysis to obtain the external chameleon solutions. The effective potential is approximated by its quadratic expansion around the minimum $V_{eff}(\phi) \simeq \frac{m^2}{2!}(\phi - \phi_b)^2$.

In the thick shell case, the effective potential inside the massive body is approximated by its density contribution alone, $V_{eff}(\phi) \simeq \beta\phi\rho/M_{Pl}$. This approximation is self-consistent given that we have $M_{Pl} > \phi > \phi_b$ and $M_{Pl} > \phi > \phi_\infty$ at the solution.

In the thin-shell case, the linear approximation should be verified, however, since higher order terms may become important for the lowest order solution (5.14) at the boundary of the massive body. Naively substituting the thin-shell solution (5.14) into the potential expansion (5.8), one realizes that the linear term in the equation of motion (the mass term) is dominated by the tri-linear and quartic interaction terms for $r \lesssim \frac{1}{2}(\alpha + 2)R$ and $r \lesssim \sqrt{\frac{1}{3!}(\alpha + 2)(\alpha + 3)R}$, respectively, which are both clearly outside the massive body. In general, the self-interaction terms ϕ^n in the expansion (5.8) for $n \geq 2$ dominate at distances

$$r \lesssim \left(\frac{1}{(n-1)!} \frac{(\alpha+n-1)!}{(\alpha+1)!} \right)^{\frac{1}{n-2}} R. \quad (5.20)$$

The fact that all of the higher order terms overcome the linear term indicates the need for a more thorough analysis into the importance of higher order terms which correspond to chameleon self-couplings.

These non-linearities have been contemplated in the literature to some extent. In one article [139], the effect of a $\lambda\phi^4$ interaction is studied using approximate analytic methods. The resulting profile for the chameleon in the thin shell case is still inversely proportional to the distance $1/r$ outside the source $r > R$ (and within the Compton wavelength of the chameleon $m_\infty r \ll 1$), but the effective coupling reduces to (5.17)

$$\beta_{eff} \simeq \frac{M_{Pl}}{M} \lambda^{-1/2} \quad \text{if} \quad \lambda > \left(\frac{M_{Pl}}{\beta M} \right)^2. \quad (5.21)$$

which occurs for large enough λ . This is a non-perturbative effect which cannot be reproduced in a perturbative analysis. In another article [142], an approximate analytic analysis of the non-linear regime is performed, and a result equivalent to thin-shell solution (5.16) is obtained (see next to last eq. in sec. IIID of [142]). They show that the full form of the potential does not substantially alter the solution close to the surface of the massive body, where the matching between the inner and the outer solutions in (5.14) is made. They argue that, at large distances, the solution can only be of the type of the second equation in (5.14) and since the chameleon is positive $\phi(r) > 0$, it should be possible to constrain the integration constant by $-\phi_\infty R < B < 0$ so that the chameleon remains above some critical value $\phi(r) > \phi_{critical}(r) \equiv \phi_\infty (1 - Re^{-m_\infty(r-R)}/r)$. The limiting value $\phi_{critical}(r)$ coincides with the approximate thin-shell solution (5.16). If, on the other hand, the chameleon is much greater than this critical value $\phi(r) \gg \phi_{critical}(r)$ outside of the body, then one would simply recover the thick-shell solution (5.19).

In sec. 5.2, we propose a thorough analysis of the chameleon non-linearities based on EFT techniques. We also verify limits imposed by the equivalence principle.

5.2 Analysis of chameleon self-interactions

So far, we have seen that the thin-shell solution for the chameleon violates the strong equivalence principle and is derived using a potentially dangerous linear approximation. In this section, we present an [EFT](#) approach to evaluate the effect of the chameleon non-linearities on the chameleon potential beyond the linear approximation. We show that the chameleon self-interactions at all orders are negligible for solar system bodies. We also show that the chameleon evades tests of EP violations. We focus on the thin-shell solution since it is relevant for extended bodies.

5.2.1 An effective field theory approach

A perturbative [EFT](#) method represented by Feynman diagrams [23] is used to systematically estimate the effect of chameleon self-interactions. These interactions induce corrections to the chameleon potential outside a massive body where the potential is very shallow. We build an action which reproduces the chameleon dynamics as follows. Let the chameleon be described by the following action,

$$S_{tot} = S_\phi + S_m \quad (5.22)$$

where

$$\begin{aligned} S_\phi &= -\frac{1}{2} \int d^4x \sqrt{-g} (\partial_\mu \phi \partial^\mu \phi + V_{eff}(\phi)) \\ S_m &= \sum_a \beta_{eff} \frac{M_b}{M_{Pl}} \phi \int d\tau_a. \end{aligned} \quad (5.23)$$

The ϕ field is redefined so that its minimum is at $\phi = 0$ and a constant term in the Lagrangian is neglected, $d\tau_a = \sqrt{\eta_{\mu\nu} x^\mu x^\nu}$ is the proper time of body- a moving along its worldline \mathbf{x}_a . This action describes a system of two bodies ($a = 1, 2$) in orbit around each other with typical small velocity $v \ll 1$ (recall that $c = 1$). In the [EFT](#) approach, the massive bodies are viewed as point-like particles, coupled to a chameleon with effective strength β_{eff} (5.17) and subject to the potential $V_{eff}(\phi)$ (5.8). The mass of the chameleon m_ϕ and the coupling constant g_n are evaluated outside the bodies. With the appropriate power counting rules, the action is expanded in powers of v and translated into Feynman diagrams. These diagrams depict the bodies moving along their respective worldlines and interacting via chameleon exchange. The non-linearities present in the effective potential V_{eff} correspond to vertices of the self-interacting chameleon. The action (5.22) reproduces the potential of the thin shell solution (5.16) outside the massive body. Following the techniques of the [EFT](#), the leading order potential is given by the exchange of a massive chameleon between the worldlines of the two bodies depicted in the Feynman diagram of figure 5.1. Notice that for solar system type objects, $\beta_{eff,1} \simeq \beta_{eff,2} \simeq \beta_{eff}$.

$$\text{Figure (5.1)} = \frac{\beta_{eff}^2 M_1 M_2}{M_{Pl}^2} \int dt \frac{e^{-m_\infty |x_1 - x_2|}}{|x_1 - x_2|}, \quad (5.24)$$

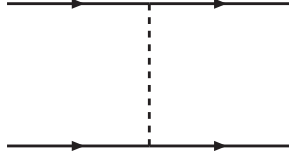


Figure 5.1: The Feynman diagrams of the effective chameleon potential to leading order.

and we recover a Yukawa type interaction at leading order.

Ideally, the expansion is performed in terms of a single small parameter. In the case of Einstein gravity, the small parameter is the typical velocity of the orbiting bodies v . Due to the proliferation of scales in the chameleon case, a consistent expansion at all orders in terms of v is not possible. For this reason, the problem is initially simplified by considering the effective potential V_{eff} to cubic order. We then analyze the effect of all higher order interactions in V_{eff} taking into account the proliferation of scales. We work in flat space but show that the back-reaction of the chameleon on Einstein gravity is negligible.

The cubic self-interacting chameleon

Let M_{b1}, M_{b2} denote the massive bodies that source the chameleon with world-lines $\mathbf{x}_1(t), \mathbf{x}_2(t)$ respectively. The action to cubic order in the effective potential V_{eff} is given by the total action (5.22) with S_ϕ replaced by

$$S_\phi = -\frac{1}{2} \int d^4x \sqrt{-g} \left(\partial_\mu \phi \partial^\mu \phi + m_\infty^2 \phi^2 + \frac{g_3 M}{3} \phi^3 \right) \quad (5.25)$$

The kinetic term of the action (5.25) is split into

$$\partial_\mu \phi \partial^\mu \phi = \delta_{ij} \partial_i \phi \partial_j \phi - \dot{\phi}^2, \quad (5.26)$$

and we treat the time derivative as an interaction term. In terms of Fourier transformed functions

$$\phi_{\mathbf{k}}(t) \equiv \int \frac{d^3x}{(2\pi)^3} \phi(t, \mathbf{x}) e^{i\mathbf{k} \cdot \mathbf{x}}, \quad (5.27)$$

and for the ϕ -propagator we have

$$\langle \phi_{\mathbf{q}}(t) \phi_{\mathbf{k}}(0) \rangle = (2\pi)^3 \delta^{(3)}(\mathbf{q} + \mathbf{k}) \delta(t) \frac{1}{k^2 + m_\phi^2}, \quad (5.28)$$

where the four-momentum $k^\mu = (k^0, \mathbf{k})$, with $k \equiv \sqrt{\mathbf{k} \cdot \mathbf{k}}$.

At next order, the contribution of the cubic interaction to the chameleon profile becomes important and is given by the amplitude represented by the Feynman diagram with three vertices, see figure 5.2(b). The 3-point function of the ϕ -field

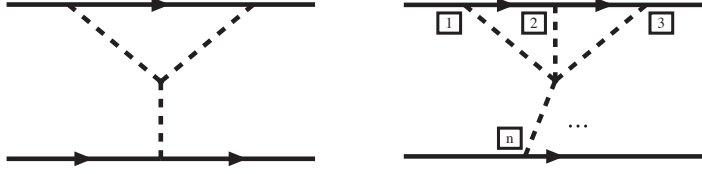


Figure 5.2: Feynman diagrams of corrections to the effective chameleon potential due to (a) the tri-linear interaction $g_3 M \phi^3$ and (b) the generic n-point interaction $g_n M^{4-n} \phi^n$.

is [143]

$$\langle T(\phi(x_1)\phi(x_2)\phi(x_3)) \rangle = 3!(-ig_3 M)\delta(t_1 - t_2)\delta(t_2 - t_3) \times \int \prod_{r=1}^3 \frac{d^3 k_r}{(2\pi)^3} e^{i\mathbf{k}_r \cdot \mathbf{x}_r} (2\pi)^3 \delta^{(3)}\left(\sum_{r=1}^3 \mathbf{k}_r\right) \prod_{r=1}^3 \frac{-i}{k_r^2 + m_\phi^2}. \quad (5.29)$$

Following EFT techniques, we assemble together the three matter vertices to the 3-point function, yielding

$$\begin{aligned} \text{fig. 5.2 (a)} &= \frac{1}{2} \left(\frac{-iM_{b1}}{M_{Pl}} \right)^2 \left(\frac{-iM_{b2}}{M_{Pl}} \right) \int dt_1 dt'_1 dt_2 \langle T(\phi(x_1)\phi(x'_1)\phi(x_2)) \rangle \\ &= -i3g_3 \frac{\beta_{eff}^3 M M_{b1}^2 M_{b2}}{M_{Pl}^3} \int dt \log(m_\phi |\mathbf{x}_1 - \mathbf{x}_2|). \end{aligned} \quad (5.30)$$

In the computation, the mass term in the propagators is neglected, as we consider distances (here and in the rest of this section) much smaller than the Compton wavelength of the chameleon $r \ll 1/m_\phi$, but it is reinserted at the end of (5.30) as an infra-red regulator [143]. Notice that this contribution (5.30) to the effective potential is directly proportional to distance, implying that this ‘correction’ eventually overcomes the lowest order solution (5.14) at some distance r_* and the perturbative expansion breaks down.

In the case of the earth, this distance r_* corresponds to

$$r_* \approx \frac{1}{g_3} \frac{M_{Pl}}{\beta_{eff} M_b M}, \quad (5.31)$$

i.e. $r_* \simeq 10^6$ Mpc (for $M = 1\text{eV}$ and $R = R_\oplus$, $\rho = \rho_\oplus$). This critical distance is larger than the Hubble radius and therefore the trilinear interaction never becomes important.

Let us pause a moment to compare self-interactions in Einstein gravity and scalar-gravity. In the case of general relativity, effects due to graviton self-interactions are suppressed because of the graviton self-coupling. The three-graviton vertex, for instance, is of the form $\partial^2 h^3$ (where h denotes the graviton with generic polarization indices and ∂ a generic spacetime derivative) and the corresponding correction to the Newtonian potential is proportional to $1/r^2$ [23]. The correction is thus suppressed with respect to the leading Newtonian contribution by a factor r_s/r (where r_s is the Schwarzschild radius of the body

sourcing the gravitational field). These corrections are indeed negligible for bodies that are sufficiently distant or diffuse. In the case of the scalar self-interactions, the behaviour is different. The fact that a scalar field can have *non-derivative* ϕ^3 self-coupling is crucial. Two powers less of momentum result in two powers more of r in the self-interaction amplitude, or the effective potential, which in turn leads to a *logarithmic* correction to the leading $1/r$ potential. This next-to-leading order correction overcomes the leading potential at large enough distances. So ϕ^3 self-interactions change the long-range behaviour of the scalar field, in contrast to the gravitational case.

The n -interacting chameleon

For all self-interactions, we can bypass the actual computations of the n -interacting Feynman diagrams 5.2. Using EFT methods, we estimate the scaling of the relative amplitude for the contribution to the effective potential mediated by all the other $g_n M^4 (\phi/M)^n$ interactions.

In EFT, we'd like to have a perturbative expansion in terms of a small parameter. For instance, in general relativity, post-Newtonian computations of two bodies gravitating around each other have the typical velocity v of the system as the expansion parameter (n th PN correction to the leading order Newtonian potential means corrections proportional to v^{2n}). In our case, we have a proliferation of dimensionless scales, so it is not possible to identify a single expansion parameter, however the method of [23] can still be applied to assess the strength of different contributions to the effective potential.

The effective action is computed perturbatively by applying systematic power counting rules. Each insertion on the world-line of a massive body, propagator, ϕ vertex, requires one of the following factors

- $\beta_{eff} dt d^3k M_b/M_{Pl}$ for a particle-chameleon vertex
- $g_n M^{4-n} dt (d^3k)^n \delta^{(3)}(k)$ for each n - ϕ vertex
- $\delta(t) \delta^{(3)}(k) \times 1/k^2$ for each propagator.

In standard Einstein gravity, two gravitating bodies exchange gravitons mediating the gravitational potential with momenta $k^\mu = (k_0, \mathbf{k})$, where $k^0 \sim v/r$ and $k \sim 1/r$ [23]. One can then assign the scaling $x^0 \sim r/v$, $x \equiv |\mathbf{x}| \sim r$, $k \sim 1/r$ and consequently $\delta^{(3)}(k) \sim r^3$, $d^3k \sim 1/r^3$, $\delta(t) \sim v/r$, $dt \sim r/v$.

These rules can be applied to a diagram contributing to the effective potential between two massive bodies due to the exchange of ϕ -fields and involving an n - ϕ vertex ($n > 2$), so the scaling can be estimated by

$$\text{fig. 5.2 (b)} \sim g_n \beta_{eff}^n M^{4-n} \left(\frac{M_b}{M_{Pl}} \right)^n \frac{r^{4-n}}{v}. \quad (5.32)$$

We recall that the simple one graviton exchange scales as [23]

$$\left(\frac{M_b}{M_{Pl}} \right)^2 \frac{t}{r} \simeq M_b v r \equiv L, \quad (5.33)$$

where the virial relation $M_b/(M_{Pl}^2 r) \sim v^2$ has been used. Using both (5.33) and the same virial relation in the chameleon amplitude scaling (5.32) one obtains

$$fig. 5.2 \sim g_n \beta_{eff}^n L \left(\frac{r_s}{l_{Pl}} \right)^2 \left(\frac{r_s}{r} \right)^{n-4} \left(\frac{M}{M_{Pl}} \right)^{4-n}, \quad (5.34)$$

where $r_s \equiv 2G_N M_b$ is the Schwarzschild radius of the massive body and the Planck length $l_{Pl} \equiv M_{Pl}^{-1}$ has been introduced. The proliferation of dimensionless ratios (r_s/r , M/M_{Pl} and M_b/M_{Pl}) makes this result less immediate to interpret, but the substitution of actual values for physical parameters provides insight as to what the scaling (5.34) means. Let us observe that L is the scaling of the action involving the Newtonian potential ($\sim dt G_N M_b^2/r$), and $\beta_{eff}^2 L$ is the scaling of the contribution to the effective action obtained by a diagram analogous to fig. 5.2 but with just one ϕ -propagator. Apart from $\beta_{eff}^2 L$, there are in eq.(5.34) extra terms involving the ratios $r_s/r < 1$, $M/M_{Pl} < 1$ and $r_s/l_{Pl} > 1$. To evaluate the importance of the diagram involving the n - ϕ vertex for the case of two orbiting bodies, an estimation of the parameters is necessary.

Numerical values are summarised by

$$\begin{aligned} \left(\frac{r_s}{l_{Pl}} \right)^2 &\simeq \left(4 \cdot 10^{37} \times \frac{M_b}{M_\odot} \right)^2, \\ \frac{r_s}{r} &\simeq 2 \cdot 10^{-8} \times \frac{M_b}{M_\odot} \left(\frac{r}{1\text{AU}} \right)^{-1}, \\ \frac{M}{M_{Pl}} &\simeq 4 \cdot 10^{-28} \times \frac{M}{1\text{eV}}, \\ \beta_{eff} &\simeq 2.2 \cdot 10^{-6} \times \left(\frac{\phi_\infty}{10^{16}\text{eV}} \right) \left(\frac{R}{R_\odot} \right) \left(\frac{M_b}{M_\odot} \right)^{-1}. \end{aligned} \quad (5.35)$$

For reasonable values of the parameters, such corrections are less and less relevant as n increases, and the resulting contribution to the two-body potential goes with distance as $1/r^{n-3}$.

The amplitude in eq. (5.30) corresponds to $n = 3$, i.e. a logarithmic potential, or as eq.(5.34) shows, a potential whose r dependence displays one power more than the usual $1/r$ Newtonian behaviour of single particle exchange. For $n = 4$ the amplitude is a times the contribution from the diagram with a single chameleon exchange, where a is given by

$$a \equiv \beta_{eff}^2 \lambda (r_s/l_{Pl})^2. \quad (5.36)$$

Taking the value for the Compton wavelength λ corresponding to the interplanetary medium from tab. 5.1, we see that a becomes a strong suppression factor. To answer the issue raised in section (5.1.4), it is of little importance that the higher order terms in the expansion are as important as the mass term near the surface of the body. Given that we are considering the case where $r \ll 1/m_\infty$, the potential is simply negligible for the determination of the chameleon profile in the region well within the Compton wavelength, where the Yukawa suppression has not yet taken place. Going from a diagram with a n -point interaction vertex to one with a $n + 1$ essentially corresponds to multiplying the amplitude

by a factor given by

$$\frac{g_{n+1}}{g_n} \beta_{eff} \left(\frac{r_s}{r} \right) \left(\frac{M_{Pl}}{M} \right) \simeq \beta_{eff} \left(\frac{r_s}{r} \right) \left(\frac{M_{Pl}}{\phi_\infty} \right), \quad (5.37)$$

which again is smaller than unity for reasonable parameters, as can be estimated from tab. 5.1 and (5.35). The perturbative series is then under full control.

Let us now consider the case where the background is curved. The kinetic term and the potential of the chameleon field, including all non-linearities, contribute to the energy-momentum tensor which, in turn, affect the background gravitational field via the Einstein equations. It is therefore necessary to verify that this chameleon induced backreaction on the gravitational field is negligible compared to the background. This verification is done by comparing the respective chameleon and gravitational potentials as follows. Let T be the generic entry of the energy-momentum tensor of the chameleon field and h the metric change due to its effect. We then obtain from Einstein equations:

$$\begin{aligned} h'' &\sim 8\pi G_N T \sim \frac{\phi'^2 + V(\phi)}{M_{Pl}^2} \sim \frac{\phi'^2 + m_\infty^2 (\phi - \phi_\infty)^2}{M_{Pl}^2} \\ &\sim \beta_{eff}^2 \frac{r_s^2}{r^4} + \beta_{eff}^2 m_\infty^2 \left(\frac{r_s}{r} \right)^2, \end{aligned} \quad (5.38)$$

where only the contribution of the quadratic part of the chameleon potential has been considered. Analogous reasoning behind eq. (5.37) leads to the conclusion that the contribution from higher order chameleon self-interactions are sub-dominant with respect to the $m_\infty^2 (\phi - \phi_\infty)^2$ term. For $r < m_\infty^{-1}$, the term proportional to $1/r^2$ is sub-dominant with respect to the one proportional to $1/r^4$, thus leading to the estimate $h \sim \beta_{eff}^2 r_s^2 / r^2$, whose effect is suppressed by a small factor β_{eff}^2 compared to the first order Post-Newtonian correction to the gravitational potential and a factor $\beta_{eff} r_s / r$ compared to the leading chameleon solution. In the opposite regime $r > m_\infty^{-1}$, the Yukawa suppression takes place. We have thus verified that the metric backreaction due to the chameleon is indeed negligible compared to the background solution.

5.2.2 Tests of the chameleon

If extra long-range forces exist, they must fulfill precise constraints imposed by experiment [65]. For the chameleon, such constraints have already been taken into consideration, see e.g. [142, 145]. In the following, we quote the constraints relevant for the EFT action (5.22) used to describe the chameleon for self-gravitating bodies in orbit.

The Nordvedt effect refers to the fall of bodies that have gravitational self-energy. A non-zero Nordvedt effect means that one would expect the Earth to fall towards the Sun at a different rate than the Moon. Lunar laser ranging, in which laser light is sent to the moon and reflected back, has lead to stringent bounds on this differential rate. This differential acceleration is estimated to be [11]

$$\eta_{\oplus-m}^{(exp)} \sim 10^{-13} \quad (5.39)$$

On the other hand, the chameleon violates the EP, so its mediated force is expected to induce a differential acceleration $\eta_{\oplus-m}^{(cham)}$ (normalized to the ordinary acceleration towards the sun at $1AU$). This differential acceleration can be approximated by

$$\begin{aligned}\eta_{\oplus-m}^{(cham)} &\simeq \beta_{eff\odot} \left| \beta_{eff\oplus} - \beta_{effm} \right| \\ &\simeq 16\pi^2 \frac{\phi_\infty^2 R_\odot R_m}{M_\odot M_m / M_{Pl}^2} \\ &\simeq 3.6 \cdot 10^{-7} \times \left(\frac{M}{1\text{eV}} \right)^{2\frac{\alpha+4}{\alpha+1}},\end{aligned}\tag{5.40}$$

Comparing this result with (5.39), we conclude that the chameleon can evade being detected for $M \lesssim 3 \times 10^{-7 \frac{\alpha+1}{2(\alpha+4)}} \text{ eV}$ (where α and β have been set to 1 everywhere except in the exponent).

Another astrophysical constraint for orbiting bodies can be expressed in terms of the Brans-Dicke parameter ω_{BD} . This parameter is defined by the action S_{BD} ruling the dynamics of the Brans-Dicke scalar field Φ ,

$$S_{BD} = S_\Phi + S_m = \frac{M_{Pl}^2}{2} \int d^4x \sqrt{-g} \left[e^\Phi \left(R - \omega_{BD} (\partial\Phi)^2 \right) \right] + \int d^4x \sqrt{-g} \mathcal{L}_{mat}(\psi^i, g_{\mu\nu}).\tag{5.41}$$

Once Φ is canonically normalized, i.e. $\Phi^c \equiv \Phi / (M_{Pl} \omega_{BD}^{1/2})$, and the metric rescaled by a factor $e^{-\Phi}$, eq. (5.41) gives a coupling to matter

$$S_m = \frac{m}{2M_{Pl} \omega_{BD}^{1/2}} \Phi^c \int dt.\tag{5.42}$$

Present bounds from Mercury perihelion precession, for instance, give $\omega_{BD} > 10^3$ [11], translating into $\beta_{eff}^2 < 10^{-3}$ for the chameleon which is easily evaded.

5.3 Discussion

We have given a systematic analysis of the corrections to the chameleon mediated potential due to non-derivative n -th order self-interactions, performed through the implementation of the EFT method originally proposed in [23] for general relativity. The analysis of the effects of self interaction is crucial for understanding if the result for the free field can be extended to the fully interacting case. Trilinear interactions have been shown to be potentially dangerous, as their contribution to the potential grows with distance with respect to the lowest order effect, but for ordinary values of the parameters at play, such contributions are actually harmless. Contributions from higher order interactions decrease faster with distance and they are also negligible.

We have presented a thorough perturbative analysis of such effects with the help of EFT methods and the powerful tool of Feynman diagrams. Once the relevant scales in the problem are identified, even if they are multiple, as in this case, it is possible to set a perturbative expansion which allows for the assessment of different diagrams.

Acronyms

BH black hole.

EEP Einstein equivalence principle.

EFT effective field theory.

EIH Einstein, Infeld and Hoffmann.

GWO gravitational wave observatories.

IR infrared.

NRGR non-relativistic General Relativity.

NS neutron star.

PN post-Newtonian.

PPN parametrized post-Newtonian.

SEP strong equivalence principle.

TT transverse-traceless.

UV ultraviolet.

WEP weak equivalence principle.

Bibliography

- [1] J. M. Weisberg and J. H. Taylor, “Relativistic Binary Pulsar B1913+16: Thirty Years of Observations and Analysis,” *ASP Conf. Ser.* **328** (2005) 25, [arXiv:astro-ph/0407149](#).
- [2] M. V. Gerard 't Hooft, “One loop divergencies in the theory of gravitation,”.
- [3] J. F. Donoghue, “Introduction to the effective field theory description of gravity,” [arXiv:gr-qc/9512024 \[gr-qc\]](#).
- [4] **Supernova Search Team** Collaboration, A. G. Riess *et al.*, “Observational Evidence from Supernovae for an Accelerating Universe and a Cosmological Constant,” *Astron. J.* **116** (1998) 1009–1038, [arXiv:astro-ph/9805201](#).
- [5] R. Durrer, “What do we really know about Dark Energy?,” [arXiv:1103.5331 \[astro-ph.CO\]](#).
- [6] R. Durrer and R. Maartens, “Dark Energy and Modified Gravity,” [arXiv:0811.4132 \[astro-ph\]](#).
- [7] T. Clifton, P. G. Ferreira, A. Padilla, and C. Skordis, “Modified Gravity and Cosmology,” [arXiv:1106.2476 \[astro-ph.CO\]](#).
- [8] R. Wagoner and C. Will, “Postnewtonian gravitational radiation from orbiting point masses,” *Astrophys.J.* **210** (1976) 764–775.
- [9] R. Epstein and R. V. Wagoner, “Post-Newtonian generation of gravitational waves,” *APJL* **197** (May, 1975) 717–723.
- [10] C. Will, “Theory and experiment in gravitational physics,”.
- [11] C. M. Will, “The confrontation between general relativity and experiment,” *Living Reviews in Relativity* **9** no. 3, (2006) . <http://www.livingreviews.org/lrr-2006-3>.
- [12] E. Bertschinger, “On the Growth of Perturbations as a Test of Dark Energy,” *Astrophys.J.* **648** (2006) 797–806, [arXiv:astro-ph/0604485 \[astro-ph\]](#).
- [13] R. Caldwell, A. Cooray, and A. Melchiorri, “Constraints on a New Post-General Relativity Cosmological Parameter,” *Phys.Rev.* **D76** (2007) 023507, [arXiv:astro-ph/0703375 \[ASTRO-PH\]](#).

- [14] W. Hu and I. Sawicki, “A Parameterized Post-Friedmann Framework for Modified Gravity,” *Phys.Rev.* **D76** (2007) 104043, [arXiv:0708.1190 \[astro-ph\]](#).
- [15] M. Kunz, L. Amendola, and D. Sapone, “Dark Energy Phenomenology,” [arXiv:0806.1323 \[astro-ph\]](#).
- [16] P. Horava, “Quantum Gravity at a Lifshitz Point,” *Phys. Rev.* **D79** (2009) 084008, [arXiv:0901.3775 \[hep-th\]](#).
- [17] D. Mattingly, “Modern tests of Lorentz invariance,” *Living Rev.Rel.* **8** (2005) 5, [arXiv:gr-qc/0502097 \[gr-qc\]](#).
- [18] D. Blas, O. Pujolas, and S. Sibiryakov, “Consistent Extension of Horava Gravity,” *Phys. Rev. Lett.* **104** (2010) 181302, [arXiv:0909.3525 \[hep-th\]](#).
- [19] D. Blas, O. Pujolas, and S. Sibiryakov, “On the Extra Mode and Inconsistency of Horava Gravity,” *JHEP* **0910** (2009) 029, [arXiv:0906.3046 \[hep-th\]](#).
- [20] D. Blas, O. Pujolas, and S. Sibiryakov, “Models of non-relativistic quantum gravity: The Good, the bad and the healthy,” *JHEP* **1104** (2011) 018, [arXiv:1007.3503 \[hep-th\]](#).
- [21] T. Damour and G. Esposito-Farese, “Tensor multiscalar theories of gravitation,” *Class. Quant. Grav.* **9** (1992) 2093–2176.
- [22] B. Z. Foster, “Radiation Damping in Einstein-Aether Theory,” *Phys. Rev.* **D73** (2006) 104012, [arXiv:gr-qc/0602004](#).
- [23] W. D. Goldberger and I. Z. Rothstein, “Effective field theory of gravity for extended objects,” *Phys. Rev. D* **73** no. 10, (May, 2006) 104029.
- [24] W. D. Goldberger, “Les Houches lectures on effective field theories and gravitational radiation,” [arXiv:hep-ph/0701129](#).
- [25] D. Blas and H. Sanctuary, “Gravitational Radiation in Horava Gravity,” *Phys.Rev.* **D84** (2011) 064004, [arXiv:1105.5149 \[gr-qc\]](#).
- [26] U. Cannella, S. Foffa, M. Maggiore, H. Sanctuary, and R. Sturani, “Extracting the three- and four-graviton vertices from binary pulsars and coalescing binaries,” *Phys. Rev.* **D80** (2009) 124035, [arXiv:0907.2186 \[gr-qc\]](#).
- [27] H. Sanctuary and R. Sturani, “Effective field theory analysis of the self-interacting chameleon,” *Gen.Rel.Grav.* **42** (2010) 1953–1967, [arXiv:0809.3156 \[gr-qc\]](#).
- [28] R. M. Wald, “General Relativity,”. Book, The University of Chicago Press, 1984.
- [29] S. M. Carroll, *Spacetime and geometry: An introduction to general relativity*. 2004.
- [30] E. E. Flanagan and S. A. Hughes, “The basics of gravitational wave theory,” *New J. Phys.* **7** (2005) 204, [arXiv:gr-qc/0501041](#).

- [31] M. Maggiore, *Gravitational Waves. Vol. 1: Theory and Experiments*. 2007.
- [32] L. Blanchet, “Gravitational radiation from post-Newtonian sources and inspiralling compact binaries,” *Living Rev.Rel.* **9** (2006) 4.
- [33] L. Blanchet and T. Damour, “POSTNEWTONIAN GENERATION OF GRAVITATIONAL WAVES,” *Annales Poincare Phys.Theor.* **50** (1989) 377–408.
- [34] E. Poisson, *Post-Newtonian theory for the common reader*. Lecture Notes, 2007.
- [35] M. E. Pati and C. M. Will, “PostNewtonian gravitational radiation and equations of motion via direct integration of the relaxed Einstein equations. 2. Two-body equations of motion to second postNewtonian order, and radiation reaction to 3.5 postNewtonia order,” *Phys.Rev.* **D65** (2002) 104008, [arXiv:gr-qc/0201001 \[gr-qc\]](#).
- [36] R. L. Arnowitt, S. Deser, and C. W. Misner, “The dynamics of general relativity,” [arXiv:gr-qc/0405109](#).
- [37] T. Jacobson and D. Mattingly, “Einstein-Aether waves,” *Phys.Rev.* **D70** (2004) 024003, [arXiv:gr-qc/0402005 \[gr-qc\]](#). 5 pages: v2: Remarks added concerning gauge invariance of the waves and hyperbolicity of the equations. Essentially the version published in PRD Journal-ref: *Phys.Rev.* D70 (2004) 024003.
- [38] S. Weinberg, *Gravitation and Cosmology: Principles and Applications of the General Theory of Relativity*. John Wiley & Sons, Inc. (1972), 657 p., 1972.
- [39] R. A. Porto and I. Z. Rothstein, “Spin(1)Spin(2) Effects in the Motion of Inspiralling Compact Binaries at Third Order in the Post-Newtonian Expansion,” *Phys.Rev.* **D78** (2008) 044012, [arXiv:0802.0720 \[gr-qc\]](#).
- [40] R. A. Porto, “New results at 3PN via an effective field theory of gravity,” [arXiv:gr-qc/0701106 \[gr-qc\]](#).
- [41] V. Cardoso, O. J. Dias, and P. Figueras, “Gravitational radiation in $d > 4$ from effective field theory,” *Phys.Rev.* **D78** (2008) 105010, [arXiv:0807.2261 \[hep-th\]](#).
- [42] C. R. Galley, “A Nonlinear scalar model of extreme mass ratio inspirals in effective field theory II. Scalar perturbations and a master source,” [arXiv:1107.0766 \[gr-qc\]](#).
- [43] T. Damour and G. Esposito-Farese, “Tensor - scalar gravity and binary pulsar experiments,” *Phys.Rev.* **D54** (1996) 1474–1491, [arXiv:gr-qc/9602056 \[gr-qc\]](#).
- [44] C. W. Misner, K. Thorne, and J. Wheeler, “Gravitation,”.
- [45] P. Peters and J. Mathews, “Gravitational radiation from point masses in a Keplerian orbit,” *Phys.Rev.* **131** (1963) 435–439.

- [46] S. Schlamminger, K.-Y. Choi, T. Wagner, J. Gundlach, and E. Adelberger, “Test of the equivalence principle using a rotating torsion balance,” *Phys.Rev.Lett.* **100** (2008) 041101, [arXiv:0712.0607 \[gr-qc\]](#).
- [47] T. Chupp, R. Haore, R. Loveman, E. Oteiza, J. Richardson, *et al.*, “Results of a new test of local Lorentz invariance: A Search for mass anisotropy in Ne-21,” *Phys.Rev.Lett.* **63** (1989) 1541–1545.
- [48] S. Shapiro, J. Davis, D. Lebach, and J. Gregory, “Measurement of the Solar Gravitational Deflection of Radio Waves using Geodetic Very-Long-Baseline Interferometry Data, 1979-1999,” *Phys.Rev.Lett.* **92** (2004) 121101.
- [49] B. Bertotti, L. Iess, and P. Tortora, “A test of general relativity using radio links with the Cassini spacecraft,” *Nature* **425** (2003) 374.
- [50] J. Anderson, M. Slade, R. Jurgens, and *et al.*, “Radar and spacecraft ranging to Mercury between 1966 and 1988,” *Proceedings of the Astronomical Society of Australia* **9** (1991) 324.
- [51] E. V. Pitjeva, “Experimental testing of relativistic effects, variability of the gravitational constant and topography of Mercury surface from radar observations 1964-1989,” *Celestial Mechanics and Dynamical Astronomy* **55** (Apr., 1993) 313–321.
- [52] J. G. Williams, S. G. Turyshev, and D. H. Boggs, “Progress in lunar laser ranging tests of relativistic gravity,” *Phys.Rev.Lett.* **93** (2004) 261101, [arXiv:gr-qc/0411113 \[gr-qc\]](#).
- [53] J. M. G. R.J. Warburton, “Search for evidence of a preferred reference frame,” *Astrophysical Journal* **208** (1976) 881–886.
- [54] J. Müller, K. Nordtvedt, and D. Vokrouhlický, “Improved constraint on the α_1 ppn parameter from lunar motion,” *Phys. Rev. D* **54** (Nov, 1996) R5927–R5930.
<http://link.aps.org/doi/10.1103/PhysRevD.54.R5927>.
- [55] K. Nordtvedt, “Probing gravity to the second post-newtonian order and to one part in 10 to the 7th using the spin axis of the sun,” *Astrophys.J.* **320** (1987) 871–874.
- [56] I. H. Stairs, A. Faulkner, A. Lyne, M. Kramer, D. Lorimer, *et al.*, “Discovery of three wide-orbit binary pulsars: Implications for binary evolution and equivalence principles,” *Astrophys.J.* **632** (2005) 1060–1068, [arXiv:astro-ph/0506188 \[astro-ph\]](#).
- [57] J. Taylor and J. Weisberg, “A new test of general relativity: Gravitational radiation and the binary pulsar PS R 1913+16,” *Astrophys.J.* **253** (1982) 908–920.
- [58] J. H. Taylor, A. Wolszczan, T. Damour, and J. Weisberg, “Experimental constraints on strong field relativistic gravity,” *Nature* (1991) .
- [59] A. Lyne, M. Burgay, M. Kramer, A. Possenti, R. Manchester, *et al.*, “A Double - pulsar system - A Rare laboratory for relativistic gravity and

- plasma physics,” *Science* **303** (2004) 1153–1157, [arXiv:astro-ph/0401086](#) [astro-ph].
- [60] S. Pireaux, J. Rozelot, and S. Godier, “Solar quadrupole moment and purely relativistic gravitation contributions to mercury’s perihelion advance,” *Astrophys.Space Sci.* **284** (2003) 1159–1194, [arXiv:astro-ph/0109032](#) [astro-ph].
- [61] H. Thirring, “Über die wirkung rotierender ferner massen in der einsteinschen gravitationstheorie,” *Physikalische Zeitschrift* **19** (1918) .
- [62] T. H. Lense J., “Über den einfluß der eigenrotation der zentralkörper auf die bewegung der planeten und monde nach der einsteinschen gravitationstheorie,” *Physikalische Zeitschrift* **19** (1918) .
- [63] I. Ciufolini and E. C. Pavlis, “A confirmation of the general relativistic prediction of the lense-thirring effect,” *Nature* **431** no. 7011, (10, 2004) 958–960. <http://dx.doi.org/10.1038/nature03007>.
- [64] C. Everitt, M. Adams, W. Bencze, S. Buchman, B. Clarke, *et al.*, “Gravity Probe B data analysis status and potential for improved accuracy of scientific results,” *Class.Quant.Grav.* **25** (2008) 114002.
- [65] C. M. Will, “The confrontation between general relativity and experiment,” *Living Rev. Rel.* **9** (2005) 3, [arXiv:gr-qc/0510072](#).
- [66] C. Cutler and E. E. Flanagan, “Gravitational waves from merging compact binaries: How accurately can one extract the binary’s parameters from the inspiral wave form?,” *Phys.Rev.* **D49** (1994) 2658–2697, [arXiv:gr-qc/9402014](#) [gr-qc].
- [67] C. Cutler and K. S. Thorne, “An Overview of gravitational wave sources,” [arXiv:gr-qc/0204090](#) [gr-qc]. Report.
- [68] T. Futamase and Y. Itoh, “The post-newtonian approximation for relativistic compact binaries,” *Living Reviews in Relativity* **10** no. 2, (2007) . <http://www.livingreviews.org/lrr-2007-2>.
- [69] M. Alcubierre, “The status of numerical relativity,” [arXiv:gr-qc/0412019](#).
- [70] N. Arkani-Hamed, H.-C. Cheng, M. A. Luty, and S. Mukohyama, “Ghost condensation and a consistent infrared modification of gravity,” *JHEP* **0405** (2004) 074, [arXiv:hep-th/0312099](#) [hep-th].
- [71] J. M. Cline, S. Jeon, and G. D. Moore, “The Phantom menaced: Constraints on low-energy effective ghosts,” *Phys.Rev.* **D70** (2004) 043543, [arXiv:hep-ph/0311312](#) [hep-ph].
- [72] T. P. Sotiriou and V. Faraoni, “f(R) Theories Of Gravity,” *Rev.Mod.Phys.* **82** (2010) 451–497, [arXiv:0805.1726](#) [gr-qc].
- [73] N. Straumann, “Problems with Modified Theories of Gravity, as Alternatives to Dark Energy,” [arXiv:0809.5148](#) [gr-qc].

- [74] J. Khoury and A. Weltman, “Chameleon fields: Awaiting surprises for tests of gravity in space,” *Phys.Rev.Lett.* **93** (2004) 171104, [arXiv:astro-ph/0309300](#) [astro-ph].
- [75] J. Khoury and A. Weltman, “Chameleon cosmology,” *Phys.Rev.* **D69** (2004) 044026, [arXiv:astro-ph/0309411](#) [astro-ph].
- [76] T. P. Waterhouse, “An Introduction to Chameleon Gravity,” [arXiv:astro-ph/0611816](#) [astro-ph].
- [77] A. Upadhye, J. Steffen, and A. Weltman, “Constraining chameleon field theories using the GammeV afterglow experiments,” *Phys.Rev.* **D81** (2010) 015013, [arXiv:0911.3906](#) [hep-ph].
- [78] **GammeV Collaboration** Collaboration, J. H. Steffen *et al.*, “Laboratory constraints on chameleon dark energy and power-law fields,” *Phys.Rev.Lett.* **105** (2010) 261803, [arXiv:1010.0988](#) [astro-ph.CO].
- [79] T. Jacobson and D. Mattingly, “Gravity with a dynamical preferred frame,” *Phys. Rev.* **D64** (2001) 024028, [arXiv:gr-qc/0007031](#).
- [80] T. Jacobson, “Einstein-aether gravity: Theory and observational constraints,” [arXiv:arXiv:0711.3822](#) [gr-qc].
- [81] T. Jacobson, “Einstein-aether gravity: A Status report,” *PoS QG-PH* (2007) 020, [arXiv:arXiv:0801.1547](#) [gr-qc].
- [82] B. Withers, “Einstein-aether as a quantum effective field theory,” *Class.Quant.Grav.* **26** (2009) 225009, [arXiv:0905.2446](#) [gr-qc].
- [83] T. Jacobson, “Extended Horava gravity and Einstein-aether theory,” *Phys. Rev.* **D81** (2010) 101502, [arXiv:1001.4823](#) [hep-th].
- [84] T. P. Sotiriou, “Horava-Lifshitz gravity: a status report,” [arXiv:1010.3218](#) [hep-th].
- [85] N. Arkani-Hamed, S. Dimopoulos, and G. Dvali, “The Hierarchy problem and new dimensions at a millimeter,” *Phys.Lett.* **B429** (1998) 263–272, [arXiv:hep-ph/9803315](#) [hep-ph].
- [86] G. Dvali, “Black Holes and Large N Species Solution to the Hierarchy Problem,” *Fortsch.Phys.* **58** (2010) 528–536, [arXiv:0706.2050](#) [hep-th].
- [87] P. Horava and C. M. Melby-Thompson, “General Covariance in Quantum Gravity at a Lifshitz Point,” *Phys.Rev.* **D82** (2010) 064027, [arXiv:1007.2410](#) [hep-th].
- [88] D. Blas, O. Pujolas, and S. Sibiryakov, “Comment on ‘Strong coupling in extended Horava-Lifshitz gravity’,” *Phys.Lett.* **B688** (2010) 350–355, [arXiv:0912.0550](#) [hep-th].
- [89] C. Armendariz-Picon, N. F. Sierra, and J. Garriga, “Primordial Perturbations in Einstein-Aether and BPSH Theories,” *JCAP* **1007** (2010) 010, [arXiv:1003.1283](#) [astro-ph.CO].

- [90] T. Kobayashi, Y. Urakawa, and M. Yamaguchi, “Cosmological perturbations in a healthy extension of Horava gravity,” *JCAP* **1004** (2010) 025, [arXiv:1002.3101 \[hep-th\]](#).
- [91] B. Z. Foster, “Strong field effects on binary systems in Einstein-aether theory,” *Phys.Rev.* **D76** (2007) 084033, [arXiv:arXiv:0706.0704 \[gr-qc\]](#).
- [92] E. Barausse, T. Jacobson, and T. P. Sotiriou, “Black holes in Einstein-aether and Horava-Lifshitz gravity,” *Phys.Rev.* **D83** (2011) 124043, [arXiv:1104.2889 \[gr-qc\]](#).
- [93] D. Blas and S. Sibiryakov, “Horava gravity versus thermodynamics: The Black hole case,” *Phys.Rev.* **D84** (2011) 124043, [arXiv:1110.2195 \[hep-th\]](#). 36 pages, 3 figures, 1 table. v2 Small changes to agree with published version.
- [94] C. Eling, T. Jacobson, and M. Coleman Miller, “Neutron stars in Einstein-aether theory,” *Phys.Rev.* **D76** (2007) 042003, [arXiv:0705.1565 \[gr-qc\]](#).
- [95] I. Kimpton and A. Padilla, “Lessons from the decoupling limit of Horava gravity,” *JHEP* **1007** (2010) 014, [arXiv:1003.5666 \[hep-th\]](#).
- [96] B. Z. Foster and T. Jacobson, “Post-Newtonian parameters and constraints on Einstein-aether theory,” *Phys.Rev.* **D73** (2006) 064015, [arXiv:gr-qc/0509083 \[gr-qc\]](#).
- [97] L. B. Szabados, “Quasi-Local Energy-Momentum and Angular Momentum in GR: A Review Article,” *Living Rev.Rel.* **7** (2004) 4.
- [98] B. Z. Foster, “Noether charges and black hole mechanics in Einstein-aether theory,” *Phys.Rev.* **D73** (2006) 024005, [arXiv:gr-qc/0509121 \[gr-qc\]](#).
- [99] V. Iyer and R. M. Wald, “Some properties of Noether charge and a proposal for dynamical black hole entropy,” *Phys.Rev.* **D50** (1994) 846–864, [arXiv:gr-qc/9403028 \[gr-qc\]](#).
- [100] R. D. Sorkin, “The Gravitational electromagnetic Noether operator and the second order energy flux,” *Proc.Roy.Soc.Lond.* **A435** (1991) 635–644.
- [101] T. Regge and C. Teitelboim, “Role of Surface Integrals in the Hamiltonian Formulation of General Relativity,” *Annals Phys.* **88** (1974) 286.
- [102] R. M. Wald and A. Zoupas, “A General definition of ‘conserved quantities’ in general relativity and other theories of gravity,” *Phys.Rev.* **D61** (2000) 084027, [arXiv:gr-qc/9911095 \[gr-qc\]](#).
- [103] J. Weisberg and J. Taylor, “GRAVITATIONAL RADIATION FROM AN ORBITING PULSAR,” *Gen.Rel.Grav.* **13** (1981) 1–6.
- [104] D. M. Eardley, *Observable effects of a scalar gravitational field in a binary pulsar*, vol. 196. Astrophysical Journal, 1975.

- [105] G. Esposito-Farese, “Tests of scalar-tensor gravity,” *AIP Conf.Proc.* **736** (2004) 35–52, [arXiv:gr-qc/0409081](#) [gr-qc].
- [106] R. A. Porto and I. Z. Rothstein, “The Hyperfine Einstein-Infeld-Hoffmann potential,” *Phys.Rev.Lett.* **97** (2006) 021101, [arXiv:gr-qc/0604099](#) [gr-qc].
- [107] R. A. Porto, “Post-Newtonian corrections to the motion of spinning bodies in NRGR,” *Phys.Rev.* **D73** (2006) 104031, [arXiv:gr-qc/0511061](#) [gr-qc].
- [108] W. D. Goldberger and A. Ross, “Gravitational radiative corrections from effective field theory,” *Phys.Rev.* **D81** (2010) 124015, [arXiv:0912.4254](#) [gr-qc].
- [109] S. M. Carroll and E. A. Lim, “Lorentz-violating vector fields slow the universe down,” *Phys.Rev.* **D70** (2004) 123525, [arXiv:hep-th/0407149](#) [hep-th].
- [110] D. Blas and S. Sibiryakov, “Technically natural dark energy from Lorentz breaking,” *JCAP* **1107** (2011) 026, [arXiv:1104.3579](#) [hep-th]. published version, references updated.
- [111] N. Yunes and F. Pretorius, “Fundamental Theoretical Bias in Gravitational Wave Astrophysics and the Parameterized Post-Einsteinian Framework,” *Phys.Rev.* **D80** (2009) 122003, [arXiv:0909.3328](#) [gr-qc].
- [112] N. Yunes and S. A. Hughes, “Binary Pulsar Constraints on the Parameterized post-Einsteinian Framework,” *Phys.Rev.* **D82** (2010) 082002, [arXiv:1007.1995](#) [gr-qc].
- [113] W. Del Pozzo, J. Veitch, and A. Vecchio, “Testing General Relativity using Bayesian model selection: Applications to observations of gravitational waves from compact binary systems,” *Phys.Rev.* **D83** (2011) 082002, [arXiv:1101.1391](#) [gr-qc].
- [114] A. De Rujula, R. Petronzio, and B. Lautrup, “On the Challenge of Measuring the Color Charge of Gluons,” *Nucl.Phys.* **B146** (1978) 50.
- [115] J. Ellison and J. Wudka, “Study of trilinear gauge boson couplings at the Tevatron collider,” *Ann.Rev.Nucl.Part.Sci.* **48** (1998) 33–80, [arXiv:hep-ph/9804322](#) [hep-ph].
- [116] **ALEPH Collaboration** Collaboration, S. Schael *et al.*, “Improved measurement of the triple gauge-boson couplings $\gamma W W$ and $Z W W$ in $e^+ e^-$ collisions,” *Phys.Lett.* **B614** (2005) 7–26.
- [117] **Particle Data Group** Collaboration, C. Amsler *et al.*, “Review of Particle Physics,” *Phys.Lett.* **B667** (2008) 1.
- [118] M. Kramer, I. H. Stairs, R. Manchester, M. McLaughlin, A. Lyne, *et al.*, “Tests of general relativity from timing the double pulsar,” *Science* **314** (2006) 97–102, [arXiv:astro-ph/0609417](#) [astro-ph].

- [119] I. H. Stairs, “Testing general relativity with pulsar timing,” *Living Rev.Rel.* **6** (2003) 5, [arXiv:astro-ph/0307536 \[astro-ph\]](#). * Brief entry *.
- [120] L. E. Kidder, C. M. Will, and A. G. Wiseman, “Spin effects in the inspiral of coalescing compact binaries,” *Phys.Rev.* **D47** (1993) 4183–4187, [arXiv:gr-qc/9211025 \[gr-qc\]](#).
- [121] E. Poisson and C. M. Will, “Gravitational waves from inspiraling compact binaries: Parameter estimation using second postNewtonian wave forms,” *Phys.Rev.* **D52** (1995) 848–855, [arXiv:gr-qc/9502040 \[gr-qc\]](#).
- [122] L. Blanchet, T. Damour, B. R. Iyer, C. M. Will, and A. Wiseman, “Gravitational radiation damping of compact binary systems to second postNewtonian order,” *Phys.Rev.Lett.* **74** (1995) 3515–3518, [arXiv:gr-qc/9501027 \[gr-qc\]](#).
- [123] E. Racine, A. Buonanno, and L. E. Kidder, “Recoil velocity at 2PN order for spinning black hole binaries,” *Phys.Rev.* **D80** (2009) 044010, [arXiv:0812.4413 \[gr-qc\]](#).
- [124] K. Arun, B. R. Iyer, M. Qusailah, and B. Sathyaprakash, “Probing the non-linear structure of general relativity with black hole binaries,” *Phys.Rev.* **D74** (2006) 024006, [arXiv:gr-qc/0604067 \[gr-qc\]](#).
- [125] L. Blanchet, A. Buonanno, and G. Faye, “Higher-order spin effects in the dynamics of compact binaries. II. Radiation field,” *Phys.Rev.* **D74** (2006) 104034, [arXiv:gr-qc/0605140 \[gr-qc\]](#).
- [126] T. Damour and G. Esposito-Farese, “Gravitational wave versus binary - pulsar tests of strong field gravity,” *Phys.Rev.* **D58** (1998) 042001, [arXiv:gr-qc/9803031 \[gr-qc\]](#).
- [127] C. Van Den Broeck and A. S. Sengupta, “Binary black hole spectroscopy,” *Class.Quant.Grav.* **24** (2007) 1089–1114, [arXiv:gr-qc/0610126 \[gr-qc\]](#).
- [128] S. Minwalla, M. Van Raamsdonk, and N. Seiberg, “Noncommutative perturbative dynamics,” *JHEP* **0002** (2000) 020, [arXiv:hep-th/9912072 \[hep-th\]](#).
- [129] T. Damour and J. H. Taylor, “Strong field tests of relativistic gravity and binary pulsars,” *Phys.Rev.* **D45** (1992) 1840–1868.
- [130] T. Damour and G. Esposito-Farese, “Nonperturbative strong field effects in tensor - scalar theories of gravitation,” *Phys.Rev.Lett.* **70** (1993) 2220–2223.
- [131] C. M. Will, “Testing scalar - tensor gravity with gravitational wave observations of inspiraling compact binaries,” *Phys.Rev.* **D50** (1994) 6058–6067, [arXiv:gr-qc/9406022 \[gr-qc\]](#).
- [132] T. Damour and G. Esposito-Farese, “Testing gravity to second postNewtonian order: A Field theory approach,” *Phys.Rev.* **D53** (1996) 5541–5578, [arXiv:gr-qc/9506063 \[gr-qc\]](#).

- [133] P. G. Bergmann, “Comments on the scalar tensor theory,” *Int. J. Theor. Phys.* **1** (1968) 25–36.
- [134] R. V. Wagoner, “Scalar tensor theory and gravitational waves,” *Phys. Rev.* **D1** (1970) 3209–3216.
- [135] T. Damour and A. M. Polyakov, “The String dilaton and a least coupling principle,” *Nucl.Phys.* **B423** (1994) 532–558, [arXiv:hep-th/9401069 \[hep-th\]](#).
- [136] G. W. Anderson and S. M. Carroll, “Dark matter with time dependent mass,” [arXiv:astro-ph/9711288 \[astro-ph\]](#).
- [137] R. Brustein and P. J. Steinhardt, “Challenges for superstring cosmology,” *Phys.Lett.* **B302** (1993) 196–201, [arXiv:hep-th/9212049 \[hep-th\]](#).
- [138] S. Kachru, M. B. Schulz, and S. Trivedi, “Moduli stabilization from fluxes in a simple IIB orientifold,” *JHEP* **0310** (2003) 007, [arXiv:hep-th/0201028 \[hep-th\]](#).
- [139] B. Feldman and A. E. Nelson, “New regions for a chameleon to hide,” *JHEP* **0608** (2006) 002, [arXiv:hep-ph/0603057 \[hep-ph\]](#).
- [140] S. S. Gubser and J. Khoury, “Scalar self-interactions loosen constraints from fifth force searches,” *Phys.Rev.* **D70** (2004) 104001, [arXiv:hep-ph/0405231 \[hep-ph\]](#).
- [141] D. F. Mota and D. J. Shaw, “Strongly coupled chameleon fields: New horizons in scalar field theory,” *Phys.Rev.Lett.* **97** (2006) 151102, [arXiv:hep-ph/0606204 \[hep-ph\]](#).
- [142] D. F. Mota and D. J. Shaw, “Evading Equivalence Principle Violations, Cosmological and other Experimental Constraints in Scalar Field Theories with a Strong Coupling to Matter,” *Phys.Rev.* **D75** (2007) 063501, [arXiv:hep-ph/0608078 \[hep-ph\]](#).
- [143] R. A. Porto and R. Sturani, “Scalar gravity: Post-Newtonian corrections via an effective field theory approach,” [arXiv:gr-qc/0701105 \[gr-qc\]](#).
- [144] M. Grana, “Flux compactifications in string theory: A Comprehensive review,” *Phys.Rept.* **423** (2006) 91–158, [arXiv:hep-th/0509003 \[hep-th\]](#).
- [145] P. Brax, C. van de Bruck, A.-C. Davis, D. F. Mota, and D. J. Shaw, “Detecting chameleons through Casimir force measurements,” *Phys.Rev.* **D76** (2007) 124034, [arXiv:arXiv:0709.2075 \[hep-ph\]](#).

